# I. THE CRYSTAL STRUCTURE OF A NEW DIMER OF TRIPHENYLFLUOROCYCLOBUTADIENE

# II. A LOW TEMPERATURE REFINEMENT OF THE CYANURIC TRIAZIDE STRUCTURE

Thesis by

Thomas Andrew Beineke

In Partial Fulfillment of the Requirements
For the Degree of
Doctor of Philosophy

California Institute of Technology
Pasadena, California
1966
(Submitted August 12, 1965)

## ACKNOWLEDGMENTS

Grateful acknowledgment is given my faculty advisor, Dr. E. W. Hughes, who, through his valuable suggestions, encouragement, and continued interest in these projects, is in large part responsible for their successful completion. I would also like to express my gratitude to Dr. D. J. Duchamp for his invaluable assistance in the writing of the computer programs which were used in connection with the work reported herein, and to Dr. R. E. Marsh and Dr. C. M. Gramaccioli for their assistance in the use of the CRYRM computing system. For their helpful suggestions and informative discussions, I would like to thank Dr. D. R. Dyroff, Mr. Chi Tsun Lin, and Dr. B. D. Sharma. For proofreading a major portion of this thesis, I thank Mr. E. Kent Gordon.

The financial assistance given me by the National Science Foundation in the form of an N. S. F. Cooperative Graduate Fellowship and by the California Institute of Technology in the form of a graduate teaching assistantship is gratefully appreciated. Further, I thank the Danforth Foundation and the Woodrow Wilson Foundation for their encouragement in the form of honorary fellowships.

Finally, I thank my parents, who, through personal sacrifice and continued encouragement during my undergraduate days at Ohio University, are responsible for my presence at this institution.

## ABSTRACT

### I. THE CRYSTAL STRUCTURE OF A NEW DIMER OF TRIPHENYLFLUOROCYCLOBUTADIENE

The crystal structure of the thermal isomer of the "head-to-head" dimer of triphenylfluorocyclobutadiene was determined by the direct method. The $\Sigma_2$ relationships involving the low angle reflections with the largest E's were found and solved for the signs by the symbolic method of Zachariasen. The structure was seen in the electron density map and the E-map, and was refined anisotropically by the method of least squares. The residual R was 0.065.

The structure is a gem-difluorohexaphenyldihydropentalene. All of the phenyl groups are planar as is the cyclopentadiene ring of the dihydropentalene skeleton. Overcrowding at the position of the flourines causes some deviations from the normal bond angles in the cyclopentene ring.

The list of observed and calculated structure factors on pages 32 - 34 will not be legible on the microfilm. Photographic copies may be obtained from the California Institute of Technology.

### II. A LOW TEMPERATURE REFINEMENT OF THE CYANURIC TRIAZIDE STRUCTURE

The structure of cyanuric triazide was refined anisotropically by the method of least squares. Three-dimensional intensity data, which had been collected photographically with $MoK_\alpha$ radiation at $-110^\circ C$, were used in the refinement. The residual R was reduced to 0.081.

The structure is completely planar, and there is no significant bond alternation in the cyanuric ring. The packing of the molecules causes the azide groups to deviate from linearity by 8 degrees.

TABLE OF CONTENTS

# I. THE CRYSTAL STRUCTURE OF A NEW DIMER OF TRIPHENYLFLUOROCYCLOBUTADIENE

## INTRODUCTION

In the course of an investigation of small ring compounds, Nagarajan, Caserio, and Roberts (23) observed the thermal isomerization of the "head-to-head" dimer I * of triphenylfluorocyclobutadiene to a yellow crystalline material, m.p. 219° - 220° dec. Attempts to characterize this new dimer by n.m.r. and infrared methods indicated magnetically nonequivalent fluorines located on the

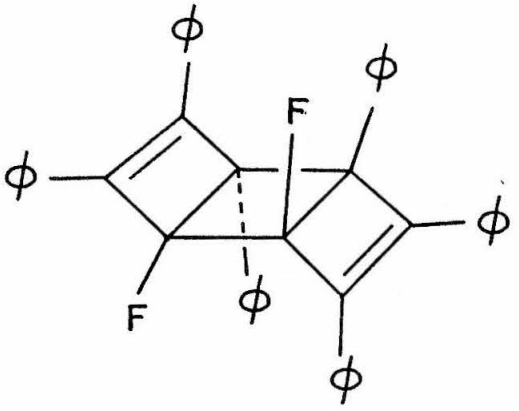


I

same carbon and suggested for the central molecular skeleton two fused, five-membered rings. The complete molecular structure, however, remained a matter of speculation. The present investigation was undertaken to determine the molecular structure of this new dimer.

---

* The structure of I was established by the x-ray investigation of Fritchie and Hughes (6, 7).

## EXPERIMENTAL

### Preliminary Observations

A sample of this new dimer (hereafter called DHB, an abbreviation for the systematic name according to the nomenclature rules of the International Union of Chemistry, hereafter abbreviated i. u. c.) consisting of small, yellow, approximately equidimensional prisms was supplied by Drs. Roberts and Caserio. No difficulty was encountered in selecting single crystals with well developed faces for optical examination; no twins were observed. The crystalline habit appeared to be centrosymmetric, but a stereographic projection of the spectral reflections obtained on a two circle, optical goniometer indicated no additional symmetry. On a polarizing microscope, DHB was observed to be dichroic; the most intense yellow color was observed when the crystal was viewed perpendicular to the (010) face and with the electric vector making an angle of about $60^{\circ}$ with the $\underset{\sim}{c}$ axis in the direction of the negative $\underset{\sim}{a}$ axis.

### Unit Cell Parameters

In the absence of higher symmetry, a triclinic cell was chosen with the most prominent zones as crystallographic axes. The well developed forms are {010}, {$\bar{1}$10}, {001}, and {101}. Since preliminary oscillation and Weissenberg photographs failed to indicate additional symmetry elements, the triclinic cell was established. The original choice of crystallographic axes was also seen to be consistent with a primitive cell. Rough values for the lengths of these axes were obtained from oscillation photographs, and the angles between

the reciprocal axes were measured on the optical goniometer. Accurate unit cell parameters were subsequently calculated from back reflection data measured on photographs of crystals rotated about the three crystallographic axes. A precision Straumanis-type Weissenberg camera was used with Cu $K_\alpha$ radiation for these measurements. The wave length of Cu $K_{\alpha_1}$ was assumed to be 1.54051 Å for these calculations. Cell parameters were adjusted by the method of least squares by a program which was written by Dr. N. D. Jones (16) for the Burroughs 220 computer. The function which was minimized was

$$\sum_i (\sqrt{w_i}\ \sin^2\Theta_{obs.} - \sqrt{w_i}\ \sin^2\Theta_{calc.})^2 ,$$

where $\sqrt{w_i}$ is the weight of the particular reflection. $\sqrt{w_i}$ was set equal to $\frac{\epsilon}{\sin 2\theta}$, where $\epsilon$ is an estimate of the reliability of each reflection. Eight reflections from the $\underset{\sim}{a}$ axis photograph, nine from the $\underset{\sim}{b}$ axis photograph, and eight from the $\underset{\sim}{c}$ axis photograph were used in this refinement. The following unit cell parameters were obtained*:

$\underset{\sim}{a} = 13.370 \pm 0.003$ Å  $\underset{\sim}{b} = 11.800 \pm 0.003$ Å  $\underset{\sim}{c} = 11.306 \pm 0.003$ Å

$\alpha = 69.67^\circ \pm 0.02^\circ$  $\beta = 94.42^\circ \pm 0.02^\circ$  $\gamma = 108.47^\circ \pm 0.02^\circ$

$V = 1585$ Å$^3$

The estimated uncertainties are an order of magnitude larger than the $\sigma$'s which were obtained from the least squares calculation. They were estimated by assuming an average coefficient of thermal expansion for organic crystals and allowing for a tempe rature variation

* A primitive cell in which all angles are obtuse can be assigned to this lattice; however, the present cell makes interpretation of the Weissenberg pictures more convenient.

of $\pm$ 5°C during the exposures.

The density of the crystals was measured by dissolving $ZnCl_2$ in water until a solution was obtained in which crystals of DHB would remain suspended. The density of this solution was then measured with a small pycnometer. The density of DHB crystals measured in this way is 1.25 g./cm.$^3$; whereas, the density calculated from the cell parameters with the assumption of two molecules per unit cell is 1.2498 g./cm.$^3$. The presence of two molecules in a unit cell was, therefore, established.

Assignment of Space Group

The choice between the two triclinic space groups, P1 and $P\bar{1}$, is not easy; however, an early indication of a center of symmetry was seen in the apparent centric crystalline habit of DHB. A Howells, Phillips, and Rogers (10) statistical treatment of the three-dimensional intensity data was performed*. The results are compared with the theoretical distributions for centric and acentric crystals in figure 1. This plot, although ambiguous, tends to favor the centric space group. The subsequent structure determination and refinement in terms of $P\bar{1}$ confirm this assignment.

Measurement of Intensity Data

Two approximately equidimensional crystals measuring less than 0.3 mm. in any direction were used for the intensity measurements. In order to estimate the magnitude of errors due to absorption, the linear coefficient of absorption, $\mu$, for DHB in $CuK_\alpha$ radi-

* See Appendix for a description of the computer program which was used.

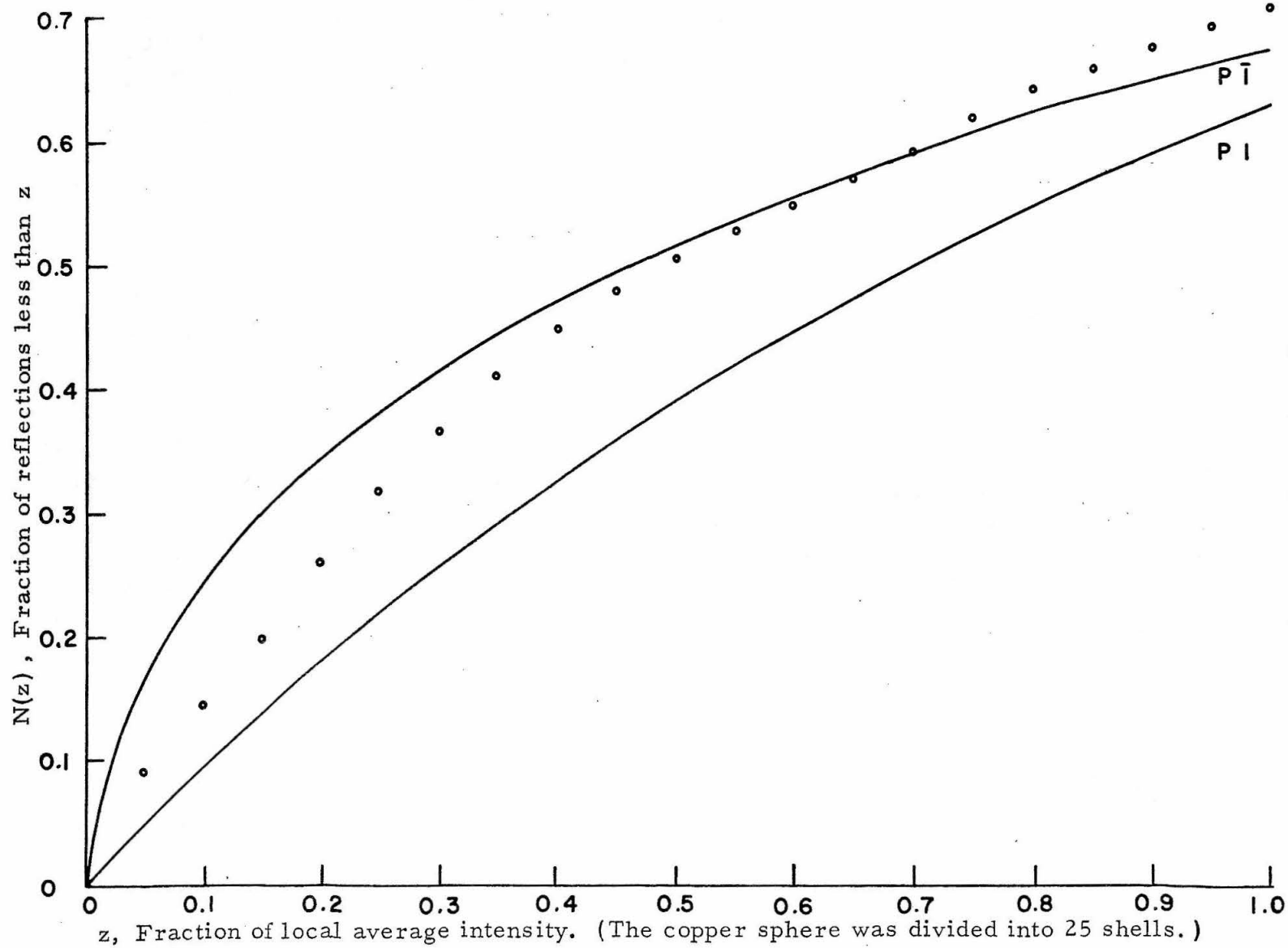


Figure 1. Howells, Phillips, and Rogers Plot for DHB.

ation was calculated and found to be 6.44 cm.$^{-1}$. The maximum value for $\mu R$ is therefore 0.19, from which the maximum variation in the absorption correction factor, A* , calculates to be $\sim 2$ per cent in the cylindrical approximation (14). Consequently, the intensity data were not corrected for absorption. Intensity data were collected photographically by the multiple-film, equi-inclination Weissenberg method. Layers zero through eight for axis $\underset{\sim}{c}$ and layers zero through four for axis $\underset{\sim}{b}$ were photographed with $CuK_\alpha$ radiation which had been filtered through Ni foil, to remove the $\beta$ radiation. Two packs of three films were used for each half layer, except for layer eight about axis $\underset{\sim}{c}$ for which one pack of three films was sufficient. The intensity of $CuK_\alpha$ radiation is decreased by a factor of about one fourth in passing through one sheet of x-ray film. Consequently, for each half layer, one film pack was exposed about 64 times as long as the other in order to provide a continuous attenuation in intensity of about one fourth between films. Intensities were estimated by visually comparing the diffraction spots on the films with an intensity scale which had been prepared for each crystal by timed exposures.

Data Reduction

All calculations except for the aforementioned least squares refinement of the unit cell parameters were done on the IBM 7094 computer with the CRYRM crystallographic computing system which has recently been developed at the California Institute of Technology (5). The data reduction was performed by the "Initial Data Processing Program" which was written by Dr. D. J. Duchamp, Dr. C. M.

Gramaccioli, and Mrs. B. Stroll (reference 5, chapter 4). As each reflection was entered in this calculation, it was assigned a standard deviation, $\sigma(I)$, according to the following function (reference 5, chapter 4):

$$\sigma(I) = \frac{1}{w_e}\left[1.333 + 0.1I + \frac{0.1I^2}{(45.0-I)^2}\right]\left[1 + 0.25\, e^{-50.0(0.5-\sin^2\theta)^2}\right]$$

for $I < 45.0$

$\sigma(I)$ = a very large number for $I \geq 45.0$ .

The $w_e$ is an external weight which is assumed to be 1.0 unless a different value is entered. (Values of 0.2 and 0.5 were frequently entered for questionable reflections.) The $\sigma(I)$'s were carried through the rest of the data reduction and scaling by propagation-of-error methods. Weights for each reflection were then set equal to the reciprocal of $\sigma(I)$. These weights were subsequently used in the final stages of the least squares refinement where they corresponded to the quantity $\sqrt{w}$.

Factors for film to film scaling were calculated in the usual way from intensities measurable on more than one film. The raw intensity data were then reduced to the scale of the most intense film of each half layer and corrected for the Lorentz and polarization factors. The data from both axes were then scaled together by a least squares procedure. A total of 6,017 reflections were recorded, of which 3,596 were observed above the background. These data are listed in Table X.

A data tape suitable for use with subsequent CRYRM programs was prepared by the "Data Tape Preparation Program" which

was written by Dr. D. J. Duchamp (reference 5, chapter 5). Subroutines which were written by the author (see Appendix) placed the data on an absolute scale by Wilson's method (30) and performed the aforementioned Howells, Phillips, and Rogers statistical test. The overall isotropic temperature factor was 4.5.

## DETERMINATION OF THE TRIAL STRUCTURE

On the basis of their n. m. r. and infrared measurements, Nagarajan, Caserio, and Roberts proposed structure II for DHB (23), although consideration had previously been given to structure III (25). In neither case is the molecular skeleton expected to be completely

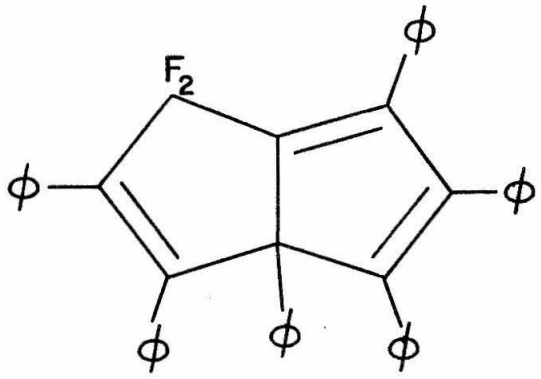


II

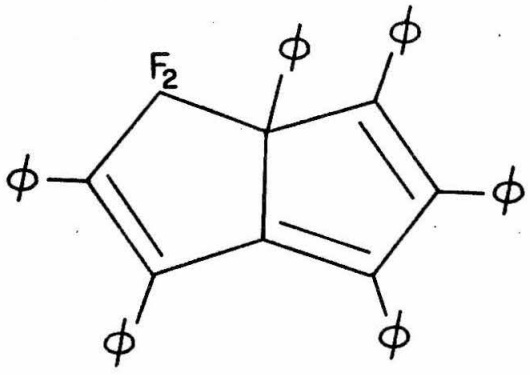


III

planar. For both structures, however, a great many intramolecular vectors will make only small deviations from the plane of the paper. Consequently, many Patterson peaks are expected to be located near the best molecular plane. A three-dimensional Patterson map was constructed by the "Fourier and Patterson Program" which was written by Dr. D. J. Duchamp (reference 5, chapter 7). This map revealed a concentration of peaks near a plane which contained the origin and passed obliquely through three unit cells. The coordinates of a number of the more prominent peaks about this plane were used to compute a "best" molecular plane by least squares. The direction cosines of this plane with respect to the crystallographic axes $\underset{\sim}{a}$, $\underset{\sim}{b}$ and $\underset{\sim}{c}$, are -0.6643, -0.3744, and 0.2369, respectively. Further information could not be obtained from the Patterson map even after

sharpening.

The Direct Solution of the Phase Problem

In the following discussion, use will be made of the unitary structure factor, the normalized unitary structure factor, and unitary scattering factors. The unitary structure factor is defined by

$$U_{\underset{\sim}{h}} = \frac{F_{\underset{\sim}{h}}}{\sum_{j=1}^{N} f_j} \qquad (1)$$

where $f_j$ is the atomic scattering factor for the $j^{th}$ atom corrected for thermal vibration. N is the number of atoms in the unit cell, and the vector $\underset{\sim}{h}$ represents the reciprocal lattice point $hk\ell$. $\sum_{j=1}^{N} f_j$ is the maximum possible value for $F_{\underset{\sim}{h}}$ when all atoms scatter in phase. $U_{\underset{\sim}{h}}$, therefore, has a maximum value of 1.0. The unitary scattering factor is defined by

$$n_j = \frac{f_j}{\sum_{j=1}^{N} f_j} \quad . \qquad (2)$$

The unitary structure factor becomes, for any centrosymmetric space group,

$$U_{\underset{\sim}{h}} = \sum_{j=1}^{N} n_j \cos 2\pi \underset{\sim}{h} \cdot \underset{\sim}{r}_j \quad , \qquad (3)$$

where $\underset{\sim}{r}_j$ is the vector from the origin to the $j^{th}$ atom. From equation 3 it can be shown that the expectation value for $|U_{\underset{\sim}{h}}^2|$ is

$$\langle |U_{\underset{\sim}{h}}^2| \rangle = \sum_{j=1}^{N} n_j^2 = \epsilon_2 \quad . \qquad (4)$$

The normalized unitary structure factor, $E_{\underset{\sim}{h}}$, is defined so that $\langle |E_{\underset{\sim}{h}}^2| \rangle = 1$.

$$E_{\underset{\sim}{h}} = \frac{U_{\underset{\sim}{h}}}{\epsilon_2^{\frac{1}{2}}} \tag{5}$$

An equivalent definition which is often seen in the literature is

$$E_{\underset{\sim}{h}}^2 = \frac{F_{\underset{\sim}{h}}^2}{\sum_{j=1}^{N} f_j^2} \quad . \tag{6}$$

From arguments similar to those of Wilson (31) it can be shown that unitary structure factors for centrosymmetric crystals follow a normal distribution curve about a mean of zero with a standard deviation of $\epsilon_2^{\frac{1}{2}}$. When the unitary structure factors are normalized according to equation 5, a standard normal distribution is obtained.

Another quantity which will be needed is

$$\epsilon_3 = \sum_{j=1}^{N} n_j^3 \quad . \tag{7}$$

For centrosymmetric space groups, a relationship similar to equation 8 (below) involving the signs* of structure factors may be obtained by any of a number of different approaches (1, 8, 9, 13, 26, 33).

$$s(\underset{\sim}{h}) \approx s(\underset{\sim}{h'})\, s(\underset{\sim}{h}+\underset{\sim}{h'}) \tag{8}$$

The symbol $s(\underset{\sim}{h})$ represents the sign of the structure factor for re-

---

* For acentric space groups, similar relationships can be derived which involve phase angles. For example, Karle and Karle (19) have used

$$\varphi_{\underset{\sim}{h}} \approx \left\langle \varphi_{\underset{\sim}{h'}} + \varphi_{\underset{\sim}{h}+\underset{\sim}{h'}} \right\rangle_{\underset{\sim}{h'}}$$

which follows directly from the relationship of Hughes (13)

$$\overline{U_{\underset{\sim}{h}} \cdot U_{\underset{\sim}{h'}}}^{h+h'} = U_{\underset{\sim}{h}+\underset{\sim}{h'}}/N \quad .$$

flection $\underset{\sim}{h}$. In simple structures, equation 8 may be shown to be absolutely true (8, 12); however, for moderately complex structures, equation 8 must be expressed in terms of a probability. This probability, $P_+(\underset{\sim}{h}, \underset{\sim}{h}')$, in terms of the magnitudes of the unitary structure factors, is (2)

$$P_+(\underset{\sim}{h}, \underset{\sim}{h}') = \tfrac{1}{2} + \tfrac{1}{2} \tanh \left\{ \frac{\epsilon_3}{\epsilon_2^{3}} \left| U_{\underset{\sim}{h}} U_{\underset{\sim}{h}'} U_{\underset{\sim}{h}+\underset{\sim}{h}'} \right| \right\} . \tag{9}$$

Confidence in $s(\underset{\sim}{h})$ is improved if the term on the right of equation 8 is replaced by the sum of products of unitary structure factors.

$$s(\underset{\sim}{h}) = s \sum_{\underset{\sim}{h}'} (U_{\underset{\sim}{h}'} U_{\underset{\sim}{h}+\underset{\sim}{h}'}) \tag{10}$$

The corresponding probability (2) is

$$P_+(\underset{\sim}{h}) = \tfrac{1}{2} + \tfrac{1}{2} \tanh \left\{ \frac{\epsilon_3}{\epsilon_2^{3}} \left| U_{\underset{\sim}{h}} \right| \sum_{\underset{\sim}{h}'} U_{\underset{\sim}{h}'} U_{\underset{\sim}{h}+\underset{\sim}{h}'} \right\} . \tag{11}$$

The expectation value for $U_{\underset{\sim}{h}}^{2}$ which is given in equation 4 is dependent on the number of atoms in the structure. This is easily demonstrated by considering a structure composed of atoms of equal scattering power. In such a structure, $\epsilon_2 = 1/N$ (12). Because of this, it is convenient to use the normalized unitary structure factor which is independent of N. Equation 10, in terms of $E_{\underset{\sim}{h}}$'s, is

$$s(\underset{\sim}{h}) \approx s \sum_{\underset{\sim}{h}'} (E_{\underset{\sim}{h}'} E_{\underset{\sim}{h}+\underset{\sim}{h}'}) \tag{12}$$

which is the $\Sigma_2$ relationship described by Hauptman and Karle (9). The corresponding probability in terms of $E_{\underset{\sim}{h}}$'s is

$$P_+(\underset{\sim}{h}) = \tfrac{1}{2} + \tfrac{1}{2} \tanh \left\{ \frac{\epsilon_3}{\epsilon_2^{3/2}} \left| E_{\underset{\sim}{h}} \right| \sum_{\underset{\sim}{h}'} E_{\underset{\sim}{h}'} E_{\underset{\sim}{h}+\underset{\sim}{h}'} \right\} . \tag{13}$$

All of these relationships are strictly true only for structures of atoms of equal scattering power, but most organic structures do not deviate sufficiently from this ideal to cause serious errors. If infinite data were available for such a structure, equation 13 would yield a probability, $P_+(\underset{\sim}{h})$, of one for every reflection. The phase problem would then have an exact solution. In practice, however, infinite data cannot be measured, and equation 12 can be made to yield useful information only for sufficiently large values for $|\underset{\sim}{E_h}|\Sigma_{\underset{\sim}{h}'}\underset{\sim}{E_h}\underset{\sim}{E_{h+h'}}$. As a consequence, knowledge of the signs of structure factors is usually restricted to reflections for which $|\underset{\sim}{E_h}|$ and the corresponding $|\underset{\sim}{F_h}|$ are large. Fortunately, a knowledge of the signs for the larger $|\underset{\sim}{F_h}|$'s is often sufficient to compute a recognizable electron density map.

In the most general centrosymmetric space group, $P\bar{1}$, there are eight independent centers of symmetry, any one of which may be chosen as the origin of the unit cell. The way in which the sign of any given structure factor varies with the choice of origin depends upon the parity of the indices h, k, and $\ell$. For example, the sign of F is invariant if h, k, and $\ell$ are all even. For any of the other seven parity combinations, four of the origins will produce a plus sign; and the other four, a minus sign. This multiplicity of origins enables the signs of three* reflections to be chosen arbitrarily if each is a member of a different linearly independent parity combination, excluding the combination in which each index is even (9, 32). Three signs

* The number of arbitrarily chosen signs is reduced to two in tetragonal and one in hexagonal, trigonal, and cubic crystals (9).

can therefore be chosen at the outset of any structure determination.

The application of equation 12 is straightforward when the signs of every term on the right side are known. However, when only a few signs are known, as is the case at the outset of every large structure determination, equation 12 is not nearly as useful as is equation 8. If the three signs which define the origin are judiciously chosen, a number of additional signs are easily obtained by a systematic application of equation 8. Whenever signs are known for two of the three reflections, the third one is given the sign of the product of the other two, provided that the probability given by equation 9 is sufficiently large. These new signs may then be used to determine additional signs. The process may be repeated a few times, but the probabilities that correct signs are being determined rapidly diminish. Even if this process were carried as far as possible, a great many reflections would remain undetermined. To surmount this difficulty, Zachariasen (33) has suggested the use of symbolic signs. Accordingly, reflections which participate in a large number of sign relationships are given letters which represent their undetermined signs. These symbolic signs, along with those which are already known, are then used to obtain additional signs. Usually, the use of only a few symbolic signs will facilitate the determination of the signs for all the larger E's .

At this point equation 12 is used in an iterative procedure to produce the most consistent set of signs. In this process, several symbolic signs develop a dependence upon one another, and in fortunate cases, each symbolic sign will eventually be uniquely deter-

mined. In less favorable cases, the remaining unknown symbolic signs are given values which produce the fewest discrepancies in the equations of type 12. The resulting sets of signs are then used with the appropriate F's to calculate electron density maps. If a recognizable map is obtained, the corresponding set of signs may be used to obtain additional signs by setting up more equations of type 12 which involve smaller E's , or the refinement may be started from the original map.

A Trial Structure for DHB.

Normalized unitary structure factors were calculated for all reflections by the author's "Statistical Phasing Program" (reference 5, chapter 13). The distribution of experimental E's is compared with theoretical two-tail probabilities for a standard normal distribution in Table I. The agreement with the theoretical distribution is

TABLE I

Distribution of E's

| K | P(\|E\|>K) | Theoretical P (22) |
|---|---|---|
| 1.04 | 0.297 | 0.30 |
| 1.15 | 0.248 | 0.25 |
| 1.29 | 0.203 | 0.20 |
| 1.44 | 0.147 | 0.15 |
| 1.64 | 0.102 | 0.10 |
| 1.70 | 0.090 | 0.09 |
| 1.75 | 0.080 | 0.08 |
| 1.81 | 0.071 | 0.07 |
| 1.88 | 0.062 | 0.06 |
| 1.96 | 0.053 | 0.05 |
| 2.05 | 0.043 | 0.04 |

| K | P(\|E\|>K) | Theoretical P (22) |
|---|---|---|
| 2.17 | 0.034 | 0.03 |
| 2.33 | 0.022 | 0.02 |
| 2.58 | 0.011 | 0.01 |
| 2.81 | 0.007 | 0.005 |
| 3.09 | 0.003 | 0.002 |
| 3.29 | 0.002 | 0.001 |

remarkable. Average values for $|E|$, $|E^2-1|$, and $E^2-1$ are compared with the theoretical values for acentric and centric crystals in Table II. For $<|E|>$ and $<|E^2-1|>$, the experimental values fall between the theoretical values for centric and acentric crystals, which is not unexpected in view of the Howells, Phillips, and Rogers plot (see page 6). For the purpose of these distribution criteria, those reflections which could not be seen above the background (hereafter called "less-thans") were treated as if their $|F_{obs.}|$'s were half the minimum observable value. "Less-thans" were not considered in the following sign determining procedure.

For DHB, a total of 6,017 reflections were recorded, of which 3,596 had observed intensities which were greater than the background. Because of this large number of reflections, a straightforward application of the method described in the preceding section would be unduly laborious. The size of the problem was therefore reduced by considering in the following treatment only those reflections for which $(\sin^2\theta)/\lambda^2 < 0.2$. A consequence of this restriction is the loss of resolution in the electron density map. This, however, presented no problem because the first objective in this procedure was the location of the phenyl groups which are large enough to be seen at very low resolution.

TABLE II

Distribution Criteria

| | Experimental Value | Theoretical Values (18) Centric | Acentric |
|---|---|---|---|
| $\langle \lvert E \rvert \rangle$ | 0.858 | 0.798 | 0.886 |
| $\langle \lvert E^2-1 \rvert \rangle$ | 0.941 | 0.968 | 0.736 |
| $\langle E^2-1 \rangle$ | 0.053 | 0.000 | 0.000 |

In the following discussion, the term "sign relationship" will be used for single relationships of type 8, whereas "$\Sigma_2$ relationship" will mean an equation of type 12. (It should be noted that a sign relationship is a special case of a $\Sigma_2$ relationship.) $\Sigma_2$ relationships were found and listed by the "Statistical Phasing Program" for the 137 reflections for which $|E| \geq 1.96$. The program also calculated the probability connected with each sign relationship. Signs were arbitrarily given to three reflections to define the origin. In addition, six symbolic signs were needed to completely solve the sign relationships. These nine standards, upon which the other 128 signs depend, are presented in Table III along with values for $|E|$ and the number of terms on the right hand side of the corresponding $\Sigma_2$ relationship.

TABLE III

| h | k | $\ell$ | Sign | $\lvert E \rvert$ | n |
|---|---|---|---|---|---|
| 2 | 1 | 1 | + | 3.20 | 18 |
| 3 | -9 | 0 | + | 2.58 | 10 |
| 0 | 3 | 4 | + | 2.19 | 12 |
| 0 | 3 | 1 | a | 2.37 | 14 |
| 2 | 0 | 0 | b | 2.08 | 14 |
| -4 | 6 | 2 | c | 2.77 | 10 |
| 2 | 1 | 3 | d | 2.45 | 10 |
| -7 | 6 | 8 | e | 3.90 | 8 |
| 2 | 1 | -5 | f | 3.06 | 9 |

The following relationships involving the symbolic signs developed in the course of the sign determination.

$$ab = d \qquad b = e \qquad a = c$$

There remained three variables and consequently eight possible sets of signs. The sign set in which all signs are positive was neglected because space group $P\bar{1}$ with two molecules per unit cell will not permit an atom at the origin* unless the molecule has a center at an atom. The remaining seven sign sets are given in Tavle IV. At the bottom of each column is listed for each sign set the number of sign relationships which fail. This number is a criterion of the validity of the particular sign set. It is seen that sign sets III and IV are

TABLE IV

Sign Sets

| Symbolic Sign | I | II | III | IV | V | VI | VII |
|---|---|---|---|---|---|---|---|
| a | + | + | - | - | + | - | - |
| b | - | - | - | - | + | + | + |
| c | + | + | - | - | + | - | - |
| d | - | - | + | + | + | - | - |
| e | - | - | - | - | + | + | + |
| f | + | - | + | - | - | + | - |
| Discrepancies | 26 | 25 | 16 | 15 | 19 | 23 | 20 |

more consistent with the sign relationships than are the others. Sets III and IV were used along with the observed F's to compute two three-dimensional electron density maps. The map based on sign set

* This argument is generally valid, but in a recent example, all of the stronger reflections had positive signs even in the absence of an atom at the origin (20).

IV had peaks at three of the centers of symmetry. Sign set III produced no peaks at the centers. Moreover, there were three or four disk shaped volumes of electron density which resembled phenyl rings in orientations consistent with both proposed structures and the least squares molecular plane.

The more reliable of the original 137 signs based on set III were used as standards to obtain the signs for the 101 reflections for which $1.96 > |E| \geq 1.64$ by repeating the procedure described above. The resulting set of 238 signs which are listed in Table V were then used with the corresponding F's to compute a third electron density map. This map indicated the positions of all six phenyl rings as well as the dihydropentalene skeleton. The indicated structure is III. According to the i. u. c. rules, this is 2, 2-difluoro-1, 3, 4, 6, 7, 8-hexaphenylbicyclo[3. 3. 0]octa-3, 5, 7-triene, which in this work has been abbreviated DHB. Atomic coordinates could not be obtained directly from the electron density map because of its low resolution. An E-map (17), which is a sharpened electron density map, was then calculated from the 238 signs and the corresponding E's . So many sharp peaks were present in the E-map that no sensible interpretation could be made without the aid of the electron density map. Those peaks in the E-map which concurred with the very broad peaks in the electron density map were recorded as atomic positions. Structure factors were calculated from these atomic coordinates and the overall isotropic temperature factor, 4. 5, which had been obtained from the Wilson plot. For the 2, 296 reflections with $\sin^2\theta/\lambda^2 < 0.2$ , the R-value $(R = \Sigma\big||F_o|-|F_c|\big|/\Sigma|F_o|)$ was about .65.

# TABLE V.

## Signs determined from sign relationships

| | h | k | l | Fx10² | Ex10² | | h | k | l | Fx10² | Ex10² | | h | k | l | Fx10² | Ex10² | | h | k | l | Fx10² | Ex10² |
|---|---|---|---|---|---|---|---|---|---|---|---|---|---|---|---|---|---|---|---|---|---|---|---|
| | -10 | 3 | 5 | 339 | 217 | | -2 | 7 | 3 | -862 | -270 | | 2 | -7 | 3 | -450 | -259 | | 5 | -1 | 8 | 317 | 208 |
| | -10 | 6 | 2 | 308 | 174 | | -2 | 8 | 1 | -481 | -202 | | 2 | -5 | 0 | 837 | 173 | | 5 | 0 | 8 | -310 | -195 |
| | -10 | 7 | 1 | 454 | 289 | | -2 | 9 | 2 | 510 | 267 | | 2 | -5 | 4 | 526 | 210 | | 5 | 1 | -5 | 428 | 167 |
| | -10 | 7 | 4 | 362 | 235 | | -2 | 10 | 5 | -322 | -217 | | 2 | -5 | 6 | 361 | 227 | § | 5 | 1 | 2 | 860 | 179 |
| | -10 | 8 | 4 | -296 | -213 | | -1 | 1 | 3 | -1302 | -168 | § | 2 | -4 | 4 | 650 | 209 | | 5 | 2 | -7 | 346 | 242 |
| | -9 | 2 | 6 | 258 | 168 | | -1 | 2 | 5 | -896 | -181 | | 2 | -4 | 7 | -452 | -293 | | 5 | 2 | 2 | 1016 | 236 |
| | -9 | 4 | 7 | 367 | 258 | § | -1 | 2 | 9 | 321 | 184 | | 2 | -2 | 0 | -1855 | -208 | | 5 | 2 | 7 | 415 | 205 |
| | -9 | 5 | 7 | -367 | -256 | | -1 | 6 | 2 | 889 | 221 | | 2 | -2 | 5 | -691 | -198 | | 5 | 3 | 2 | -638 | -174 |
| | -9 | 6 | 1 | -375 | -180 | § | -1 | 6 | 7 | -452 | -189 | | 2 | -1 | 2 | -1408 | -178 | | 5 | 3 | 7 | -430 | -223 |
| | -9 | 7 | 2 | 317 | 170 | | -1 | 9 | 6 | 432 | 266 | § | 2 | 0 | -5 | 702 | 168 | § | 5 | 4 | -5 | 292 | 196 |
| | -9 | 7 | 5 | 300 | 184 | | -1 | 10 | 2 | 364 | 254 | | 2 | 0 | 0 | -2011 | -208 | | 6 | -8 | 3 | 351 | 252 |
| | -9 | 7 | 6 | 304 | 202 | | -1 | 10 | 3 | 361 | 245 | | 2 | 0 | 9 | 278 | 181 | | 6 | -7 | 1 | 435 | 195 |
| § | -9 | 8 | 2 | -334 | -207 | | 0 | 0 | 0 | 11500 | | | 2 | 1 | -5 | 1118 | 306 | | 6 | -7 | 3 | -290 | -173 |
| | -9 | 8 | 3 | 327 | 203 | | 0 | 0 | 7 | -509 | -191 | | 2 | 1 | -4 | -791 | -169 | | 6 | -6 | 1 | -542 | -198 |
| § | -9 | 8 | 4 | -567 | -357 | | 0 | 1 | -5 | -753 | -185 | § | 2 | 1 | -2 | -1368 | -193 | | 6 | -3 | 7 | 248 | 169 |
| | -8 | 3 | 7 | -281 | -178 | | 0 | 1 | -2 | 2002 | 239 | | 2 | 1 | 1 | 2829 | 320 | | 6 | -1 | 8 | 319 | 230 |
| | -8 | 5 | 8 | -325 | -234 | | 0 | 1 | 3 | -1865 | -237 | | 2 | 1 | 3 | 1677 | 245 | § | 6 | 0 | -1 | 851 | 194 |
| § | -8 | 6 | 7 | 272 | 173 | | 0 | 2 | 3 | -1442 | -193 | | 2 | 2 | -2 | -1333 | -225 | | 6 | 2 | -5 | 364 | 197 |
| § | -8 | 7 | 2 | -373 | -173 | | 0 | 3 | 1 | -1744 | -222 | | 2 | 2 | 4 | -1116 | -206 | | 6 | 2 | 4 | 562 | 193 |
| | -8 | 7 | 7 | 335 | 223 | | 0 | 3 | 2 | 1493 | 200 | § | 2 | 4 | -6 | 366 | 222 | § | 6 | 3 | 2 | -508 | -169 |
| | -8 | 8 | 2 | 319 | 175 | | 0 | 3 | 4 | 1252 | 219 | § | 2 | 4 | -5 | 406 | 196 | § | 7 | -4 | 6 | 306 | 209 |
| | -8 | 9 | 2 | -324 | -209 | § | 0 | 4 | -1 | -527 | -176 | | 2 | 4 | 7 | 558 | 222 | § | 7 | -2 | 6 | 349 | 199 |
| § | -8 | 9 | 3 | 281 | 180 | | 0 | 4 | 5 | -760 | -177 | § | 2 | 5 | -3 | -426 | -173 | § | 7 | -1 | 7 | -451 | -293 |
| | -7 | 1 | 6 | 350 | 179 | § | 0 | 4 | 8 | 411 | 183 | | 2 | 8 | 3 | 349 | 185 | | 7 | 0 | 7 | -404 | -254 |
| § | -7 | 1 | 7 | 395 | 249 | | 0 | 5 | -6 | -436 | -282 | | 2 | 9 | 5 | -289 | -203 | | 7 | 1 | 5 | -408 | -182 |
| § | -7 | 3 | 8 | -381 | -251 | | 0 | 5 | 2 | -823 | -168 | | 3 | -9 | 0 | 441 | 258 | | 7 | 1 | 7 | 420 | 264 |
| | -7 | 4 | 8 | -337 | -216 | | 0 | 5 | 6 | -682 | -217 | | 3 | -9 | 1 | 280 | 177 | | 7 | 2 | -4 | 487 | 261 |
| § | -7 | 5 | 7 | 411 | 222 | | 0 | 6 | -3 | 428 | 190 | | 3 | -6 | 5 | 321 | 200 | § | 7 | 2 | 3 | 578 | 218 |
| | -7 | 5 | 8 | 363 | 232 | | 0 | 6 | 8 | 391 | 205 | | 3 | -5 | 0 | -955 | -202 | § | 7 | 3 | 6 | -380 | -226 |
| | -7 | 6 | 8 | -593 | -390 | | 0 | 8 | -2 | -301 | -192 | | 3 | -5 | 6 | -292 | -185 | | 7 | 4 | 0 | -326 | -164 |
| | -7 | 9 | 2 | 298 | 179 | | 0 | 8 | 4 | -517 | -233 | | 3 | -3 | 8 | 306 | 221 | | 8 | -8 | 1 | 265 | 172 |
| § | -7 | 9 | 4 | -275 | -167 | | 0 | 9 | 0 | -281 | -182 | § | 3 | -2 | 8 | 287 | 182 | | 8 | -7 | 2 | 358 | 221 |
| § | -7 | 9 | 5 | -326 | -208 | | 0 | 9 | 2 | -489 | -284 | | 3 | -1 | 4 | -970 | -205 | | 8 | -1 | 6 | -272 | -170 |
| | -6 | 1 | 1 | 954 | 201 | | 0 | 9 | 3 | 430 | 245 | | 3 | 0 | -8 | -326 | -184 | | 8 | 0 | -6 | 432 | 286 |
| | -6 | 1 | 7 | 320 | 175 | | 0 | 9 | 7 | 395 | 278 | | 3 | 0 | -6 | 597 | 200 | | 8 | 0 | -5 | -304 | -173 |
| | -6 | 1 | 8 | -406 | -272 | | 1 | -9 | 1 | -450 | -305 | | 3 | 1 | -8 | 284 | 181 | | 8 | 1 | -5 | -305 | -194 |
| | -6 | 2 | 3 | 733 | 177 | | 1 | -8 | 0 | -433 | -205 | | 3 | 1 | -6 | -511 | -196 | | 8 | 1 | 0 | -484 | -185 |
| § | -6 | 2 | 8 | -272 | -171 | | 1 | -8 | 1 | -385 | -203 | | 3 | 1 | -3 | -1093 | -211 | | 8 | 1 | 6 | -266 | -167 |
| | -6 | 6 | 8 | -296 | -180 | | 1 | -7 | 4 | 373 | 240 | § | 3 | 3 | -6 | 326 | 177 | § | 8 | 2 | -1 | -478 | -221 |
| § | -6 | 9 | 3 | -304 | -168 | | 1 | -6 | 5 | -609 | -386 | | 3 | 3 | 5 | 642 | 175 | | 8 | 2 | 0 | 406 | 178 |
| | -6 | 10 | 3 | -318 | -214 | | 1 | -5 | 4 | -529 | -214 | | 3 | 3 | 6 | 527 | 174 | | 8 | 3 | -2 | 331 | 198 |
| | -5 | 1 | 6 | 482 | 183 | | 1 | -4 | 4 | 534 | 172 | | 3 | 8 | 6 | 268 | 183 | | 9 | -7 | 0 | -359 | -207 |
| § | -5 | 1 | 7 | -506 | -243 | | 1 | -4 | 7 | 446 | 291 | | 4 | -7 | 3 | 377 | 203 | § | 9 | -5 | 0 | -435 | -195 |
| | -5 | 1 | 8 | -371 | -226 | | 1 | -3 | 6 | 428 | 184 | | 4 | -6 | 5 | 363 | 231 | § | 9 | -3 | 3 | 344 | 174 |
| | -5 | 2 | 8 | 309 | 174 | | 1 | -2 | 3 | -1163 | -201 | | 4 | -4 | 1 | 829 | 170 | | 9 | 0 | -5 | 378 | 253 |
| § | -5 | 5 | 6 | 462 | 167 | | 1 | 2 | 6 | -631 | -170 | § | 4 | -4 | 2 | -816 | -193 | | 9 | 2 | 1 | 371 | 200 |
| | -5 | 6 | 3 | 591 | 169 | | 1 | 3 | 1 | 1578 | 221 | | 4 | -4 | 7 | 467 | 318 | | 9 | 2 | 5 | 350 | 238 |
| | -5 | 7 | 3 | -491 | -168 | | 1 | 5 | -6 | 256 | 174 | | 4 | -3 | 2 | -1271 | -254 | | 9 | 3 | -1 | 378 | 250 |
| § | -4 | 1 | 2 | 1384 | 214 | § | 1 | 5 | 2 | -835 | -186 | § | 4 | -3 | 5 | 471 | 174 | § | 9 | 4 | 1 | -352 | -253 |
| | -4 | 1 | 5 | -1009 | -270 | | 1 | 6 | -5 | 376 | 259 | § | 4 | -2 | 8 | -406 | -270 | | 10 | -7 | 1 | 330 | 233 |
| | -4 | 6 | 2 | -1077 | -277 | | 1 | 6 | -3 | -392 | -187 | | 4 | -1 | 7 | -508 | -243 | § | 10 | -6 | 1 | -264 | -168 |
| § | -4 | 6 | 7 | -545 | -238 | | 1 | 6 | 2 | -695 | -199 | | 4 | -1 | 8 | -419 | -259 | | 10 | -3 | 3 | -350 | -213 |
| | -3 | 5 | 3 | 961 | 199 | | 1 | 7 | -4 | -289 | -208 | | 4 | 0 | -8 | -339 | -208 | | 10 | -2 | 3 | -291 | -172 |
| | -3 | 6 | 1 | 946 | 238 | | 1 | 7 | 6 | -355 | -166 | | 4 | 0 | 6 | -618 | -217 | | 10 | 1 | -1 | -400 | -250 |
| § | -3 | 6 | 7 | 580 | 243 | | 1 | 8 | -1 | 273 | 165 | | 4 | 1 | -8 | 370 | 252 | | 10 | 1 | 1 | 307 | 184 |
| | -3 | 8 | 4 | -525 | -214 | | 1 | 8 | 4 | -351 | -172 | | 4 | 3 | 1 | -893 | -196 | | 10 | 1 | 2 | -452 | -279 |
| | -3 | 10 | 3 | -364 | -232 | | 1 | 8 | 8 | -306 | -219 | | 4 | 3 | 5 | -719 | -225 | | 10 | 2 | 0 | -342 | -229 |
| | -2 | 1 | 2 | -1470 | -170 | | 1 | 9 | 1 | -289 | -188 | | 5 | -7 | 3 | -314 | -175 | | 10 | 2 | 1 | -535 | -353 |
| | -2 | 1 | 6 | -617 | -175 | | 2 | -8 | 0 | 352 | 165 | | 5 | -7 | 4 | 268 | 176 | § | 11 | -4 | 1 | -311 | -198 |
| | -2 | 4 | 1 | -1248 | -193 | | 2 | -8 | 2 | 290 | 169 | § | 5 | -2 | 6 | -631 | -284 | | | | | | |

§ These reflections as listed have incorrectly determined signs. See Table X for complete list of data.

## REFINEMENT

The signs (which had been obtained from the structure factor calculation) of the 2, 296 reflections with $\sin^2\theta/\lambda^2 < 0.2$ were used with the observed F's to calculate another three-dimensional electron density map. This map was a tremendous improvement over the previous maps which had been calculated from only 238 reflections. An improved set of atomic coordinates was obtained from this new electron density map. This reduced the R-value to about .55 . The refinement was continued by the method of least squares (11) on the IBM 7094 computer with the "Triclinic Least Squares Program" (reference 5, chapter 6) which was written by Dr. R. E. Marsh. The atomic scattering factors for hydrogen, fluorine, and carbon (valence) were taken from the "International Tables for X-ray Crystallography" (15). The function which was minimized is

$$\Sigma\left(\sqrt{w}\,|F_o|^2 - \frac{\sqrt{w}}{k^2}\,|F_c|^2\right)^2$$

where $\sqrt{w}$ is the weight of each reflection and k is the scaling factor by which $|F_o|$ must be multiplied to be on an absolute scale. "Less-thans" were included only if $|F_c|$ was larger than the minimum observable $F_o$ . The course of the least squares refinement is summarized in Table VI.

The initial stage of the refinement consisted of 15 least squares cycles which were restricted to the 609 reflections for which $\sin^2\theta/\lambda^2 < 0.08$ in order to minimize the effect of incorrect signs. The spatial parameters for the heavy atoms were put in a full matrix.

TABLE VI

Summary of Least Squares Refinement

Initial R = .55

| L. S. Cycle | $\sqrt{w}$ * | R | $\left(\frac{\sin^2\theta}{\lambda^2}\right)_{max}$ * | Remarks |
|---|---|---|---|---|
| 1 | $1/F_o$ | .443 | 0.08 | Full matrix. Isotropic temperature factors not refined. |
| 2 | | .377 | | |
| 3 | | .345 | | |
| 4 | | .299 | | |
| Atoms C(2) and F(46) Interchanged | | | | |
| 5 | | .278 | | |
| 6 | | .266 | | |
| 7 | | .258 | | |
| 8 | | .250 | | |
| Atom C(1) Moved Closer to C(5) | | | | |
| 9 | | .244 | | |
| 10 | | .384 § | | |
| Difference Fourier Computed; 7 Atoms Moved | | | | |
| 11 | | .197 | | |
| 12 | | .155 | | |
| 13 | | .112 | | |
| 14 | | .108 | | |
| 15 | | .202 § | | |
| 16 | $1/\sigma(I)$ ** | .165 | 0.20 | All spatial parameters in one matrix. Isotropic temperature factors in second matrix. |
| 17 | | .144 | | |
| 18 | | .134 | | |
| 19 | | .151 † | | |
| 20 | | .148 | all data | |
| 21 | | .146 | | |
| 22 | | .120 | | Anisotropic temperature factors - block matrix. Shift factor = 0.5 . |

| L. S. Cycle | $\sqrt{w}$ * | R | $\left(\frac{\sin^2\theta}{\lambda^2}\right)_{max}$ * | Remarks |
|---|---|---|---|---|
| 23 | $1/\sigma(I)$ | .128 | all data | Hydrogens added but not refined. |
| 24 | | .092 | | |
| 25 | | .083 | | |
| 26 | | .078 | | |
| 27 | | .077 | | Shift factor = 0.6. |
| 28 | | .076 | | |
| 29 | | .075 | | Shift factor = 0.7. |
| 30 | | .073 | | |
| 31 | | .072 | | Hydrogen in at new calculated positions but not refined. |
| 32 | | .071 | | Shift factor = 0.8. |
| 33 | | .070 | | Hydrogen spatial parameters refined in special matrix (see text). |
| 34 | | .069 | | |
| 35 | | .068 | | All hydrogen parameters refined. |
| 36 | | .066 | | |
| 37 | | .065 | | |

* Values for these quantities are carried from cycle to cycle unless otherwise noted.

§ These R's are larger than the preceding values because data out to $\sin^2\theta/\lambda^2 = 0.2$ were used in the structure factor calculation.

† This R is larger than the preceding values because all data were used in the structure factor calculation.

** See discussion of weights in the experimental section, page 8.

The overall isotropic temperature factor, 4.5 , was not refined during this stage of the refinement. The weighting function was

$$\sqrt{w} = \frac{1}{|F_o|} \qquad \text{for } |F_o| > 4|F_o|_{min.}$$

$$\sqrt{w} = \frac{1}{\sqrt{|F_o| 4|F_o|_{min.}}} \qquad \text{for } |F_o| \leq 4|F_o|_{min.}$$

After four cycles, interatomic distances and angles were calculated by the "Distances, Angles, and Planes Program" (reference 5, chapter 8), which was written by Mr. J. K. Lo. It was apparent that carbon, C(2) , and fluorine, F(46) , (see figure 2 for the numbering of the atoms) had moved to positions which, from chemical considerations, appeared to be interchanged. The R-value was reduced from .32 to .30 by exchanging the atomic coordinates of these two atoms. After the next four cycles, 5 - 8 , the distance between carbon atoms C(1) and C(5) was 1.62 Å , and the angle C(5) - C(1) - C(2) was 78.7°. Carbon, C(1) , was moved by hand along a line joining C(1) and C(5) until the C(1) - C(5) distance was 1.5 Å. Two more cycles of least squares, 9 - 10 , moved C(1) back to its original position. A difference Fourier was then calculated utilizing reflections out to $\sin^2\theta/\lambda^2 = 0.2$ . At this stage of the refinement, the difference Fourier contained a great many positive and negative peaks. The more prominent peaks are summarized in Table VII. A consideration of interatomic distances and angles, however, indicated that only atoms C(1), C(5), C(9), C(10), C(14), C(27), and C(29) needed to be moved. After moving these atoms, five additional least squares cycles, 11 - 15 , completed the initial stage of refinement. The R-value for data out to $\sin^2\theta/\lambda^2 = 0.08$ was about .11,

TABLE VII

Prominent Peaks in the Difference Fourier

| Atom | Negative Peak | | | Positive Peak | | |
|---|---|---|---|---|---|---|
| | x | y | z | x | y | z |
| C(1) | 0.225 | 0.441 | 0.786 | 0.267 | 0.502 | 0.822 |
| C(2) | 0.325 | 0.552 | 0.717 | 0.375 | 0.546 | 0.718 |
| C(5) | 0.225 | 0.562 | 0.830 | 0.238 | 0.649 | 0.799 |
| C(9) | 0.100 | 0.422 | 0.734 | 0.167 | 0.394 | 0.785 |
| C(10) | 0.150 | 0.301 | 0.792 | 0.188 | 0.261 | 0.761 |
| C(14) | 0.092 | 0.461 | 0.542 | 0.062 | 0.442 | 0.653 |
| C(27) | 0.212 | 0.764 | 0.965 | 0.175 | 0.693 | 0.946 |
| C(29) | 0.288 | 0.960 | 0.945 | 0.225 | 0.878 | 0.909 |
| C(38) | 0.112 | 0.422 | 0.182 | 0.175 | 0.434 | 0.252 |
| C(40) | 0.192 | 0.177 | 0.137 | 0.200 | 0.100 | 0.185 |
| F(45) | 0.388 | 0.462 | 0.660 | 0.500 | 0.552 | 0.776 |
| F(46) | 0.425 | 0.586 | 0.764 | 0.500 | 0.787 | 0.683 |

and there were no bad distances and angles.

The final stage of refinement was begun by expanding the data to $\sin^2\theta/\lambda^2 = 0.20$, including individual isotropic temperature factors, and changing the weights from $1/F_o$ to $1/\sigma(I)$ as described on page 8. All spatial parameters were put in one matrix, and the temperature parameters were put in a second matrix. The inclusion of data out to $\sin^2\theta/\lambda^2 = 0.20$ increased the R to .20, but four cycles, 16 - 19, reduced R to .13. All data were then included, and two further isotropic cycles, 20 - 21, caused convergence at R = .14.

Anisotropic temperature factors of the following form were used.

$$e^{-(\beta_{11}h^2 + \beta_{22}k^2 + \beta_{33}\ell^2 + \beta_{12}hk + \beta_{13}h\ell + \beta_{23}k\ell)}$$

For each atom, a three-by-three matrix of spatial parameters and a six-by-six matrix of anisotropic temperature factors were used. (This is referred to as a block matrix in Table VI.) Two cycles, 22 - 23, caused convergence. Hydrogen atoms were then added (but not refined) at positions 1.1 Å along the ring diagonals out from the corresponding carbons. An overall isotropic temperature factor, B = 5.5 , was used for the hydrogens. After seven cycles, 24 - 30, the hydrogen positions were adjusted, and two more cycles, 31 - 32, were performed.

All spatial parameters for the carbons and hydrogens were then put into a separate 33 x 33 matrix for each phenyl group. The remaining spatial parameters for the carbons of the dihydropentalene skeleton and the two fluorines were put into a 30 x 30 matrix. A six-by-six matrix was used for the anisotropic temperature parameters for each heavy atom. (This arrangement is called the "special matrix" in Table VI.) After two cycles, 33 - 34, with the special matrix, the isotropic temperature factors for the hydrogens were added to the refinement by placing them in one 30 x 30 matrix. Three additional cycles, 35 - 37 , were performed in which only the hydrogen parameters showed appreciable shifts. Further refinement did not appear to be justified. The final R-value was .065 .

In the initial data reduction, 123 reflections were given weights of zero because of large discrepancies in the intensities which were measured on more than one film. Reflection 0 2 4

was given a weight of zero because it was thought to be a double reflection. Extinction errors were seen in 41 low angle reflections which were given weights of zero. Of the 2,421 "less-thans", only 146 were used in the last cycle of least squares refinement because their calculated F's were larger than the minimum observable F. Consequently, only 3,577 of the 6,017 recorded reflections were used in the last cycle of least squares refinement.

A difference Fourier was computed as an independent check on the correctness of the structure. This map had a noise level which averaged about 0.2 or 0.3 electrons/$\mathring{A}^3$, although there were two negative peaks of - 0.43 and - 0.48 electrons/$\mathring{A}^3$. The difference map, therefore, gives no indication of serious errors in the structure.

The final atomic coordinates in terms of fractions of cell edges are listed in Table VIII along with the shifts in the coordinates which were calculated in the last cycle, and the $\sigma$'s which are calculated from the least squares matrix.

$$\sigma_i = \left\{(A^{-1})_{ii}\left[\frac{\Sigma w(k^2F_o^2 - F_c^2)^2}{m - s}\right]\right\}^{\frac{1}{2}} \qquad (14)$$

In equation 14, $\sigma_i$ is the standard deviation of the variable i, $(A^{-1})_{ii}$ is the diagonal element of the inverse matrix corresponding to variable i, m is the number of reflections, and s is the number of variables. The final values for the anisotropic temperature parameters are listed in Table IX along with the corresponding shifts which were calculated in the last cycle, and the $\sigma$'s. The values of F which are calculated from these parameters are compared with the

TABLE VIII.

## Spacial parameters

| Atom | X | Y | Z | σ(X) | σ(Y) | σ(Z) | sh(X) | sh(Y) | sh(Z) |
|---|---|---|---|---|---|---|---|---|---|
| C(1) | 25664 | 49584 | 80786 | 21 | 25 | 21 | 5 | 6 | 4 |
| C(2) | 35231 | 55912 | 71463 | 22 | 27 | 23 | -1 | 2 | 1 |
| C(3) | 32745 | 66844 | 61542 | 21 | 25 | 21 | 1 | 0 | 2 |
| C(4) | 26186 | 70684 | 66852 | 22 | 25 | 22 | 7 | -1 | 8 |
| C(5) | 23121 | 61460 | 79573 | 22 | 25 | 21 | 4 | 0 | -6 |
| C(6) | 21392 | 61884 | 91088 | 22 | 26 | 22 | -6 | 1 | 0 |
| C(7) | 23396 | 50591 | 100647 | 21 | 26 | 22 | -3 | 0 | -5 |
| C(8) | 26590 | 43790 | 95004 | 22 | 26 | 22 | 4 | 10 | -7 |
| C(9) | 16998 | 40282 | 75991 | 23 | 27 | 22 | -4 | -3 | 2 |
| C(10) | 17648 | 28394 | 77291 | 28 | 31 | 26 | -7 | -4 | 0 |
| C(11) | 09825 | 19968 | 72922 | 31 | 32 | 27 | 1 | 8 | 1 |
| C(12) | 01231 | 23367 | 67135 | 32 | 37 | 31 | 1 | -2 | -8 |
| C(13) | 00479 | 35060 | 65698 | 28 | 38 | 30 | 8 | -6 | 10 |
| C(14) | 08264 | 43489 | 70058 | 25 | 31 | 26 | 5 | -15 | -2 |
| C(15) | 37228 | 72011 | 48460 | 24 | 27 | 23 | 0 | -6 | -2 |
| C(16) | 47630 | 73240 | 46194 | 29 | 35 | 30 | -14 | -5 | -11 |
| C(17) | 51478 | 77713 | 33703 | 34 | 41 | 36 | 0 | -6 | 9 |
| C(18) | 45018 | 80511 | 23965 | 41 | 36 | 35 | 4 | -9 | 7 |
| C(19) | 34643 | 78865 | 26110 | 36 | 33 | 28 | 17 | 2 | 9 |
| C(20) | 30714 | 74624 | 38399 | 27 | 30 | 24 | 14 | 5 | -2 |
| C(21) | 22851 | 82127 | 61605 | 24 | 26 | 22 | -13 | -1 | 2 |
| C(22) | 29747 | 93706 | 54062 | 30 | 32 | 26 | -14 | 1 | 5 |
| C(23) | 26472 | 104543 | 49756 | 37 | 34 | 30 | -7 | -1 | 9 |
| C(24) | 16601 | 103903 | 52908 | 39 | 38 | 33 | 4 | 8 | -7 |
| C(25) | 09781 | 92614 | 60303 | 33 | 38 | 32 | 7 | 3 | -6 |
| C(26) | 12848 | 81833 | 64624 | 27 | 32 | 26 | 5 | 4 | -7 |
| C(27) | 19456 | 72403 | 93795 | 23 | 26 | 21 | 0 | -2 | -6 |
| C(28) | 27030 | 84305 | 90482 | 28 | 32 | 27 | 1 | 3 | 3 |
| C(29) | 24969 | 94325 | 92474 | 33 | 34 | 29 | -14 | -21 | 6 |
| C(30) | 15380 | 92554 | 97793 | 36 | 38 | 31 | 6 | 13 | 8 |
| C(31) | 07866 | 80860 | 101068 | 33 | 39 | 30 | 3 | 10 | -7 |
| C(32) | 09818 | 70792 | 99219 | 28 | 32 | 26 | 4 | 2 | 0 |
| C(33) | 23207 | 47776 | 114557 | 23 | 26 | 22 | -2 | 4 | -1 |
| C(34) | 32494 | 48517 | 120974 | 26 | 31 | 25 | -5 | -6 | 12 |
| C(35) | 32600 | 45682 | 133930 | 29 | 32 | 27 | -9 | -3 | -8 |
| C(36) | 23254 | 41988 | 140696 | 28 | 30 | 29 | 9 | 3 | -5 |
| C(37) | 13964 | 41294 | 134420 | 28 | 33 | 26 | 3 | -4 | -6 |
| C(38) | 13950 | 44214 | 121480 | 27 | 33 | 25 | 8 | -3 | 8 |
| C(39) | 29884 | 32414 | 101633 | 25 | 27 | 23 | 5 | -2 | 1 |
| C(40) | 23382 | 21963 | 110871 | 32 | 34 | 28 | 7 | -3 | 4 |
| C(41) | 27111 | 11804 | 117509 | 48 | 39 | 33 | 21 | 13 | -4 |
| C(42) | 37026 | 11938 | 115105 | 52 | 44 | 39 | 13 | 14 | 1 |
| C(43) | 43454 | 22130 | 105968 | 40 | 45 | 38 | 20 | 14 | -6 |
| C(44) | 39845 | 32215 | 99114 | 32 | 36 | 30 | 4 | 9 | -2 |
| F(45) | 37719 | 47837 | 66784 | 13 | 15 | 13 | 2 | 4 | 2 |
| F(46) | 44251 | 60234 | 77574 | 13 | 16 | 13 | -2 | 0 | -4 |
| H(47) | 24090 | 25932 | 81563 | 245 | 280 | 258 | -178 | -31 | -94 |
| H(48) | 10524 | 11682 | 74316 | 244 | 286 | 247 | -28 | 246 | -22 |
| H(49) | -04038 | 16976 | 63886 | 251 | 308 | 267 | 130 | 65 | 14 |
| H(50) | -05959 | 37113 | 61381 | 282 | 314 | 283 | 227 | -26 | 28 |
| H(51) | 07601 | 51693 | 69820 | 256 | 299 | 268 | 116 | -496 | 314 |
| H(52) | 52862 | 71647 | 52901 | 243 | 285 | 261 | -56 | 320 | -414 |
| H(53) | 59622 | 78383 | 32267 | 301 | 349 | 311 | -44 | -252 | 342 |
| H(54) | 46939 | 83536 | 15031 | 285 | 330 | 336 | -419 | -92 | 133 |
| H(55) | 29614 | 80525 | 19091 | 260 | 302 | 287 | 42 | -285 | 482 |
| H(56) | 23324 | 73951 | 39261 | 229 | 269 | 237 | 359 | 172 | -178 |
| H(57) | 37018 | 93944 | 52095 | 254 | 279 | 243 | -268 | -40 | 164 |
| H(58) | 32120 | 112689 | 44737 | 237 | 298 | 255 | 131 | -150 | 164 |
| H(59) | 14334 | 111108 | 50088 | 274 | 326 | 272 | 131 | -280 | 116 |
| H(60) | 02295 | 92614 | 62762 | 258 | 302 | 266 | 56 | 76 | 66 |
| H(61) | 07988 | 73936 | 70358 | 242 | 287 | 259 | 215 | 277 | -97 |
| H(62) | 33911 | 85042 | 86368 | 254 | 294 | 263 | -217 | -225 | 67 |
| H(63) | 30416 | 102885 | 90312 | 251 | 304 | 252 | -207 | -267 | 226 |
| H(64) | 13597 | 99286 | 99092 | 244 | 294 | 254 | 27 | -206 | -138 |
| H(65) | 00665 | 80390 | 105336 | 285 | 331 | 311 | 52 | 460 | 32 |
| H(66) | 04312 | 61628 | 101692 | 245 | 299 | 247 | 232 | 109 | -60 |
| H(67) | 39249 | 51218 | 115761 | 238 | 270 | 251 | -142 | -119 | 56 |
| H(68) | 39728 | 46591 | 138337 | 263 | 302 | 267 | -150 | 84 | -153 |
| H(69) | 22918 | 39869 | 150594 | 254 | 295 | 294 | -134 | 180 | -193 |
| H(70) | 06985 | 37875 | 140364 | 243 | 279 | 250 | -12 | -164 | 34 |
| H(71) | 07236 | 43871 | 116780 | 236 | 276 | 246 | 184 | -41 | 95 |
| H(72) | 16420 | 22589 | 112570 | 274 | 313 | 284 | 397 | 110 | -84 |
| H(73) | 21992 | 04901 | 123819 | 284 | 355 | 318 | -1036 | 900 | -623 |
| H(74) | 40158 | 04978 | 120383 | 269 | 338 | 292 | 165 | 414 | -46 |
| H(75) | 51145 | 21550 | 103848 | 293 | 346 | 304 | -59 | -164 | 29 |
| H(76) | 44780 | 40494 | 92295 | 257 | 356 | 296 | 67 | 232 | 216 |

All values for parameters, σ's , and shifts have been multiplied by $10^5$. sh(x), etc. represent the shift in parameter x , etc. in the final least squares cycle.

TABLE IX

## a. Anisotropic temperature factors for heavy atoms

| Atom | $\beta_{11}$ | $\beta_{22}$ | $\beta_{33}$ | $\beta_{12}$ | $\beta_{13}$ | $\beta_{23}$ | σ(11) | σ(22) | σ(33) | σ(12) | σ(13) | σ(23) | sh(11) | sh(22) | sh(33) | sh(12) | sh(13) | sh(23) |
|---|---|---|---|---|---|---|---|---|---|---|---|---|---|---|---|---|---|---|
| C(1) | 00573 | 00712 | 00543 | 00447 | 00098 | -00366 | 22 | 31 | 25 | 42 | 34 | 39 | 0 | -3 | 5 | -5 | 2 | -2 |
| C(2) | 00547 | 00891 | 00717 | 00489 | -00089 | -00621 | 23 | 34 | 28 | 45 | 36 | 45 | -1 | 0 | 6 | -3 | 10 | -8 |
| C(3) | 00532 | 00735 | 00543 | 00300 | 00028 | -00313 | 22 | 31 | 25 | 41 | 33 | 39 | -4 | 4 | 4 | 2 | 0 | 1 |
| C(4) | 00565 | 00695 | 00623 | 00376 | -00083 | -00348 | 23 | 31 | 26 | 43 | 35 | 41 | 1 | -2 | 1 | -6 | -5 | -5 |
| C(5) | 00571 | 00809 | 00501 | 00497 | -00017 | -00338 | 22 | 32 | 25 | 43 | 33 | 40 | -2 | 1 | 4 | 1 | -2 | -1 |
| C(6) | 00573 | 00829 | 00623 | 00480 | 00018 | -00475 | 23 | 33 | 27 | 44 | 35 | 43 | -6 | 2 | 8 | -5 | -3 | -6 |
| C(7) | 00541 | 00793 | 00567 | 00324 | 00039 | -00421 | 23 | 32 | 26 | 43 | 34 | 41 | -6 | 6 | 6 | 0 | -2 | 3 |
| C(8) | 00640 | 00763 | 00587 | 00470 | -00005 | -00353 | 24 | 32 | 27 | 45 | 36 | 42 | -5 | -4 | 7 | -12 | -3 | -4 |
| C(9) | 00669 | 00807 | 00502 | 00449 | 00136 | -00346 | 24 | 32 | 25 | 44 | 35 | 40 | 0 | 0 | 7 | 4 | 8 | 4 |
| C(10) | 00883 | 00899 | 00774 | 00614 | 00065 | -00622 | 29 | 37 | 30 | 52 | 43 | 48 | -3 | 10 | 1 | 2 | -17 | -16 |
| C(11) | 01130 | 00940 | 00794 | 00497 | 00132 | -00739 | 34 | 38 | 31 | 58 | 48 | 51 | 19 | -5 | 17 | 13 | -5 | -2 |
| C(12) | 00980 | 01223 | 00954 | 00022 | 00076 | -00990 | 33 | 46 | 34 | 62 | 50 | 58 | 3 | -1 | 9 | 21 | -15 | -11 |
| C(13) | 00723 | 01335 | 01157 | 00258 | -00131 | -00851 | 30 | 48 | 36 | 60 | 48 | 61 | -4 | -3 | 12 | -20 | 7 | -14 |
| C(14) | 00619 | 00971 | 00954 | 00403 | -00015 | -00704 | 26 | 38 | 32 | 50 | 42 | 50 | 3 | 11 | 5 | 13 | 1 | -10 |
| C(15) | 00648 | 00827 | 00662 | 00401 | 00156 | -00387 | 24 | 34 | 27 | 46 | 37 | 43 | -2 | -2 | 1 | -11 | 0 | 5 |
| C(16) | 00772 | 01410 | 01087 | 00511 | 00623 | -00325 | 31 | 49 | 36 | 62 | 48 | 60 | -3 | 6 | 8 | 10 | -32 | -2 |
| C(17) | 01005 | 01345 | 01362 | 00780 | 01198 | -00315 | 36 | 64 | 42 | 76 | 60 | 74 | 21 | -3 | -17 | 38 | -8 | 23 |
| C(18) | 01795 | 01301 | 00909 | 00705 | 01042 | -00502 | 50 | 51 | 37 | 80 | 64 | 61 | -2 | -2 | 17 | -9 | 18 | -21 |
| C(19) | 01425 | 01175 | 00566 | 00806 | 00006 | -00431 | 41 | 45 | 32 | 69 | 52 | 53 | 15 | 3 | -1 | 24 | -16 | 5 |
| C(20) | 00906 | 00973 | 00606 | 00684 | -00071 | -00428 | 29 | 38 | 27 | 53 | 42 | 46 | -14 | 9 | 19 | 0 | 5 | 1 |
| C(21) | 00741 | 00825 | 00545 | 00563 | -00130 | -00518 | 25 | 34 | 26 | 47 | 37 | 43 | 4 | 3 | 3 | -2 | 5 | -3 |
| C(22) | 01021 | 01819 | 00817 | 01455 | 00034 | -00382 | 32 | 37 | 31 | 55 | 46 | 48 | -1 | 6 | 7 | 12 | -5 | -7 |
| C(23) | 01365 | 00763 | 01074 | 00588 | -00209 | -00387 | 40 | 39 | 36 | 64 | 56 | 53 | -10 | 6 | 7 | -11 | 22 | 7 |
| C(24) | 01594 | 01185 | 01206 | 01748 | -00851 | -00998 | 45 | 46 | 38 | 75 | 61 | 62 | 13 | 9 | 12 | 29 | -24 | -6 |
| C(25) | 01060 | 01309 | 01207 | 01381 | -00547 | -00952 | 35 | 47 | 37 | 67 | 53 | 61 | -4 | 8 | 5 | 2 | 8 | 8 |
| C(26) | 00805 | 01042 | 00878 | 00904 | -00187 | -00661 | 28 | 39 | 32 | 55 | 43 | 51 | 3 | -9 | 2 | -10 | 18 | 26 |
| C(27) | 00715 | 00796 | 00480 | 00641 | -00136 | -00395 | 25 | 32 | 25 | 46 | 36 | 41 | 0 | 5 | 0 | 3 | 1 | -1 |
| C(28) | 00783 | 00953 | 00898 | 00595 | -00186 | -00593 | 28 | 38 | 31 | 53 | 43 | 49 | 4 | 5 | 8 | 3 | 21 | 3 |
| C(29) | 01216 | 00886 | 01036 | 00642 | -00231 | -00626 | 37 | 40 | 34 | 62 | 53 | 53 | 3 | -4 | 18 | -18 | 16 | -3 |
| C(30) | 01491 | 01204 | 01017 | 01543 | -00124 | -00929 | 42 | 45 | 35 | 73 | 57 | 59 | 16 | 7 | 5 | 27 | 1 | 1 |
| C(31) | 01156 | 01428 | 01141 | 01344 | 00306 | -00927 | 36 | 50 | 37 | 70 | 55 | 64 | 16 | -8 | 7 | -5 | 21 | 7 |
| C(32) | 00855 | 01081 | 00887 | 00816 | 00256 | -00663 | 29 | 41 | 32 | 57 | 45 | 52 | 0 | -11 | 12 | -17 | 6 | -4 |
| C(33) | 00659 | 00759 | 00596 | 00539 | -00035 | -00347 | 24 | 32 | 26 | 45 | 36 | 41 | 5 | -4 | 8 | 0 | 5 | -5 |
| C(34) | 00612 | 01337 | 00727 | 00573 | -00095 | -00697 | 25 | 44 | 29 | 53 | 39 | 52 | -4 | 0 | 4 | -4 | 0 | 0 |
| C(35) | 00811 | 01350 | 00796 | 00798 | -00430 | -00738 | 29 | 46 | 31 | 59 | 44 | 55 | 0 | -8 | 13 | 8 | -9 | 0 |
| C(36) | 00988 | 01167 | 00685 | 00749 | -00123 | -00679 | 32 | 42 | 29 | 60 | 45 | 51 | 0 | -9 | 2 | 11 | -2 | 18 |
| C(37) | 00771 | 01655 | 00677 | 00642 | 00116 | -00707 | 29 | 51 | 31 | 62 | 43 | 57 | 13 | -1 | -14 | -4 | 7 | 15 |
| C(38) | 00644 | 01639 | 00601 | 00605 | 00069 | -00576 | 26 | 49 | 29 | 57 | 39 | 54 | 2 | -1 | 13 | 5 | -10 | -6 |
| C(39) | 00872 | 00867 | 00561 | 00749 | -00237 | -00535 | 28 | 35 | 27 | 50 | 39 | 44 | -1 | 6 | 0 | 8 | -6 | -5 |
| C(40) | 01301 | 00904 | 00818 | 00667 | 00084 | -00275 | 38 | 40 | 32 | 62 | 51 | 51 | -1 | -3 | 15 | 20 | -18 | -26 |
| C(41) | 02188 | 00962 | 00926 | 00925 | -00316 | -00236 | 55 | 46 | 37 | 81 | 66 | 57 | 80 | -17 | -20 | 28 | -51 | 9 |
| C(42) | 02507 | 01399 | 01391 | 02522 | -01608 | -01160 | 64 | 55 | 45 | 101 | 82 | 72 | -34 | 20 | -3 | 1 | 24 | -6 |
| C(43) | 01588 | 01678 | 01468 | 02230 | -01112 | -01367 | 46 | 58 | 43 | 87 | 67 | 75 | 12 | -11 | -3 | -6 | 7 | 10 |
| C(44) | 01102 | 01341 | 01125 | 01510 | -00428 | -00759 | 36 | 49 | 36 | 69 | 53 | 61 | -8 | -25 | 6 | -36 | 5 | 22 |
| F(45) | 00785 | 01050 | 00837 | 00872 | 00232 | -00532 | 15 | 21 | 16 | 28 | 22 | 27 | 3 | -2 | 5 | 1 | 0 | 3 |
| F(46) | 00603 | 01208 | 00854 | 00471 | -00227 | -00429 | 14 | 24 | 17 | 29 | 22 | 28 | 1 | -1 | 2 | 0 | -1 | 1 |

All values listed in part a. are multiplied by $10^5$.

## b. Isotropic temperature factors for hydrogens

| Atom | B | σ(B) | sh(B) |
|---|---|---|---|
| H(47) | 382 | 76 | -40 |
| H(48) | 374 | 75 | -47 |
| H(49) | 402 | 78 | -54 |
| H(50) | 560 | 87 | 14 |
| H(51) | 463 | 80 | -32 |
| H(52) | 367 | 76 | -65 |
| H(53) | 744 | 99 | 54 |
| H(54) | 700 | 96 | 33 |
| H(55) | 514 | 84 | -15 |
| H(56) | 287 | 69 | -52 |
| H(57) | 338 | 74 | -71 |
| H(58) | 365 | 74 | -38 |
| H(59) | 563 | 88 | -01 |
| H(60) | 460 | 79 | -13 |
| H(61) | 375 | 77 | -62 |
| H(62) | 392 | 77 | -60 |
| H(63) | 428 | 79 | -25 |
| H(64) | 333 | 76 | -107 |
| H(65) | 678 | 91 | 62 |
| H(66) | 421 | 81 | -55 |
| H(67) | 339 | 72 | -54 |
| H(68) | 504 | 84 | -02 |
| H(69) | 510 | 85 | -30 |
| H(70) | 392 | 75 | -11 |
| H(71) | 358 | 74 | -24 |
| H(72) | 510 | 84 | -31 |
| H(73) | 706 | 94 | 74 |
| H(74) | 626 | 93 | 24 |
| H(75) | 754 | 100 | 78 |
| H(76) | 522 | 84 | -18 |

All values listed in part b. are multiplied by $10^2$.

sh(11), etc. and sh(B) represent the shifts in the anisotropic temperature factors, $\beta_{11}$, etc., and the isotropic temperature factor, B , in the final least squares cycle.

observed F's in Table X. Each data group in Table X is preceded by the value for h , the value for k , and the letter L , which define the indices for the particular data group. The columns in Table X are L, $10\times F_{obs.}$, and $10\times F_{calc.}$, in that order. A negative sign in the second column indicates a "less-than," and the numerical value which follows the negative sign is the minimum observable F . An asterisk following a value in the second column means that the reflection in question has been given a weight of zero in the least squares refinement. A comparison of Table V and Table X reveals 50 incorrectly determined signs in the original 238 signs.

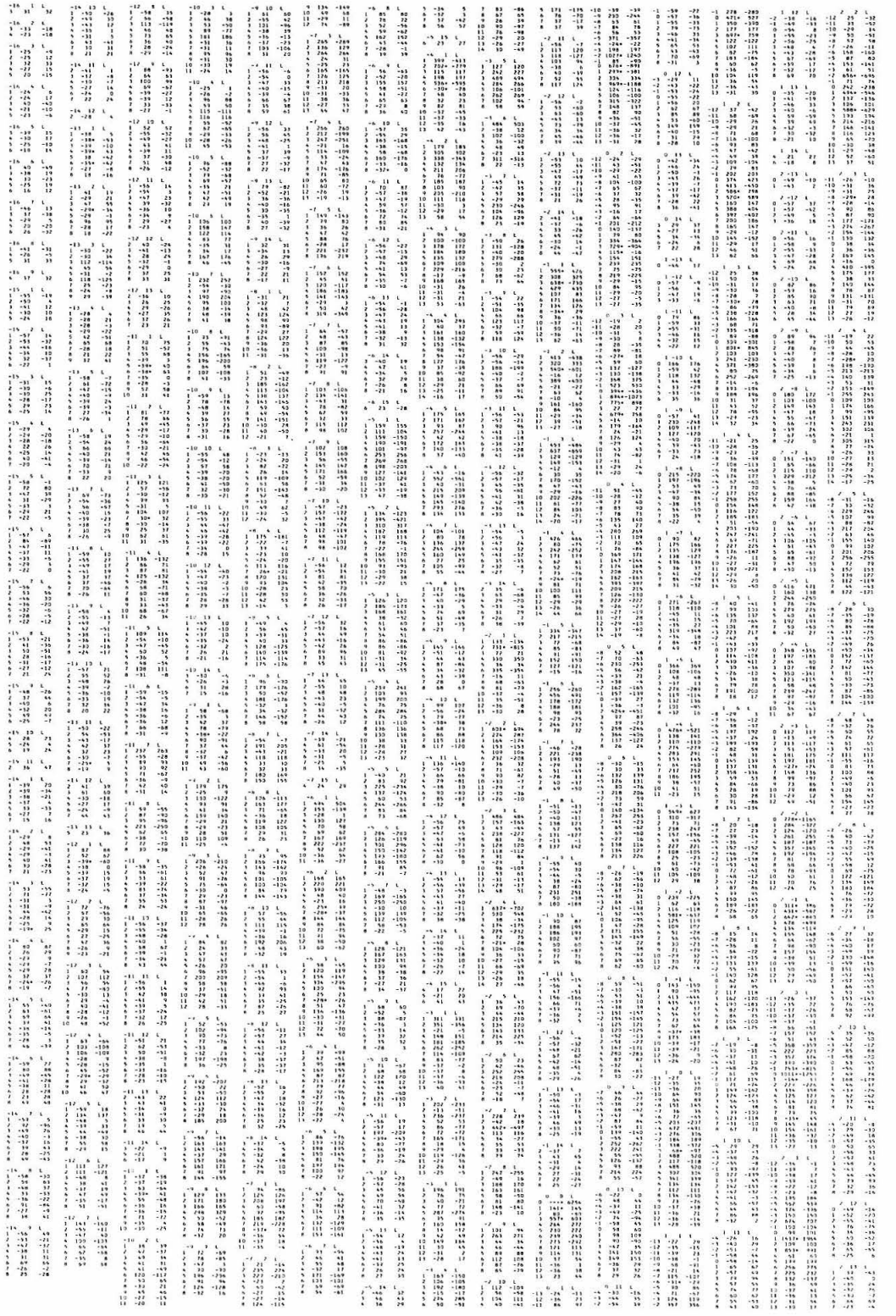

TABLE X. Columns are $\ell$, $10\times F_{obs.}$, and $10\times F_{calc.}$

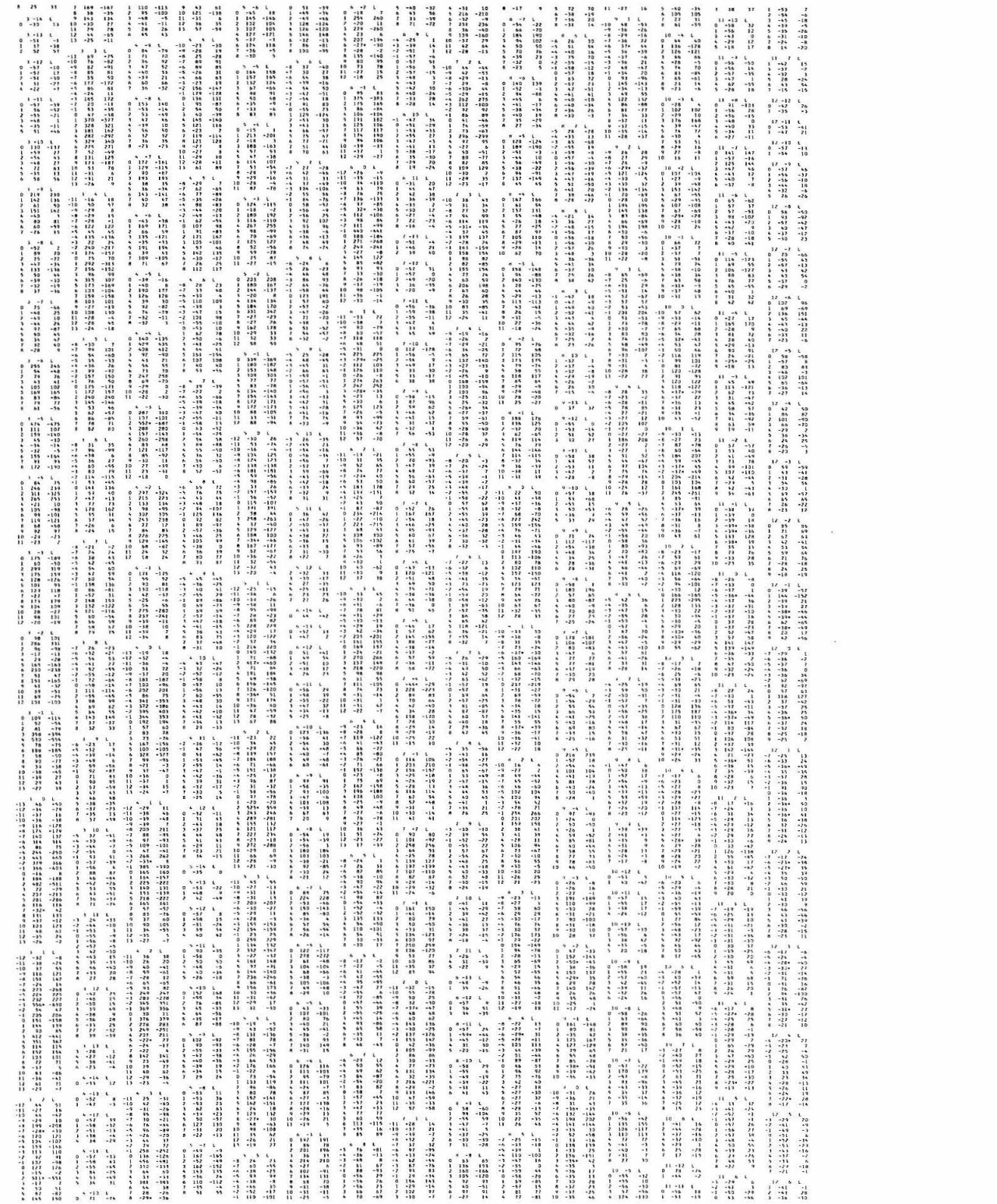

TABLE X (continued)

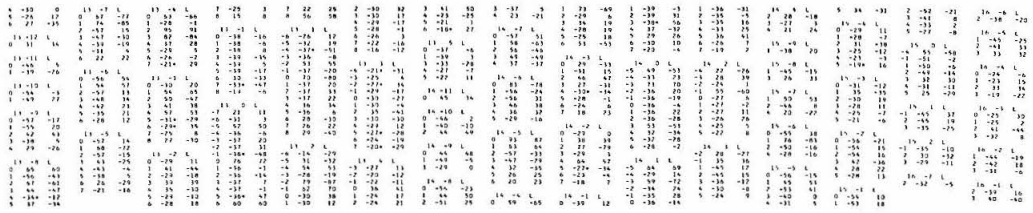

TABLE X (continued)

## DISCUSSION

As indicated in Table VIII, the shifts for the hydrogen parameters in the last cycle of the least squares refinement were of the same order of magnitude as the standard deviations. Since, therefore, the refinement had not reached convergence with respect to the hydrogens, there is no reason to list individual C-H distances and C-C-H angles. The average C-H distance is 1.018 Å with a standard deviation of 0.041 Å calculated from the variation of individual values about the mean. The longest and shortest C-H distances are 1.087 Å and 0.936 Å, respectively. All other bond distances and angles are presented in figures 2 and 3. (Figures 2 and 3 show the molecule as viewed along a direction in the plane defined by axes $\underset{\sim}{a}$ and $\underset{\sim}{b}$ and perpendicular to axis $\underset{\sim}{b}$. The plane of the paper is approximately the plane defined by axes $\underset{\sim}{b}$ and $\underset{\sim}{c}$ with axis $\underset{\sim}{c}$ the horizontal direction increasing from left to right.) The average standard deviation for C-C distances is estimated to be 0.005 Å; for C-F distances, 0.003 Å; for angles in the central dihydropentalene skeleton, $0.2^{\circ}$; for angles in the phenyl rings, $0.4^{\circ}$.

Except for the five-membered ring containing C(2), the ring systems of DHB form well defined planes. The numbering of these planes is presented in figure 5. The direction cosines and deviations (from these planes) of the individual atoms are given in Table XI. Table XII is a list of the angles between the various normals to the planes of the DHB molecule.

There are two reasonably good planes which can be calculated for the ring containing C(2). Plane VII is calculated from C(2), C(3),

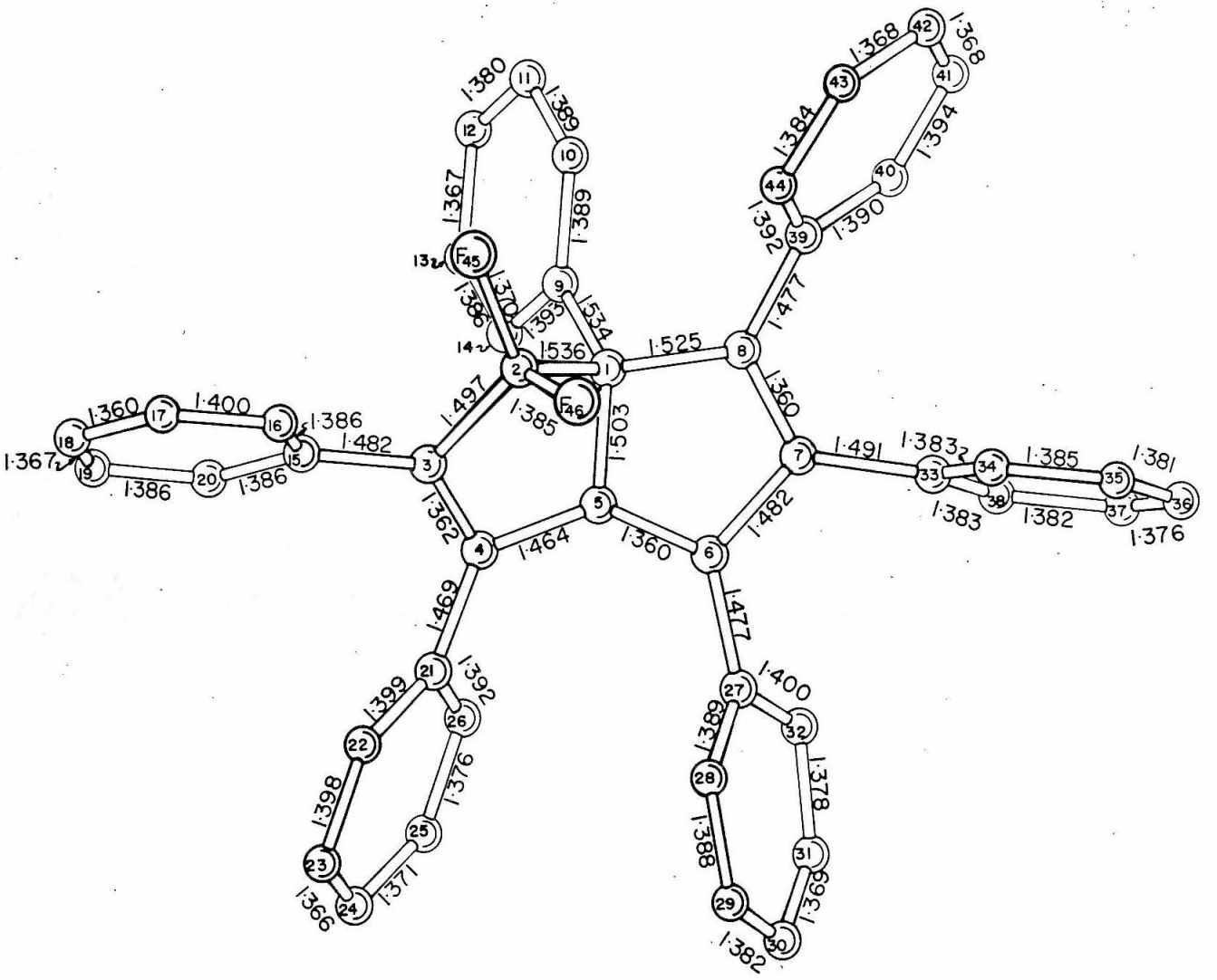


Figure 2. Bond Distances in DHB.

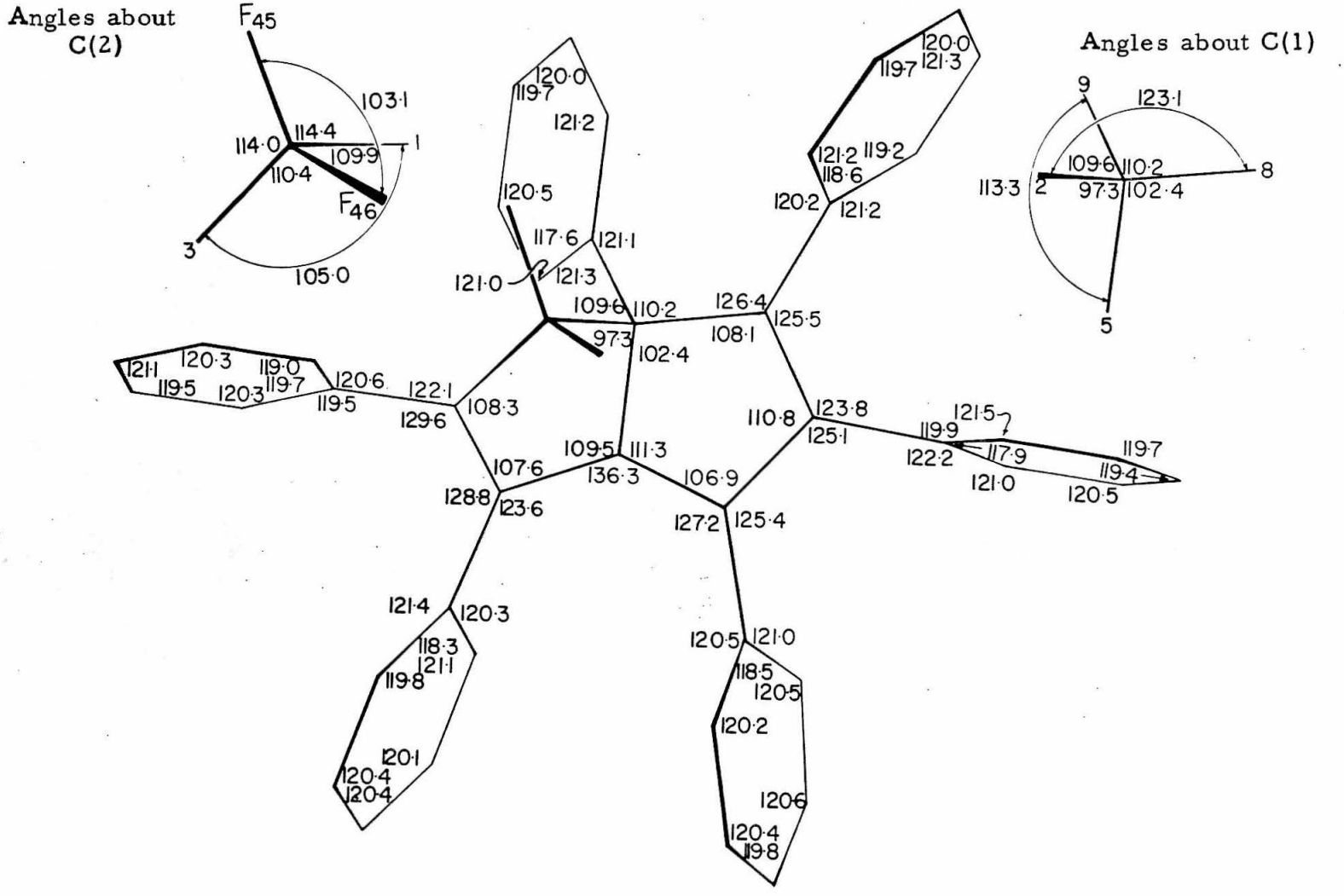


Figure 3. Bond Angles in DHB.

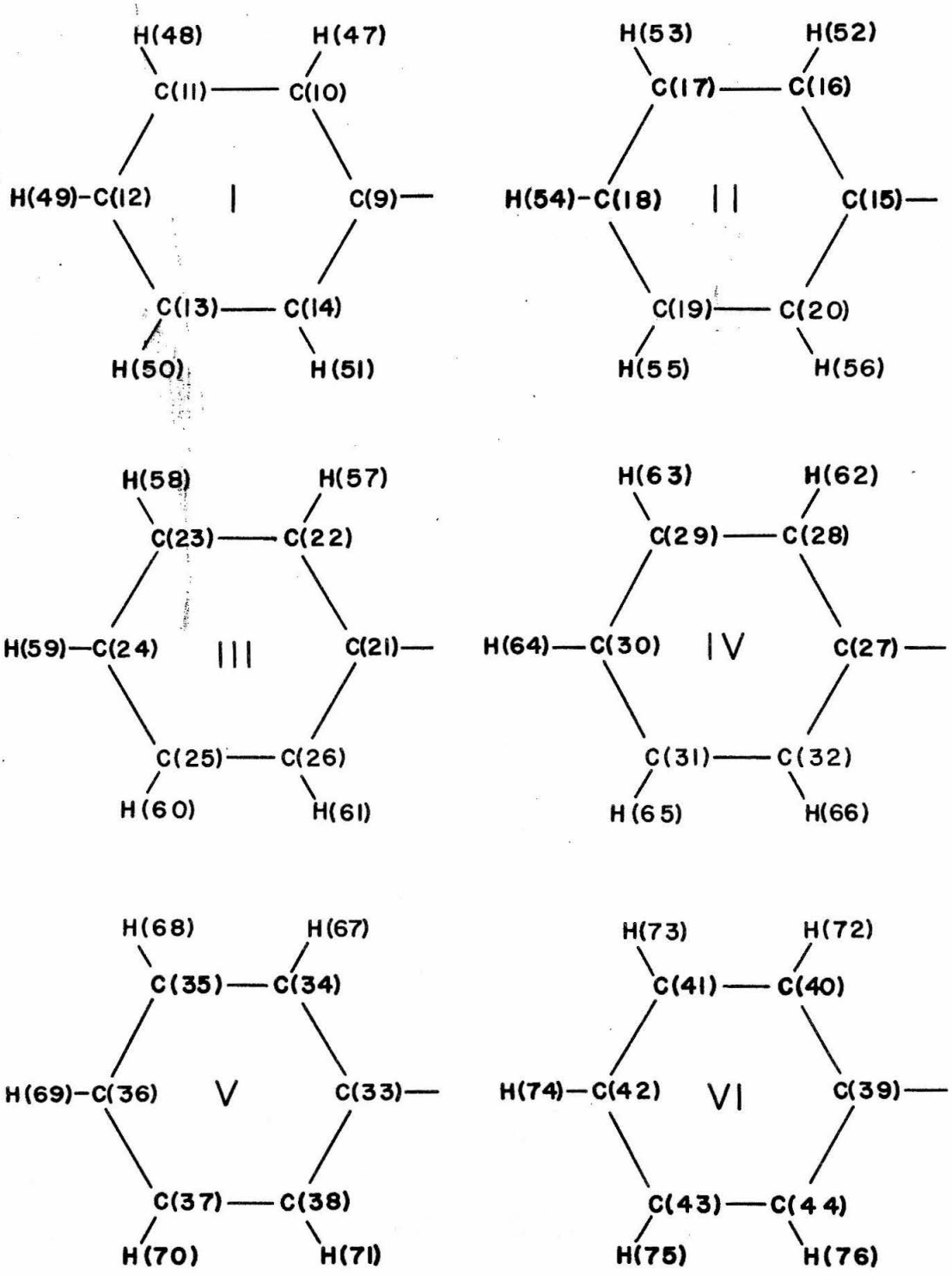


Figure 4. Numbering of Hydrogen Atoms.

TABLE XI.

# Least-squares planes

| Plane | Atom | D | Atom | D | d | cos A | cos B | cos C | Plane | Atom | D | Atom | D | d | cos A | cos B | cos C |
|---|---|---|---|---|---|---|---|---|---|---|---|---|---|---|---|---|---|
| I | C(1)§ | -0034 | C(9) | 0029 | 6441 | -4561 | 0628 | 8358 | V | C(7)§ | 0423 | C(33) | 0050 | -7902 | 1979 | -9847 | -2284 |
| | C(10) | -0021 | C(11) | -0003 | | | | | | C(34) | -0009 | C(35) | -0033 | | | | |
| | C(12) | 0020 | C(13) | -0011 | | | | | | C(36) | 0036 | C(37) | 0005 | | | | |
| | C(14) | -0013 | H(47)§ | -0094 | | | | | | C(38) | -0049 | H(67)§ | -0014 | | | | |
| | H(48)§ | 0272 | H(49)§ | -0311 | | | | | | H(68)§ | -0342 | H(69)§ | -0147 | | | | |
| | H(50)§ | -0012 | H(51)§ | 0775 | | | | | | H(70)§ | 0595 | H(71)§ | -0213 | | | | |
| II | C(3)§ | 0499 | C(15) | -0164 | -9681 | 0624 | -9662 | -3281 | VI | C(8)§ | 1154 | C(39) | 0113 | 13010 | 1772 | 6189 | 8656 |
| | C(16) | 0143 | C(17) | -0002 | | | | | | C(40) | -0017 | C(41) | -0057 | | | | |
| | C(18) | -0118 | C(19) | 0096 | | | | | | C(42) | 0036 | C(43) | 0061 | | | | |
| | C(20) | 0045 | H(52)§ | -0092 | | | | | | C(44) | -0136 | H(72)§ | 0452 | | | | |
| | H(53)§ | 0445 | H(54)§ | -0092 | | | | | | H(73)§ | -0137 | H(74)§ | 0861 | | | | |
| | H(55)§ | 0387 | H(56)§ | -0123 | | | | | | H(75)§ | -0615 | H(76)§ | 0406 | | | | |
| III | C(4)§ | 0713 | C(21) | -0007 | 11326 | 2254 | 4294 | 9296 | VII | C(1)§ | -5366 | C(2) | 0243 | 10478 | 5521 | 5508 | 5281 |
| | C(22) | 0011 | C(23) | -0010 | | | | | | C(3) | -0410 | C(4) | 0414 | | | | |
| | C(24) | 0004 | C(25) | 0000 | | | | | | C(5) | -0248 | | | | | | |
| | C(26) | 0001 | H(57)§ | 0256 | | | | | | | | | | | | | |
| | H(58)§ | 0546 | H(59)§ | 0007 | | | | | VII' | C(1) | -0479 | C(2)§ | 4972 | 9325 | 6972 | 3148 | 5520 |
| | H(60)§ | 0326 | H(61)§ | 0561 | | | | | | C(3) | 0523 | C(4) | -0849 | | | | |
| | | | | | | | | | | C(5) | 0805 | | | | | | |
| IV | C(6)§ | -0740 | C(27) | -0025 | 9459 | 4066 | -0659 | 8450 | | | | | | | | | |
| | C(28) | 0001 | C(29) | 0005 | | | | | VIII | C(1) | 0451 | C(5) | -0335 | -5423 | -8288 | -2676 | -1059 |
| | C(30) | 0011 | C(31) | -0035 | | | | | | C(6) | 0066 | C(7) | 0266 | | | | |
| | C(32) | 0042 | H(62)§ | -0245 | | | | | | C(8) | -0448 | | | | | | |
| | H(63)§ | 0235 | H(64)§ | -0240 | | | | | | | | | | | | | |
| | H(65)§ | 0164 | H(66)§ | 0124 | | | | | | | | | | | | | |

§ These atoms were given a weight of zero for the calculation of the least-squares plane.

D is the deviation of the particular atom from the plane in $A \times 10^4$.

d is the distance from the origin to the plane multiplied by $10^3$.

cos A, etc. are the direction cosines of the normal to the plane with respect to the crystallographic axes, $\underset{\sim}{a}$, $\underset{\sim}{b}$, and $\underset{\sim}{c}$.

TABLE XII

Angles Between the Normals to the Various Planes in DHB

| Plane A | Plane B | θ |
|---|---|---|
| VII | VIII | 28°35' |
| VII' | VIII | 27°52' |
| VII | VII' | 15°35' |
| II | VII | 43°41' |
| III | VII | 36°55' |
| IV | VIII | 69°15' |
| V | VIII | 67°33' |
| VI | VIII | 58°0' |
| I | VII | 88°35' |
| I | VIII | 63°33' |

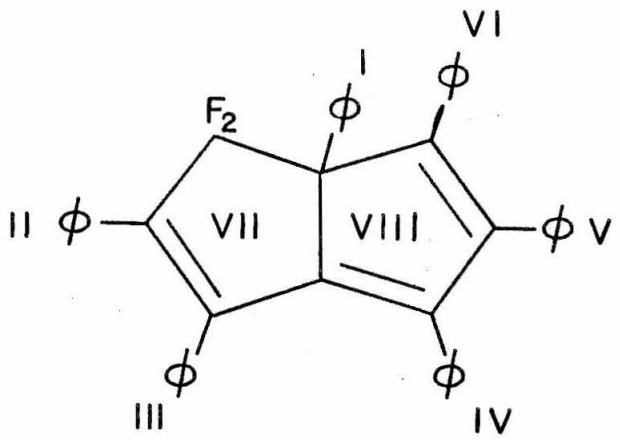


Figure 5. Numbering of the Planes in DHB.

C(4), and C(5); VII' from C(1), C(3), C(4), C(5). As is expected from the $sp^2$ hybridization of C(3) and C(4), the deviations from plane VII are smaller than from plane VII'.

The angle between the normals to the two planes, VII and VIII, of the dihydropentalene skeleton is 28°35', which is a consequence of the $sp^3$ hybridization of C(1) and C(2). The phenyl rings, as expected from steric considerations, are twisted from 36°55' to 88°35' with respect to the corresponding rings of the dihydropentalene skeleton. The 28°35' angle between the normals to planes VII and VIII is, for all practical purposes, the angle between the p-orbitals of C(4) and C(5). Therefore, the overlap integral S' for this bond is

$$S' = S_{pp} \cos 28°35'$$

where $S_{pp}$ is the usual overlap integral for a $C_{sp^2} - C_{sp^2}$ single bond. The decreased overlap does not appear to be serious enough to prevent conjugation between the C(3) = C(4) double bond and the cyclopentadiene ring. It is probably this conjugation which is responsible for the yellow color of DHB.

The C-C bond distances in DHB clearly demonstrate the relationship between the hybridization of the carbons involved and the bond distance. This effect is discussed by Dewar and Schmeisling (4), and the "expected" values with which the distances in DHB are compared, are taken from their average values. Only one $C_{sp^3} - C_{sp^3}$ single bond (between C(1) and C(2))is observed in DHB. It is 1.536Å, which is 0.008Å shorter than the expected value of 1.544Å. The four $C_{sp^3} - C_{sp^2}$ single bonds (C(1)-C(5), C(1)-C(8), C(1)-C(9), and C(2)-C(3)), 1.503, 1.525, 1.534, and 1.497Å, give an average of 1.515Å, which is 0.002Å shorter than the expected value of 1.517Å. (Dewar and Schmeisling (4), however, suspect that their 1.517Å value may be

too large.) The average value for the four $C_{sp^3} - C_{sp^2}$ single bonds in the isomer I is 1.515 Å (7). The seven $C_{sp^2} - C_{sp^2}$ single bonds (C(4)-C(5), C(6)-C(7), C(3)-C(15), C(4)-C(21), C(6)-C(27), C(7)-C(33), and C(8)-C(39)), 1.464, 1.482, 1.482, 1.469, 1.477, 1.491, and 1.477 Å, give an average of 1.477 Å, which is 0.002 Å shorter than the expected value of 1.479 Å. The corresponding average in isomer I is 1.467 Å (7). The three $C_{sp^2} - C_{sp^2}$ double bonds (C(3)-C(4), C(5)-C(6), and C(7)-C(8)), 1.362, 1.360, and 1.360 Å, give an average of 1.361 Å which is 0.023 Å longer than the expected value of 1.338 Å.

The average C-C distance in the phenyl rings is 1.383 Å with a standard deviation of 0.011 Å calculated from the variation of the individual values from the mean. This value is very close to the 1.392 Å C-C distance in benzene (3). The average C-C distance in the phenyl rings of isomer I is 1.381 Å (7). The C-F distances (1.370 and 1.385 Å) in DHB are shorter than in isomer I because both fluorines are bonded to the same carbon, but they are longer than the C-F distance (1.358 Å) in $CH_2F_2$ (21). It is, however, not surprising that the C-F distances in DHB are longer than expected for a $CF_2$ group because of short nonbonded distances involving both fluorines. The nonbonded C(1)-F(45) distance is 2.445 Å; C(1)-F(46), 2.394 Å; C(3)-F(45), 2.405 Å; C(3)-F(46), 2.368 Å; C(8)-F(46), 2.895 Å.

The planarity of the phenyl rings requires the average of the internal C-C-C bond angles in the phenyl rings to be $120^\circ$. A measure of the accuracy of this study is seen in the small $1.0^\circ$ standard

deviation which was calculated from the deviations of the individual angles from this mean. The internal C-C-C bond angles in ring VIII follow the general pattern of cyclopentadiene (27). There are no reliable structural data for a cyclopentene ring with which to compare the angles in ring VII; however, with the exception of the angles about C(1), they appear normal. The angles about tetrahedral C(1) are distorted because of the steric considerations which were discussed in the preceding paragraph. In particular, angle C(2)-C(1)-C(5) (97.3°) is much smaller than the tetrahedral angle 109.5°. Angles C(2)-C(1)-C(8) (123.1°) and C(5)-C(1)-C(9) (113.3°), on the other hand, are much larger than the tetrahedral angle.

The anisotropic temperature factors in Table IX were converted into ellipsoids of thermal vibration by Waser's method (29) with the "Temperature Ellipsoids Program" (reference 5, chapter 12) which was written by Mrs. B. Stroll. The lengths of the principal axes in "B" units and their direction cosines with respect to the cell axes are presented in Table XIII. A qualitative examination of these results indicates tremendous anisotropy of thermal vibration for the carbons in the phenyl rings. Although no quantitative vibrational analysis was performed, indications of rigid body vibrations and oscillations are seen in Table XIII. Ring I appears to be oscillating about the C(1)-C(9) bond in the plane of the ring. Rings II, III, IV, and VI exhibit the same kind of oscillation, but in addition, they oscillate along an arc which is perpendicular to each ring plane. Ring V appears to oscillate in a twisting motion about the C(7)-C(33) bond.

## TABLE XIII

## Ellipsoids of thermal vibration

| Atom | B | cos A | cos B | cos C | Atom | B | cos A | cos B | cos C | Atom | B | cos A | cos B | cos C |
|---|---|---|---|---|---|---|---|---|---|---|---|---|---|---|
| C(1) | 384 | 82982 | 22213 | 31939 | C(16) | 762 | 21639 | 75515 | 69700 | C(31) | 854 | 71864 | 40901 | 34323 |
| | 306 | -45954 | 95496 | 09524 | | 626 | 72405 | -65549 | 28161 | | 567 | 24835 | -54498 | 59556 |
| | 232 | -31653 | 19674 | 94282 | | 313 | -65491 | 00856 | 65945 | | 329 | -64951 | 73191 | 72628 |
| C(2) | 396 | -16116 | -81340 | 05689 | C(17) | 1099 | 35303 | 65462 | 68977 | C(32) | 613 | 75163 | 32444 | 41432 |
| | 340 | -98660 | 44400 | 04266 | | 840 | 64028 | -74932 | 23047 | | 448 | 27499 | -73152 | 38493 |
| | 309 | -02661 | 37603 | 99749 | | 289 | -68220 | 09987 | 68635 | | 308 | -59951 | 59966 | 82472 |
| C(3) | 375 | -79137 | 83047 | 25998 | C(18) | 1284 | 92841 | -11352 | 29215 | C(33) | 427 | 87213 | 18730 | 11928 |
| | 333 | 59641 | 54638 | 41283 | | 635 | -21853 | 99335 | 39962 | | 337 | -48160 | 95844 | 52783 |
| | 240 | -13474 | -10786 | 87288 | | 308 | -30046 | -01888 | 86887 | | 264 | 08699 | -21509 | 84092 |
| C(4) | 374 | -96115 | 45621 | 33939 | C(19) | 929 | -98835 | 16991 | 00703 | C(34) | 608 | -17489 | 97648 | 19196 |
| | 330 | 21982 | 81858 | 55801 | | 545 | -15132 | 98533 | 36526 | | 389 | -98206 | 15873 | 11355 |
| | 270 | 16692 | -34895 | 75724 | | 299 | -01594 | -01525 | 93068 | | 318 | 06974 | 14556 | 97480 |
| C(5) | 389 | 49735 | 66510 | 27452 | C(20) | 582 | 94189 | 01899 | 01391 | C(35) | 606 | 15818 | 85993 | 09592 |
| | 340 | -86712 | 74683 | 21943 | | 433 | -33465 | 99981 | 34944 | | 549 | -89507 | 51030 | 50319 |
| | 225 | -02503 | 00103 | 93621 | | 272 | 02849 | -00240 | 93685 | | 307 | 41693 | 00944 | 85882 |
| C(6) | 385 | 58108 | 58752 | 25356 | C(21) | 477 | -94647 | 01197 | 07261 | C(36) | 635 | -94408 | -00708 | 02574 |
| | 347 | 76836 | -77240 | 04504 | | 353 | -32152 | 97065 | 11177 | | 506 | -32958 | 97570 | 13390 |
| | 272 | -26816 | 24136 | 96626 | | 235 | 02776 | 24016 | 99107 | | 296 | -00879 | 21896 | 99065 |
| C(7) | 382 | -74972 | 84287 | 11131 | C(22) | 682 | -99853 | 27795 | 02973 | C(37) | 767 | -21136 | 98323 | 20593 |
| | 342 | 63053 | 52971 | 31117 | | 424 | -05381 | 77851 | 83392 | | 506 | 94276 | -06949 | 22486 |
| | 249 | -20119 | 09397 | 94380 | | 335 | -00469 | -56271 | 55107 | | 282 | -25790 | 16856 | 95237 |
| C(8) | 413 | 92892 | 05224 | 10903 | C(23) | 920 | -98846 | 28097 | 20300 | C(38) | 775 | -19531 | 98808 | 26229 |
| | 349 | -36986 | 99236 | 44449 | | 524 | 10932 | 45335 | 96372 | | 417 | 95188 | -10134 | 20661 |
| | 262 | -01578 | -11178 | 88912 | | 326 | 10478 | -84588 | 17326 | | 258 | -25614 | 11580 | 94260 |
| C(9) | 442 | 92684 | 00657 | 22550 | C(24) | 1093 | -84573 | -11454 | 25273 | C(39) | 567 | -90924 | -07081 | 10394 |
| | 367 | -30143 | 99454 | 25017 | | 490 | 12228 | 42267 | 96686 | | 348 | -40310 | 98545 | 20748 |
| | 214 | -22383 | 10310 | 94157 | | 332 | 51777 | -89900 | 03596 | | 240 | 10382 | 15450 | 97270 |
| C(10) | 574 | 94726 | -02473 | 15287 | C(25) | 786 | -69744 | -32785 | 25300 | C(40) | 853 | 98646 | -16530 | 02626 |
| | 391 | 17141 | -82888 | 22513 | | 522 | -00904 | 56916 | 95566 | | 482 | -16109 | 86448 | 76209 |
| | 322 | -27077 | 55885 | 96226 | | 369 | 71658 | -75402 | 15064 | | 329 | 03047 | -47468 | 64692 |
| C(11) | 765 | 98695 | -27845 | 08316 | C(26) | 562 | 69572 | 43590 | 00128 | C(41) | 1464 | -99284 | 24311 | 13778 |
| | 421 | -05455 | -78125 | 22062 | | 394 | -14925 | 42826 | -99496 | | 559 | -01081 | 79024 | 80648 |
| | 315 | -15146 | 55865 | 97180 | | 355 | 70274 | -79147 | 10020 | | 337 | 11891 | -56250 | 57497 |
| C(12) | 846 | -87101 | 69322 | 01217 | C(27) | 466 | -86725 | -18446 | 01079 | C(42) | 1733 | -88388 | -01984 | 28354 |
| | 460 | -47279 | -44758 | 39953 | | 327 | -48863 | 98227 | 32378 | | 556 | 04192 | 63209 | 91402 |
| | 373 | 13347 | 56486 | 91664 | | 212 | 09556 | 03312 | 94606 | | 350 | 46583 | -77463 | 29010 |
| C(13) | 701 | -63516 | 93372 | 30039 | C(28) | 514 | -93471 | 15056 | 32024 | C(43) | 1205 | -73230 | -26733 | 28202 |
| | 523 | -15113 | -05512 | 89538 | | 429 | -05496 | 92185 | 60643 | | 589 | 00144 | 60003 | 94081 |
| | 425 | 75746 | 35369 | 32869 | | 386 | 35110 | -35710 | 72776 | | 379 | 68097 | -75398 | 18797 |
| C(14) | 453 | 53543 | -72620 | 32809 | C(29) | 808 | -98528 | 23675 | 19074 | C(44) | 812 | -69036 | -43409 | 02783 |
| | 415 | -21463 | 63811 | 94261 | | 466 | 11570 | 28709 | 98139 | | 530 | -19433 | 51044 | 98129 |
| | 392 | -81745 | -25452 | 06303 | | 386 | -12552 | 92818 | 02223 | | 345 | 69686 | -74230 | 19051 |
| C(15) | 440 | 90888 | -06657 | 33322 | C(30) | 985 | 86188 | 20554 | 05807 | P(45) | 599 | 64546 | 47793 | 43541 |
| | 385 | -25862 | 99776 | 37503 | | 473 | 21274 | -32313 | 77186 | | 400 | 31494 | -62761 | 50668 |
| | 278 | -32718 | -00533 | 86504 | | 325 | -46025 | 92377 | 63313 | | 292 | -69583 | 61455 | 74410 |
| | | | | | | | | | | P(46) | 625 | -38584 | 96759 | 55651 |
| | | | | | | | | | | | 420 | -64084 | -21879 | 48437 |
| | | | | | | | | | | | 333 | 66365 | -12608 | 67503 |

Listed under B are the lengths of the principal axes of the ellipsoids in "B" units multiplied by $10^2$.

Under Cos A, etc., are listed the direction cosines multiplied by $10^5$ of these ellipsoids with respect to the crystallographic axes, $\underset{\sim}{a}$, $\underset{\sim}{b}$, and $\underset{\sim}{c}$.

Table XIV gives the labeling of symmetry related molecules which are involved in the closest intermolecular distances. All intermolecular distances which are shorter than van der Waals distances are presented in Table XV.

TABLE XIV

Symmetry Related Molecules

| Molecules | Coordinates of the Symmetry Related Molecule in Terms of Original Coordinates | | |
|---|---|---|---|
| | x | y | z |
| A | x | y | z-1 |
| B | x | y+1 | z-1 |
| C | 1-x | 2-y | 1-z |
| D | x | y | z+1 |
| E | 1-x | 1-y | 2-z |
| F | x | y-1 | z+1 |
| G | -x | 1-y | 1-z |
| H | -x | 1-y | 2-z |

TABLE XV

Intermolecular Distances Which Are Shorter than van der Walls Distances†

| | |
|---|---|
| $H(67)_E$§ - H(76) | 2.169 Å |
| $H(76)_E$ - H(67) | 2.169 Å |
| $C(10)_D$ - H(69) | 2.885 Å * |
| $H(69)_A$ - C(10) | 2.885 Å * |
| $H(74)_B$ - C(19) | 2.776 Å * |
| $C(19)_F$ - H(74) | 2.776 Å * |
| $H(52)_C$ - H(58) | 2.330 Å |
| $H(58)_G$ - H(52) | 2.330 Å |

TABLE XV (continued

| | |
|---|---|
| $H(50)_G$ - H(56) | 2.285 Å |
| $H(56)_G$ - H(50) | 2.285 Å |

† The van der Waals radius for hydrogen, 1.2 Å, was taken from Pauling (24). For carbon, half the 3.40 Å interlayer distance in graphite (28), 1.7 Å, was used.

§ The subscript refers to the symmetry related molecule (see Table XIV).

* These distances result from "nesting" (7).

"Nesting," which is defined by Fritchie as "the close approach of a hydrogen on one phenyl ring to the center of another ring," (7) is observed in the packing of DHB, although not to the extent that was observed in isomer I. Only one intramolecular "nesting" is seen. H(47) is 2.625, 3.186, and 2.883 Å from C(39), C(40), and C(44), respectively. There are six intermolecular "nestings." H(55) is 3.380, 3.115, 3.007, 3.172, 3.422, and 3.510 Å from $C(27)_A$*, $C(28)_A$, $C(29)_A$, $C(30)_A$, $C(31)_A$, and $C(32)_A$; H(68) is 3.674, 3.389, 3.371, 3.609, 3.836, and 3.865 Å from $C(15)_D$, $C(16)_D$, $C(17)_D$, $C(18)_D$, $C(19)_D$, and $C(20)_D$; H(69) is 3.057, 2.885, 2.985, 3.229, 3.358, and 3.273 Å from $C(9)_D$, $C(10)_D$, $C(11)_D$, $C(12)_D$, $C(13)_D$, and $C(14)_D$; H(74) is 3.778, 3.042, 2.776, and 3.322 Å from $C(17)_F$, $C(18)_F$, $C(19)_F$, and $C(20)_F$; H(49) is 3.672, 3.934, 3.874, 3.554, 3.260, and 3.317 Å from $C(21)_G$, $C(22)_G$, $C(23)_G$, $C(24)_G$, $C(25)_G$, and $C(26)_G$; H(65) is 3.086, 2.941, 2.904, 3.007, 3.134, and 3.168 Å from $C(9)_H$, $C(10)_H$, $C(11)_H$, $C(12)_H$,

* Subscript indicates the symmetry related molecule according to Table XIV.

$C(13)_H$, and $C(14)_H$.

From Table XV it is seen that all short intermolecular distances involving carbons result from "nesting." All of the other short intermolecular distances involve only hydrogen atoms, which, because of the uncertainty of their positions, are no cause for concern.

## REFERENCES FOR PART I


1. W. Cochran, Acta Cryst. 5, 65 (1952).

2. W. Cochran and M. M. Woolfson, Acta Cryst. 8, 1 (1955).

3. E. G. Cox, D. W. J. Cruickshank, and J. A. S. Smith, Proc. Roy. Soc. 247 A, 1 (1958).

4. M. J. S. Dewar and H. N. Schmeisling, Tetrahedron 11, 96 (1960).

5. D. J. Duchamp, "User's Guide to the CRYRM Crystallographic Computing System," Gates and Crellin Laboratories of Chemistry, California Institute of Technology (1964).

6. C. J. Fritchie, Jr. and E. W. Hughes, J. Am. Chem. Soc. 84, 2257 (1962).

7. C. J. Fritchie, Jr., Ph. D. Thesis, California Institute of Technology (1963).

8. D. Harker and J. S. Kasper, Acta Cryst. 1, 70 (1948).

9. H. Hauptman and J. Karle, "Solution of the Phase Problem I. The Centrosymmetric Crystal," A. C. A. Monograph No. 3, Edwards Brothers, Inc., Ann Arbor, Michigan (1953).

10. E. R. Howells, D. C. Phillips, and D. Rogers, Acta Cryst. 3, 210 (1950).

11. E. W. Hughes, J. Am. Chem. Soc. 63, 1737 (1941).

12. E. W. Hughes, Acta Cryst. 2, 34 (1949).

13. E. W. Hughes, Acta Cryst. 6, 871 (1953).

14. "International Tables for X-ray Crystallography," Vol. II, Birmingham: Kynoch Press (1952), p. 295.

15. "International Tables for X-ray Crystallography," Vol. III, Birmingham: Kynoch Press (1962), p. 201.

16. N. D. Jones, Ph. D. Thesis, California Institute of Technology, (1964), Appendix.

17. I. L. Karle, H. Hauptman, J. Karle, and A. B. Wing, Acta Cryst. 11, 257 (1958).

18. I. L. Karle, K. Britts, and P. Gum, Acta Cryst. 17, 496 (1964).

19. I. L. Karle and J. Karle, Acta Cryst. 17, 835 (1964).

20. I. L. Karle, J. Karle, T. B. Owen, and J. L. Hoard, Acta Cryst. 18, 345 (1965).

21. D. R. Lide, Jr., J. Am. Chem. Soc. 74, 3548 (1952).

22. B. W. Lindgren and G. W. McElrath, Introduction to Probability and Statistics, Macmillan, New York (1963), p. 255.

23. K. Nagarajan, M. C. Caserio, and J. D. Roberts, J. Am. Chem. Soc. 86, 449 (1964).

24. L. Pauling, The Nature of the Chemical Bond, 3rd Ed., Cornell University Press, Ithaca, New York (1960), p. 260.

25. J. D. Roberts, private communication.

26. D. Sayer, Acta Cryst. 5, 60 (1952).

27. V. Schomaker and L. Pauling, J. Am. Chem Soc. 61, 1769 (1939).

28. Strukturbericht, Vol. I, 28 (1931).

29. J. Waser, Acta Cryst. 8, 731 (1955).

30. A. J. C. Wilson, Nature 150, 152 (1942).

31. A. J. C. Wilson, Acta Cryst. 2, 318 (1949).

32. M. M. Woolfson, Direct Methods in Crystallography, Oxford at the Clarendon Press (1961), p. 22.

33. W. H. Zachariasen, Acta Cryst. 5, 68 (1952).

# II. A LOW TEMPERATURE REFINEMENT OF THE CYANURIC TRIAZIDE STRUCTURE

## INTRODUCTION

The crystal structure of cyanuric triazide (1, 3, 5-triazido-2, 4, 6-triazine) was investigated independently by Hughes (5) and Knaggs (2, 8). In general, the over-all molecular configuration was the same in both of these works, but the following differences were observed: 1) Hughes found that the two crystallographically different C-N bonds in the triazine ring are of equal length, whereas Knaggs found them to be unequal; 2) Hughes reported a non-linear azide group; Knaggs, a linear one. In neither study was the structure refined extensively, but Knaggs' refinement was more complete.

The distances and angles which Knaggs obtained are presented in figure 1. The estimated error for bond distances within the tria-

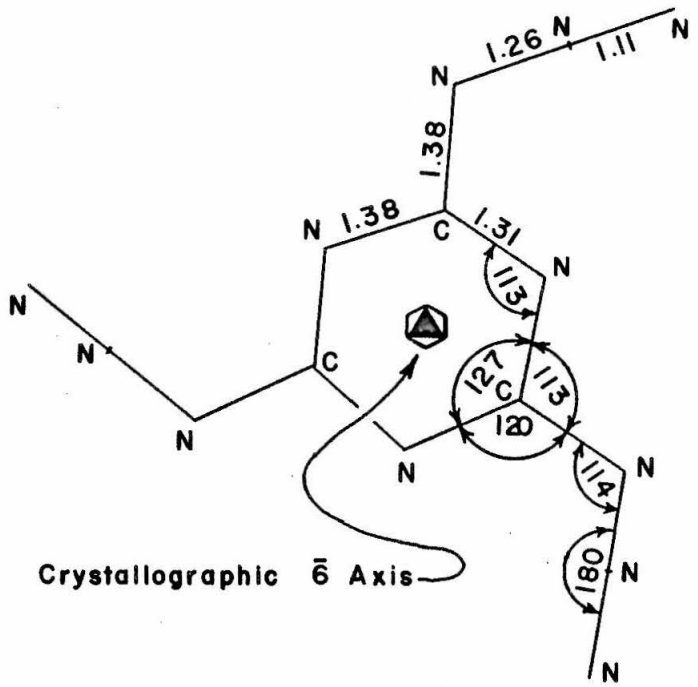


Figure 1. Cyanuric Triazide Distances and Angles from Knaggs (8).

zine ring was reported to be 1 - 2 per cent. The average C-N distance in the ring was $1.34_5$ Å. It is, therefore, apparent that the individual C-N distances deviate from the average by little more than the estimated error. Nevertheless, an explanation for this bond alternation was proposed which involved fixation of the $\pi$ bonds by the unsymmetrical position of the azide chains (8). The present work was undertaken with the objective of accurately measuring the C-N distances in order to learn if this bond alternation is significant.

# EXPERIMENTAL

## Low Temperature Equipment

Because of the low temperatures which were attained in this study, the usual method of crystal mounting (in which the crystal is glued to a glass fiber which in turn is glued to a brass pin) was abandoned. (The different coefficients of expansion for glass and brass cause sufficient strain at these temperatures to rupture the glass-to-brass joint.) Instead, the crystal was glued to a glass pin, one end of which had been pulled down to a very small diameter from a piece of 1/8" glass rod in the very narrow flame of a natural gas - oxygen torch. The other end of the pin, which was 1/8" in diameter, was clamped directly into the goniometer head. To protect the crystal from buffeting in the stream of cold nitrogen, a glass capillary 1.5 mm. in diameter with 0.01 mm. walls was then glued in place around the crystal (see figure 2). Duco cement diluted with an equal volume of amyl acetate was found to be very satisfactory for this low temperature work.

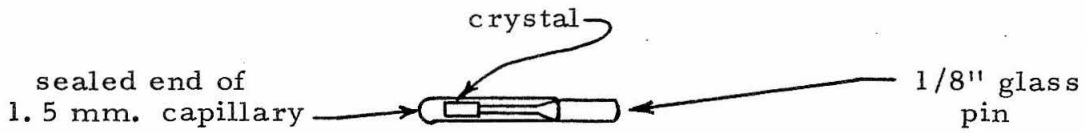


Figure 2. Crystal Mount.

The - 110°C temperature at which the intensity data for this study were collected was attained by a blower apparatus which was designed and built by J. Rollet (12). This apparatus is very similar

to the one described by Abrahams, Collins, Lipscomb, and Reed (1). A stream of very cold nitrogen was directed at the crystal by a Dewar-type blower tube which, for a Weissenberg camera, is inserted through the open end of the layer-line screen. The other end of the blower tube is bell-shaped and situated directly above a heating coil. The bell-shaped end of the tube and heating coil were submerged in a reservoir of liquid nitrogen, and the stream of cold nitrogen was provided by boiling the nitrogen into the blower tube (see figure 3).

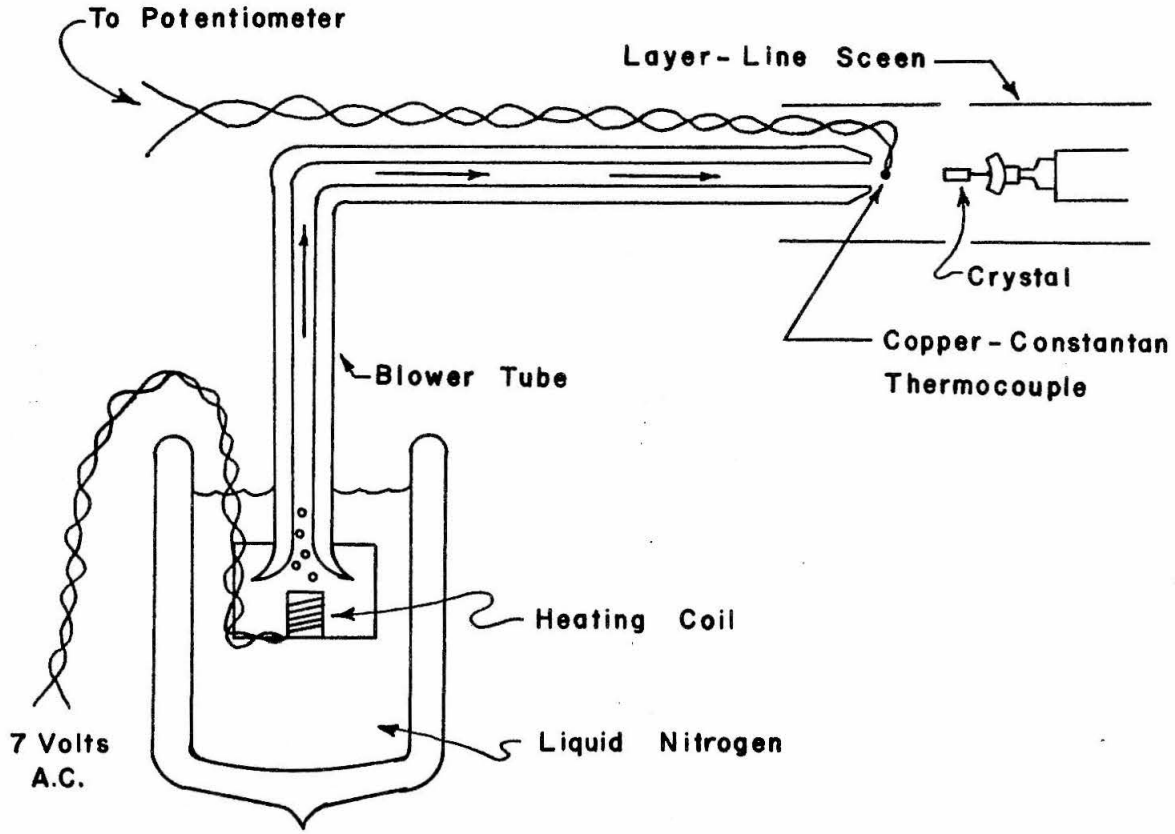


Figure 3. Schematic Drawing of the Cooling Apparatus.

The temperature was measured by a copper-constantan thermocouple which is situated at the nozzle of the blower, directly in front of the crystal. The thermocouple potential at which these measurements were made was - 4.7 mv. (reference junction at room temperature), which corresponds to a temperature of - 110°C (12).

Unit Cell Parameters

Cyanuric triazide is hexagonal, space group $P6_3/m$ with two molecules per unit cell. The crystals which were used in this study were taken from the original sample of crystals used by Hughes (5). They were elongated along the $\underset{\sim}{c}$ axis in hexagonal prisms. The crystalline faces were covered with a white powder; however, the diffraction patterns were quite normal. The colorless crystals quickly turned brown when exposed to X-rays, but a zero-layer Weissenberg picture of the $\underset{\sim}{c}$ axis crystal made at the conclusion of this work gave no evidence of disorder and showed the same relative intensities as were observed on the first zero-layer picture. Excellent cleavage perpendicular to the $\underset{\sim}{c}$ axis was observed and used to obtain approximately equidimensional crystalline fragments from the needles. Two crystal fragments approximately one millimeter in every direction were used for the measurement of intensities. One fragment was mounted along the $\underset{\sim}{c}$ axis; the other, along the $\underset{\sim}{a}$ axis.

The unit cell dimensions at - 110°C were calculated from measurements which were made on a zero-layer Weissenberg picture of the crystal which was rotated about the $\underset{\sim}{a}$ axis. Mo $K_\alpha$ radiation

was used, and the following wavelengths were assumed.

$$\text{Mo } K_{\alpha_1} = 0.70926 \text{ Å}$$
$$\text{Mo } K_{\alpha_2} = 0.71354 \text{ Å}$$
$$\text{Mo } K_{\overline{\alpha}} = 0.7107 \text{ Å}$$

The film was calibrated to eliminate errors due to film shrinkage by marking it with a known distance before developing. Ten high-angle reflections were used as input to the CRYRM "Unit Cell Least Squares Program" (reference 3, chapter 10) which was written by Mr. George Reeke. The function which was minimized was

$$\sum_{n=1}^{N} w_n (\sin^2\theta_{obs.} - \sin^2\theta_{calc.})^2 \left(\frac{4}{\lambda_n^2}\right)^2$$

where N is the total number of observations and $w_n$ is the weight for the $n^{th}$ observation. The weighting function was

$$\sqrt{w_n} = E/\sin 2\theta_n ,$$

where E is an external weight. In this calculation, E was 1.0 except for a couple of doubtful observations for which E was 0.5 . Corrections for eccentricity and absorption were included in the calculation. The following unit cell dimensions were obtained.

$$\underset{\sim}{a} = 8.75 \pm 0.03 \text{ Å}$$
$$\underset{\sim}{c} = 5.85 \pm 0.02 \text{ Å}$$

The estimated uncertainties are an order of magnitude larger than the sigmas which were obtained from the least squares calculation. They were estimated by assuming an uncertainty of 0.3 mm. in the camera radius.

Intensity Data

The intensity data were collected photographically at - 110°C by the multiple-film, equi-inclination Weissenberg method. Layers zero through seven about the $\underset{\sim}{c}$ axis and layers zero through four about the $\underset{\sim}{a}$ axis were photographed with Mo $K_\alpha$ radiation. For layers zero through four about the $\underset{\sim}{c}$ axis and the zero layer about the $\underset{\sim}{a}$ axis, two packs of four films were used. Each of the other layers was photographed with a single pack of four films. Within each film pack, the four films were separated by three sheets of 0.001 inch nickel foil which provided a film to film attenuation factor of about 0.3 for Mo $K_\alpha$ radiation. Intensities were estimated visually by comparing the diffraction maxima on the films with a calibrated intensity scale which had been prepared by timed exposures.

The data reduction and all subsequent calculations were performed on an IBM 7094 computer by the CRYRM crystallographic computing system (3). As each reflection was entered into the data reduction, a standard deviation for the intensity, $\sigma(I)$, was computed according to the following function.

$$\sigma(I) = \frac{1}{w_e}\left[B + 0.133\, I + \frac{0.1\, I^2}{(70.0 - I)^2}\right] \times \left[1 + 0.25\, e^{-50(0.5 - \sin^2\theta)^2}\right]$$

for $I < 70.0$ ,

$\sigma(I)$ = a very large number for $I \geq 70.0$ ,

$B = 0.6667$ for the data from axis $\underset{\sim}{c}$ ,

$B = 0.3333$ for the data from axis $\underset{\sim}{a}$ .

The I is the raw intensity, and $w_e$ is an external weight which was 1.0 for most reflections. Values of 0.2 or 0.5 were entered for a

few questionable reflections. The $\sigma(I)$'s were carried through the rest of the data reduction and scaling by propagation-of-error methods.

Factors for film to film scaling were calculated in the usual way from intensities which were measurable on more than one film. Since the successive films (A, B, C, and D) in each film pack had nickel foil between them, a certain amount of fluorescence was possible. There were, consequently, three different film environments within each film pack (A, B and C, and D). Therefore, the three film factors were not expected to be equal. For this reason, an over-all general film factor was not used for film to film scaling. Instead, the following procedure was used. The film factors which had been calculated during the first pass of the "Initial Data Processing Program" were sorted into three groups. The film factors relating film A to film B were put in group 1; film B to film C, group 2; and film C to film D, group 3. It was observed that the group 1 film factors for the $\underset{\sim}{a}$ axis pictures were significantly smaller than the corresponding film factors for the $\underset{\sim}{c}$ axis pictures. (This is, perhaps, due to the reduced background on the A films for the $\underset{\sim}{a}$ axis pictures which resulted from the narrower width of the layer line slit which was used for these exposures.) Consequently, group 1 was divided into two groups; group 1a for the $\underset{\sim}{a}$ axis pictures and group 1c for the $\underset{\sim}{c}$ axis pictures. After accounting for the angle of incidence between the X-rays and the film, the film factors within each group were averaged. The four average film factors which resulted

are: $F_{1a} = 2.6765$, $F_{1c} = 3.0232$, $F_2 = 3.4632$, and $F_3 = 3.4085$. The average film factors were then corrected for non-normal incidence of X-rays and applied in the film to film scaling.

The raw intensities were then corrected for the Lorentz and Polarization factors and reduced to a common scale by a comparison of reflections which were observed on photographs about both axes. Absorption corrections were neglected because of the small linear coefficient of absorption for cyanuric triazide in Mo $K_\alpha$ radiation ($\mu = 1.47$ cm.$^{-1}$). A data tape suitable for subsequent calculations with the CRYRM system was then prepared by Dr. Duchamp's "Data Tape Preparation Program" (reference 3, chapter 5). This data tape listed for each reflection the indices, the observed F, the atomic scattering factors for carbon (valence) and nitrogen (7), and a weight $\sqrt{w_i}$ which is equal to the reciprocal of $\sigma(I)$.

## REFINEMENT

The asymmetric unit consists of four nitrogen atoms and one carbon (one third of a molecule) which are all in the six-fold special positions (h) of Wyckoff (5). These positions are:

$x, y, 1/4$ ; $\bar{y}, x-y, 1/4$; $y-x, \bar{x}, 1/4$

$\bar{x}, \bar{y}, 3/4$; $y, y-x, 3/4$; $x-y, x, 3/4$ .

There are, consequently, only ten spatial parameters to be determined. The layered structure which results from atoms in these special positions produces a diffraction pattern which, except for the attenuation associated with increasing diffraction angle, depends upon $\ell$ only insofar as it is even or odd (5, 8). Nevertheless, three-dimensional data were collected in order to increase the accuracy of the spatial parameters and to calculate the $\underset{\sim}{c}$ axis temperature factors.

Knaggs' (8) spatial coordinates were used as input to a three-dimensional least squares refinement (6) which was performed by the CRYRM "Hexagonal Least Squares Program" (reference 3, chapter 6) which was written by the author. (See Appendix for details of this program.) The atomic scattering factors for nitrogen and carbon (valence) were taken from the "International Tables for X-ray Crystallography" (7). Initially, the individual isotropic temperature factors were arbitrarily set at 1.2 $\text{Å}^2$. The function which was minimized is

$$\Sigma\, w\left(|F_{obs.}|^2 - \frac{1}{k^2}|F_{calc.}|^2\right)^2 ,$$

where w is the weight; k , the scaling factor by which $F_{obs.}$ must

be multiplied to be on an absolute scale. Those reflections which were not observed above the background (hereafter called "less-thans") were included in the least squares refinement only if $F_{calc.}$ exceeded the minimum observable $F_{obs.}$. Of the 2,316 recorded reflections, 1,360 were "less-thans", of which only 74 were included in the final least squares cycles. All seven 0 0 $\ell$ reflections ($\ell$ = an even integer) were given weights of zero because of extinction. (All atoms scatter in phase for the 0 0 $\ell$ reflections.) Seven other reflections were given zero weights because of extinction errors. Another forty reflections were given zero weights because of poor agreement between values measured on both axes or other indications of unreliability. Consequently, only 976 of the 2,316 reflections were used in the final least squares cycle. The progress of the refinement is summarized in Table I.

The initial R-value,

$$R = \frac{\Sigma \left| \left| k F_{obs.} \right| - \left| F_{calc.} \right| \right|}{\Sigma \left| k F_{obs.} \right|} ,$$

for the copper sphere was .35. The first six cycles (the B series) were performed two cycles at a time with a full matrix utilizing data for which $\sin^2\theta/\lambda^2 < 0.42$ (the copper sphere).

TABLE I

Initial R-value for the Copper Sphere = .35

| L. S. Cycle | $\sqrt{w_i}$* | $\left(\frac{\sin^2\theta}{\lambda^2}\right)_{max}$* | R | Remarks |
|---|---|---|---|---|
| B1 | $1/F_{obs.}$ | 0.42 | .12 | Full matrix, isotropic. |

TABLE I (continued)

| L. S. Cycle | $\sqrt{w_i}$ * | $\left(\frac{\sin^2\theta}{\lambda^2}\right)_{max}$ * | R | Remarks |
|---|---|---|---|---|
| B2 | $1/F_{obs.}$ | 0.42 | .28** | Four negative temperature factors. |
| B3 | $1/\sigma(I)$*** | | .16 | Four negative temperature factors. |
| B4 | | | .18 | |
| B5 | $1/(F_{obs.})^2$ | | .094 | One negative temperature factor. |
| B6 | | | .082† | |
| Data Were Re-scaled | | | | |
| C1 | $1/\sigma(I)$ | | .082 | |
| C2 | | | .11†† | |
| C3 | | 1.0 | .11 | |
| C4 | | | .12††† | |
| C5 | | Complete Mo Sphere | .085 | Anisotropic |
| C6 | | | .083 | ↓ |
| C7 | | | .082 | |
| C8 | | | .081 | |
| C9 | | | .081 | |
| C10 | | | .081 | |

* Values listed under these headings remain constant from cycle to cycle unless noted otherwise.

** This R is large because new temperature factors were used in place of the negative ones from B2.

*** It was found that these $\sigma(I)$'s were in error.

† This R was improved by re-scaling the data before the structure factor calculation.

†† This R is large because data out to $\sin^2\theta/\lambda^2 = 1.0$ were used for the structure factor calculation.

TABLE I (continued)

††† This R is large because the complete Mo sphere was used for the structure factor calculation.

Isotropic temperature factors were used. The weighting scheme was $1/F_{obs.}$ for the first two cycles. Four of the isotropic temperature factors were negative after these two cycles. The assumption was made that the weighting scheme was responsible for the negative temperature factors. The temperature factors were reset at 1.2 $\AA^2$, and the weighting scheme was changed to $1/\sigma(I)$ for cycles B3 and B4. Again, four temperature factors were negative following cycle B3, but cycle B4 made them all positive. The temperature factors were reset to values in the neighborhood of 1.2 $\AA^2$, and the weighting scheme was changed to $1/(F_{obs.})^2$ for cycles B5 and B6.

In the meantime, a close examination of the data revealed serious errors in the assignment of weights by the "Initial Data Processing Program" and in the inter-axial scaling. These errors were corrected by re-scaling the data, and the final ten cycles (the C series) of least squares were performed. The data were expanded to $\sin^2\theta/\lambda^2 = 1.0$ for cycle C3 and to the molybdenum limiting sphere for cycle C5. The isotropic temperature factors were replaced at cycle C5 with anisotropic temperature factors as described in the following expression.

$$e^{-\{\beta_{11}h^2 + \beta_{22}k^2 + \beta_{33}\ell^2 + \beta_{12}hk\}}$$

Since all of the atoms are situated on a crystallographic mirror plane, one axis of each thermal ellipsoid must be perpendicular to

this plane. Therefore, $\beta_{13}$ and $\beta_{23}$ for each atom must be identically zero.

Convergence was attained with cycle C8, but two additional cycles were performed after various doubtful reflections had been given zero weights. All shifts in the final cycle of least squares were less than a tenth of the corresponding standard deviations. The final R-value was .081 .

Since the only evidence for the crystallographic mirror plane was the indirect evidence for a layered structure, four anisotropic cycles of least squares were performed in space group P $6_3$ . Convergence was reached with an R-value of 0.080 . The bond distances and angles which resulted did not differ significantly from those for the structure in P $6_3/m$ . The terminal azide nitrogen, N(5), (see figure 5 for the numbering of the atoms) showed the greatest deviation from the plane of the triazine ring. This deviation, 0.089 Å along the $\underset{\sim}{c}$ axis, however, was less than the root mean square vibrational amplitude in this direction. Consequently, the presence of the crystallographic mirror plane was considered as established.

As an independent check on the correctness of the structure, a Fourier synthesis and a difference Fourier synthesis were calculated for the section, z = 1/4 . The Fourier section is presented in figure 4. The contours are at intervals of 5 electrons/Å$^3$. The positions of the atoms as determined by least squares are indicated in the Fourier for one asymmetric unit by x's . An electron density of 40 electrons/Å$^3$ is indicated at the centers of the atoms within the ring and the first nitrogens, N(3), of the azide groups. The middle and terminal nitro-

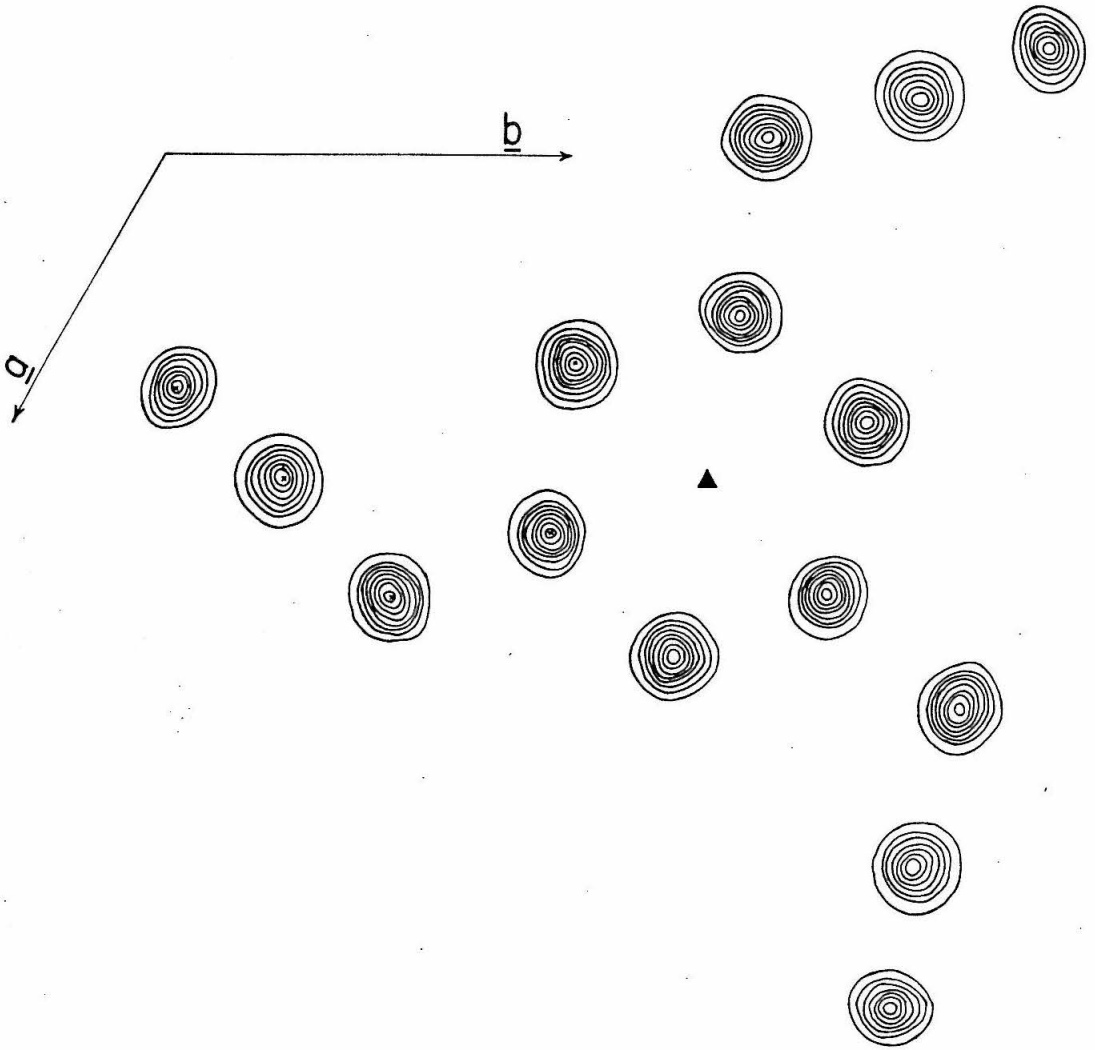


Figure 4. Fourier Synthesis of Cyauric Triazide. Section at z = 1/4. Contours are at intervals of 5 electrons/$A^3$.

gens of the azide groups possess an electron density of 35 electrons/$Å^3$ at their centers. The larger temperature factors for these middle and terminal azide nitrogens spread the atoms over a larger volume and decrease the electron densities at their centers. The sharpness of the peaks in the Fourier results from two factors: 1) Knaggs observed very sharp peaks in the room temperature Fourier, which were attributed to the absence of hydrogens in the structure (8); 2) the low temperature at which the present study was conducted substantially reduced thermal vibration. The noise level in the difference Fourier was about 1 electron/$Å^3$ with maximum positive and negative peaks, 1.75 and - 1.33 electrons/$Å^3$, respectively. The noise appeared to be concentrated in the plane of the molecule, and was substantially lower throughout the rest of the unit cell. When compared with the peak heights at the atomic centers, the noise level is insignificant.

The final spatial and temperature parameters (for the structure in space group $P\,6_3/m$) are presented in Table II. The structure factors which were calculated from the parameters in Table II

TABLE II

Final Spatial and Temperature Coordinates

(All z coordinates are 1/4.)

| Atom | x | y | $\beta_{11}$ | $\beta_{22}$ | $\beta_{33}$ | $\beta_{12}$ |
|---|---|---|---|---|---|---|
| N(1) | .2120(2)* | .4878(2) | .0025(1) | .0027(1) | .0061(2) | .0025(2) |
| C(2) | .3864(2) | .5533(2) | .0026(2) | .0024(1) | .0045(2) | .0027(2) |
| N(3) | .4543(2) | .4385(2) | .0035(1) | .0029(2) | .0075(3) | .0042(3) |

TABLE II (continued)

| Atom | x | y | $\beta_{11}$ | $\beta_{22}$ | $\beta_{33}$ | $\beta_{12}$ |
|---|---|---|---|---|---|---|
| N(4) | .3329(2) | .2772(2) | .0039(2) | .0032(2) | .0076(3) | .0045(3) |
| N(5) | .2412(2) | .1308(2) | .0060(2) | .0032(2) | .0154(4) | .0052(3) |

* The figures in the parentheses are the standard deviations multiplied by $10^4$.

are compared with the observed structure factors in Table III. Each data group in Table III is preceded by the value for h , the letter k , and the value for $\ell$ which define the indices for the particular data group. The columns of Table III are k , $F_{obs.} \times 10$ , $F_{calc.} \times 10$, in that order. A minus sign in the second column indicates a "less-than", and the numerical value which follows the negative sign is the minimum observable F . An asterisk following a value in the second column means that the reflection in question has been given a weight of zero in the least squares refinement.

TABLE III. Columns are k , $10\times F_{obs.}$ , $10\times F_{calc.}$

TABLE III (continued)

## DISCUSSION

The bond distances and angles for cyanuric triazide are presented in figure 5. For bond distances, the average standard deviation estimated from the uncertainties listed in Table II is 0.002 Å. This uncertainty is a measure of the precision of these distances. When the uncertainties in the unit cell parameters are considered, this estimate is increased by an order of magnitude and represents the accuracy of the measurements. The hexagonal symmetry and planar configuration of the structure, however, cause the standard deviations in the bond angles to be independent of errors in the unit cell parameters. The standard deviation for bond angles is 0.17°. The average C-N bond distance within the triazine ring is 1.339 Å, from which the two crystallographically distinct C-N bonds deviate by 0.003 Å. This deviation is 1.5 "precision" standard deviations from the mean and can hardly be considered as significant. (The uncertainties in the unit cell parameters cause only an uncertainty in the scale of this deviation and, thus, may be neglected.) It is concluded that the C-N bonds in the triazine ring are chemically equivalent.

Any discussion of carbon-nitrogen bond distances suffers from the fact that no carbon-nitrogen double bonds have been measured. However, reliable values for carbon-nitrogen bonds with bond numbers 1.0 and 1.5 are 1.48 and 1.31 Å, respectively (9). Several authors (4, 9, 13) have suggested 1.24 Å as the carbon-nitrogen double bond distance. These values were used to construct a plot of carbon-nitrogen bond distances versus bond number, and a smooth curve was

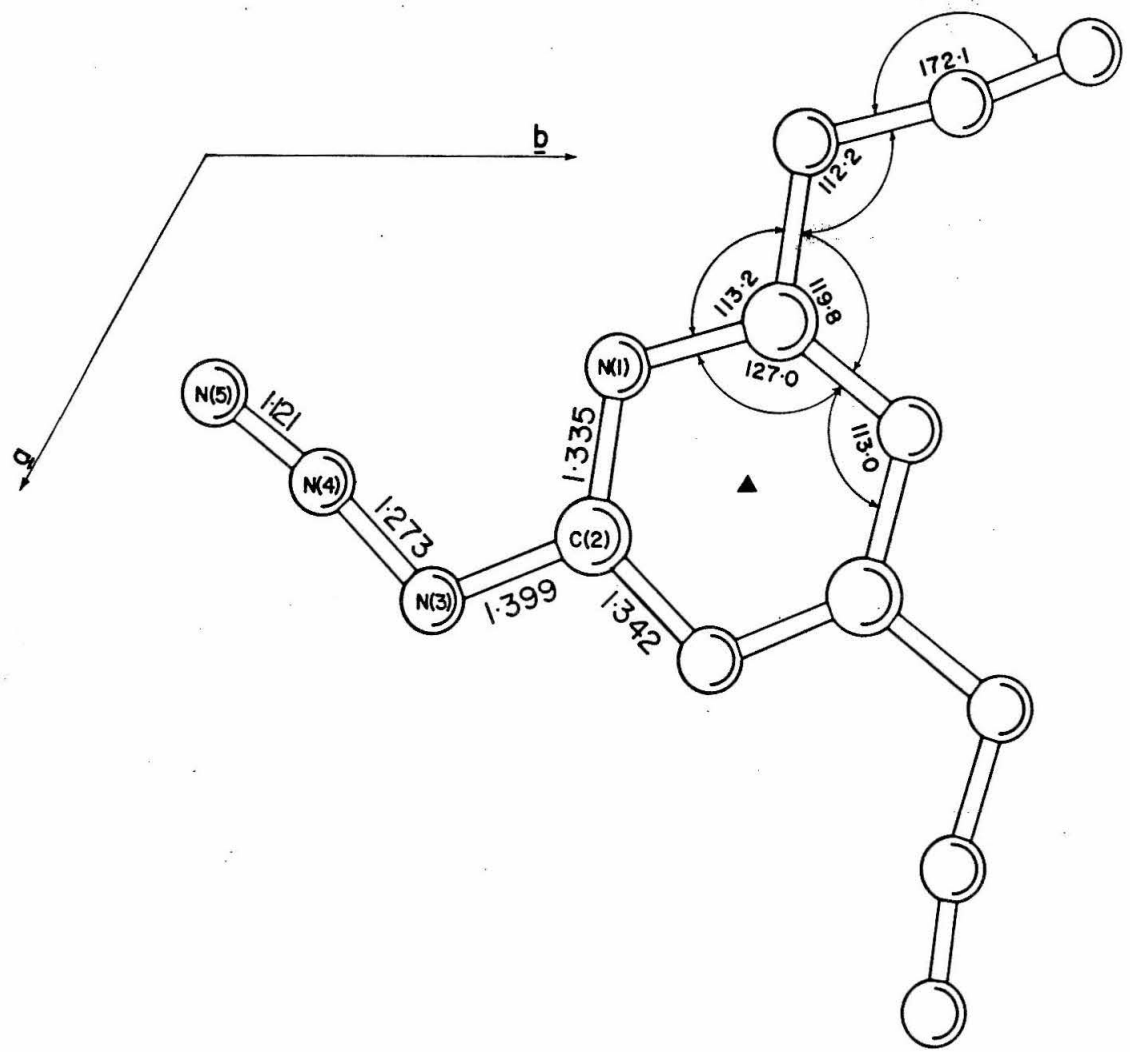


Figure 5, Bond Distances and Angles for Cyanuric Triazide.

drawn through these three points. From this curve, the bond numbers for the C-N bonds in the triazine ring of cyanuric triazide were found to be 1.39; for the C(2)-N(3) bonds, 1.22 . Further, if it is assumed that the N-N distances in the azide group (which do not differ significantly from the N-N distances in methyl azide (10)) result from equal contributions of configurations A and B (11), the bond distances in cyanuric triazide are explained by a resonance hybrid of the canonical structures I through V, each contributing to the extent which is indicated in figure 6.

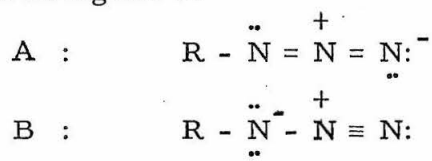

The 172.1° N-N-N bond angle in the azide group represents a significant departure from linearity. This departure, however, results from short intermolecular contacts rather than from the electronic structure of the molecule. As indicated in figure 7, the closest intermolecular approach, 3.083 Å, involves N(3) and atom H (the corresponding azide nitrogen related to N(3) by the $2_1$ screw axis at x = 1/2, y = 1/2). This interaction limits in one direction the rotation of the molecule about the $\bar{6}$ axis at the center of each molecule. Rotation in the other direction is prevented by the 3.169 Å distance between N(5) and atom A (the terminal azide nitrogen related to N(5) by the $6_3$ axis at x = 0 , y = 0). In the absence of free rotation about the $\bar{6}$ axis, the close nonbonded interactions between N(4) and atom F and between N(5) and atom A (and the third terminal azide nitrogen related to N(5) by the $6_3$ axis) supply the bending torque which is re-

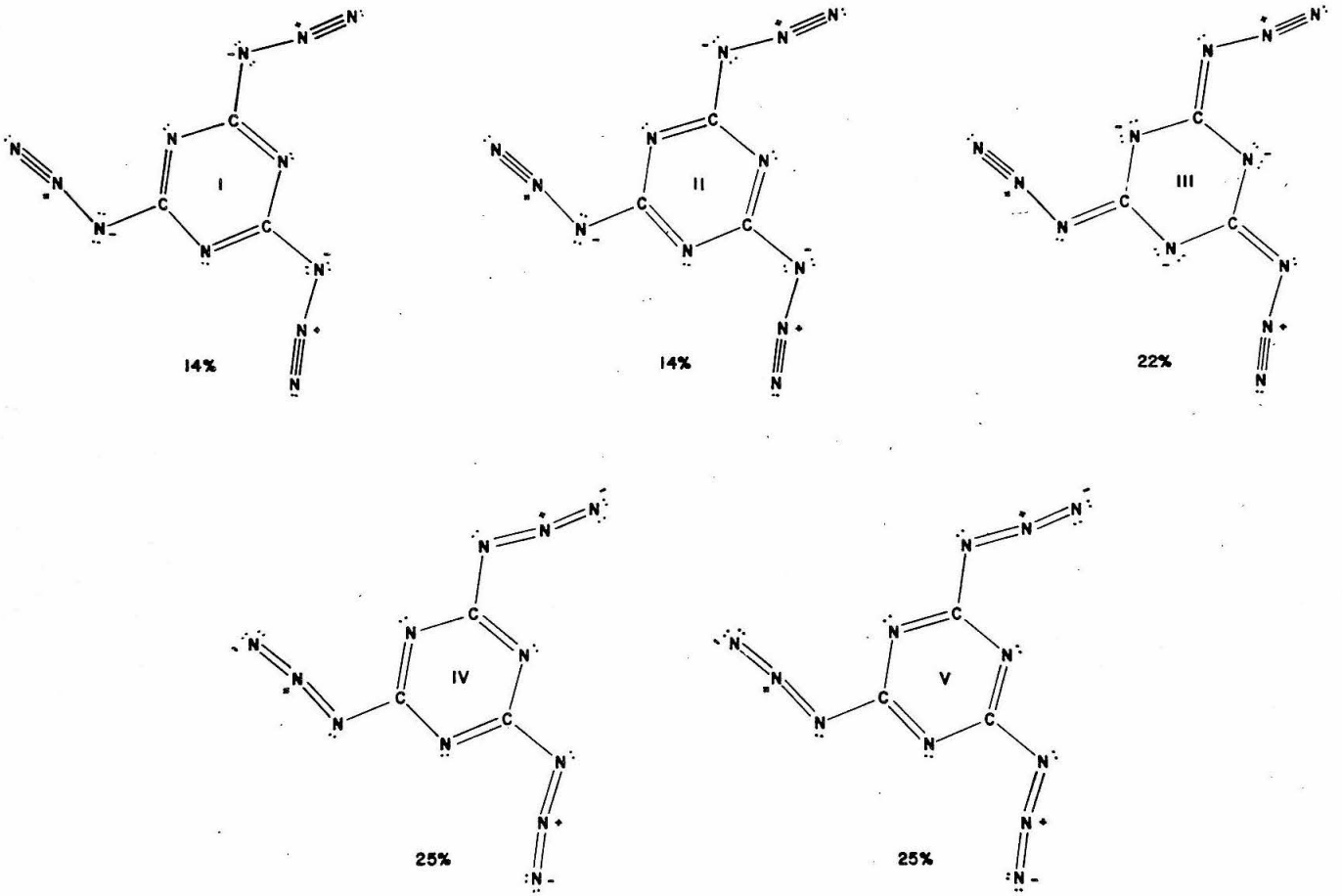


Figure 6. Canonical Structures and Percentage Contribution for the Resonance Hybrid of Cyanuric Triazide.

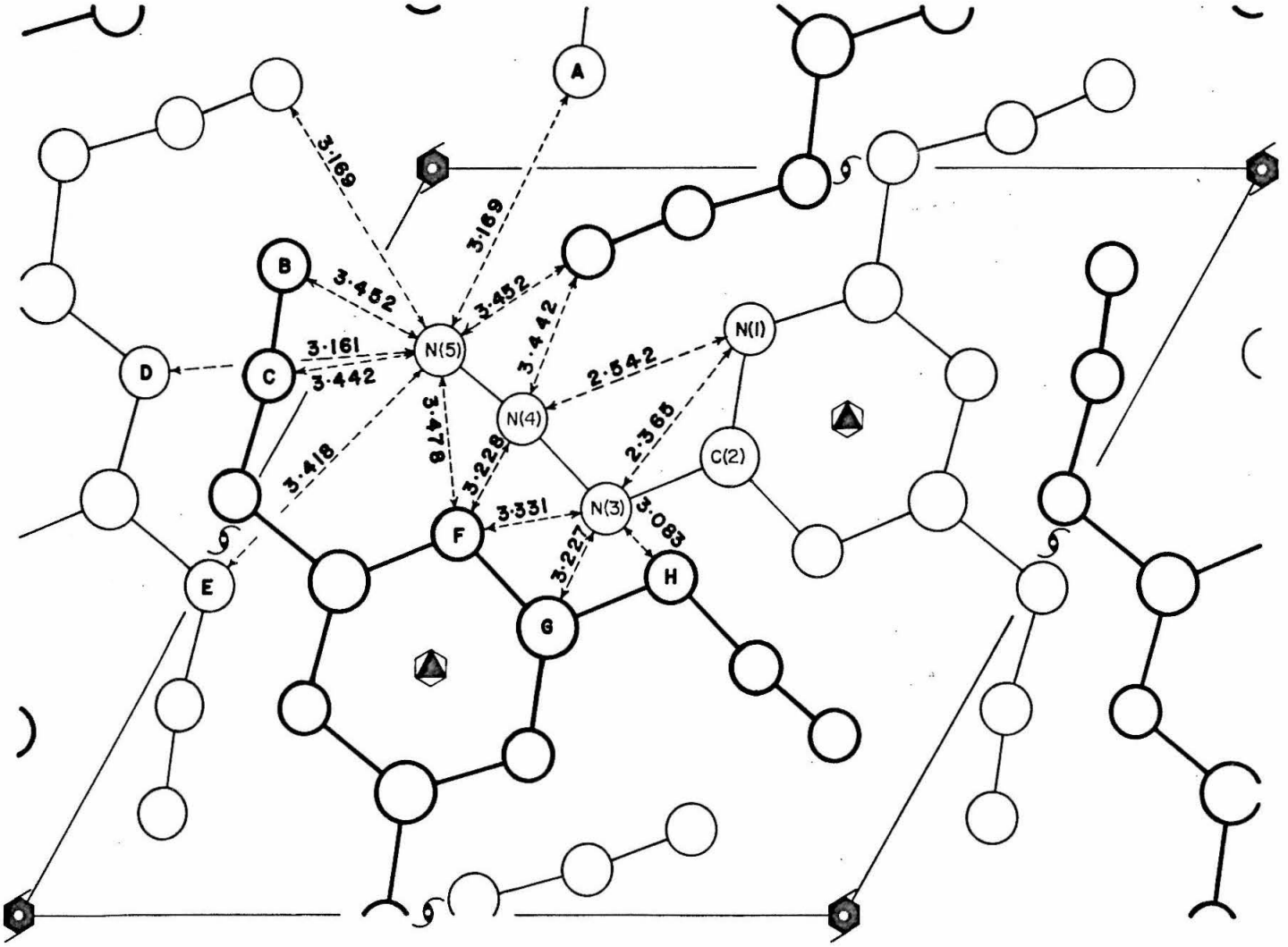


Figure 7. Packing Diagram for Cyanuric Triazide. Light lines represent molecules at z = 1/4; and heavy lines, z = 3/4.

sponsible for the non-linearity of the azide group.

All intermolecular distances which are less than 3.5 Å are shown in the packing diagram, figure 7. Also, two nonbonded intramolecular distances are shown. In spite of the short distance between N(3) and atom H, the interaction between N(1) and N(4) along with similar interactions involving C(2) (which have been omitted from figure 7 to avoid overcrowding the drawing), cause the angle N(1)-C(2)-N(3), 119.8°, to be larger than the other exterior angle, 113.2°, at C(2).

Knaggs' (8) two-dimensional data were used along with her spatial parameters as input to six isotropic least squares cycles. The R-value was reduced from .12 to 0.068†. The structure which resulted is in good agreement with this work. The spatial parameters are compared with the low temperature structure in Table IV, and the bond distances and angles are compared in Table V.

It is concluded that at room temperature, as well as -110°C, the C-N bonds in the triazine ring are chemically equivalent. Further, the azide group is bent at the middle nitrogen at both temperatures by packing considerations.

---

† The refinement was essentially complete after the first cycle. However, six cycles were calculated as one job because of the extremely short computation time. Sixteen seconds were required for the six cycles.

TABLE IV

Comparison of Refined Knaggs' Structure with This Work

| | Refinement of Knaggs' Data | | | This Work | |
|---|---|---|---|---|---|
| Atom | x | y | B | x | y |
| N(1) | .214(2)* | .488(2) | 1.9(4) | .2120(2) | .4878(2) |
| C(2) | .389(2) | .556(2) | 1.7(5) | .3864(2) | .5533(2) |
| N(3) | .454(2) | .442(2) | 1.8(4) | .4543(2) | .4385(2) |
| N(4) | .337(2) | .282(2) | 2.0(4) | .3329(2) | .2772(2) |
| N(5) | .245(2) | .134(2) | 2.6(4) | .2412(2) | .1308(2) |

* The figures within the parentheses are the standard deviations multiplied by $10^3$ for the x and y parameters from Knaggs' data; by 10 for the isotropic temperature parameters, B's; and by $10^4$ for the x and y parameters of this work.

TABLE V

Comparison of Molecular Dimensions

Distances in Å

| Bond | This Work | Refinement with Knaggs' Data | Knaggs' Structure (8) | Hughes' Structure (5) |
|---|---|---|---|---|
| N(1)-C(2) | 1.335 | 1.331 | 1.31 | 1.33 |
| C(2')-N(1)* | 1.342 | 1.326 | 1.38 | 1.33 |
| C(2)-N(3) | 1.399 | 1.380 | 1.38 | 1.50 |
| N(3)-N(4) | 1.273 | 1.250 | 1.26 | 1.29 |
| N(4)-N(5) | 1.121 | 1.129 | 1.11 | 1.09 |
| | Angles in Degrees | | | |
| Bond Angle | | | | |
| N(1)-C(2)-N(1')** | 127.0 | 127.3 | 127 | 137 |
| C(2')-N(1)-C(2) | 113.0 | 112.7 | 113 | 103 |
| N(1)-C(2)-N(3) | 119.8 | 118.5 | 120 | 112.5 |

TABLE V (continued)

| Bond Angle | This Work | Refinement with Knaggs' Data | Knaggs' Structure (8) | Hughes' Structure (5) |
|---|---|---|---|---|
| C(2)-N(3)-N(4) | 112.2 | 113.6 | 114 | 109 |
| N(3)-N(4)-N(5) | 172.1 | 172.8 | 180 | 165 |

* C(2') is the carbon in the triazine ring which is related to C(2) by the operation of the $\bar{6}$ axis.

** N(1') is the nitrogen in the triazine ring which is related to N(1) by the operation of the $\bar{6}$ axis.

## REFERENCES FOR PART II


1. S. C. Abrahams, R. S. Collins, W. N. Lipscomb, and T. B. Reed, Rev. Sci. Instrum. 21, 396 (1950).

2. W. H. Bragg, Nature 134, 138 (1934).

3. D. J. Duchamp, "User's Guide to the CRYRM Crystallographic Computing System," Gates and Crellin Laboratories of Chemistry, California Institute of Technology, Pasadena, California (1964).

4. D. Hall, Acta Cryst. 18, 955 (1965).

5. E. W. Hughes, J. Chem. Phys. 3, 1 and 650 (1935).

6. E. W. Hughes, J. Am. Chem. Soc. 63, 1737 (1941).

7. "International Tables for X-ray Crystallography," Vol. II, (1959), Kynoch Press, Birmingham, p. 295.

8. I. E. Knaggs, Proc. Roy Soc. 150A, 576 (1935); Nature 135, 268 (1935); J. Chem. Phys. 3, 241 (1935).

9. R. E. Marsh, R. Bierstedt, and E. L. Eichhorn, Acta Cryst. 15, 310 (1962).

10. L. Pauling and L. O. Brockway, J. Am. Chem. Soc. 59, 13 (1937).

11. L. Pauling, The Nature of the Chemical Bond, 3rd Ed., Cornell University Press, Ithaca, New York (1965), p. 272.

12. J. Rollet, "Instructions for Operating Low-Temperature Weissenberg Camera," Gates and Crellin Laboratories of Chemistry, California Institute of Technology, Pasadena, California (1950).

13. P. Vaughan and J. Donohue, Acta Cryst. 5, 530 (1952).

# APPENDIX

## GENERAL REMARKS

The following programs and subroutines were written in the Macro Assembly Program (MAP) language (4) as part of the CRYRM crystallographic computing system (1). All have been tested and successfully used in the computations associated with the work reported in this thesis. The Wilson and the Howells, Phillips, and Rogers routines have been successfully used by several other investigators and may be assumed to be free of error. The "Statistical Phasing Program" has been used successfully in several monoclinic space groups as well as the centric triclinic space group.

The "Hexagonal Least Squares Program" has been debugged for only two space groups, $P\,6_3/m$ and $P\,6_3$. Consequently, the user should accept the possibility of an error or two when refining in any of the other hexagonal or trigonal space groups.

The remarks in this appendix are restricted to the methods of computation which were employed in these programs. For details concerning the use of these programs (i. e., format of input cards, etc.), the reader is referred to the "User's Guide to the CRYRM Crystallographic Computing System" (1). Details about the MAP language are given in "I. B. M. 7090/7094 Programming System: Macro Assembly Program (MAP) Language," (4) and "Reference Manual I. B. M. 7090 Data Processing System" (7).

# WILSON STATISTICS SUBROUTINE

## Introduction

This subroutine is used with the "Data Tape Preparation Program" (reference 1, chapter 5), in the prepare mode, to obtain by Wilson's method (10) an approximate value for the scaling factor and for the over-all isotropic temperature factor. The following is a brief description of the method.

If $F_{\underset{\sim}{h}}$ is not on an absolute scale, a scaling factor, k , must be inserted in the usual expression for the structure factor.

$$kF_{\underset{\sim}{h}} = \sum_j f_j \exp\left(-B \frac{\sin^2\theta}{\lambda^2}\right) \exp\left(2\pi i \underset{\sim}{h} \cdot \underset{\sim}{r}_j\right) \tag{A1}$$

The observed intensity for reflection $\underset{\sim}{h}$ is proportional to $|kF_{\underset{\sim}{h}}|^2$, and for simplicity, the constant of proportionality is assumed to be unity.

$$I_{\underset{\sim}{h}} = |kF_{\underset{\sim}{h}}|^2 \tag{A2}$$

$$|kF_{\underset{\sim}{h}}|^2 = \left\{\sum_j f_j \exp\left(-B \frac{\sin^2\theta}{\lambda^2}\right)\exp\left(2\pi i \underset{\sim}{h} \cdot \underset{\sim}{r}_j\right)\right\}$$

$$\left\{\sum_i f_i \exp\left(-B \frac{\sin^2\theta}{\lambda^2}\right)\exp\left(-2\pi i \underset{\sim}{h} \cdot \underset{\sim}{r}_i\right)\right\} \tag{A3}$$

Equation A3 may be rewritten

$$k^2|F_{\underset{\sim}{h}}|^2 = \sum_j f_j^2 \exp\left(-2B \frac{\sin^2\theta}{\lambda^2}\right) + \sum_{i\neq j}\sum f_i f_j \exp\left(-2B \frac{\sin^2\theta}{\lambda^2}\right)$$

$$\exp\left\{2\pi i \underset{\sim}{h} \cdot (\underset{\sim}{r}_j - \underset{\sim}{r}_i)\right\} . \tag{A4}$$

Reciprocal space is now divided into several shells, each containing a sufficient number of reflections (about 100) for good statistics. Within each shell, equation A4 is averaged over $\underset{\sim}{h}$. Since the expectation value of $\exp\{2\pi i \underset{\sim}{h}\cdot(\underset{\sim}{r}_j - \underset{\sim}{r}_i)\}$ is zero, the following is obtained.

$$k^2 < |F_{\underset{\sim}{h}}|^2 >_{\underset{\sim}{h}} = < \Sigma f_j^2 >_{\underset{\sim}{h}} \exp\left(-2B < \frac{\sin^2\theta}{\lambda^2} >\right) \qquad \text{(A5)}$$

$$\ell n \frac{< |F_{\underset{\sim}{h}}|^2 >_{\underset{\sim}{h}}}{< \Sigma f_j^2 >_{\underset{\sim}{h}}} = -2\ell n k - 2B < \frac{\sin^2\theta}{\lambda^2} > \qquad \text{(A6)}$$

From equation A6 it is seen that a plot of $\ell n\,(< |F_{\underset{\sim}{h}}|^2 >_{\underset{\sim}{h}} / < \Sigma f_j^2 >_{\underset{\sim}{h}})$ versus $<\sin^2\theta/\lambda^2>$ should be linear with slope $-2B$ and intercept $-2\ell n\, k$.

Mechanics of the Calculation

The wavelength which is entered on the DO WILSON STATISTICS card is used only to define the outer limit of the sphere of reciprocal space. (Any reflection for which $\sin^2\theta/\lambda^2$ exceeds the reciprocal of the square of this wavelength is neglected.) This sphere is divided into ten shells (unless another number is specified on the DO WILSON STATISTICS card) of equal increments in $\sin^2\theta/\lambda^2$. This method of division puts approximately the same number of reflections in each shell. Those reflections which fall in the innermost shell (i.e., those reflections with the smallest values for $\sin^2\theta/\lambda^2$) are disregarded. For the other shells, $|F_{\underset{\sim}{h}}|^2$, $\Sigma f_j^2$, $\sin^2\theta/\lambda^2$ are summed, and the reflections in the particular shell are counted. At the conclusion of the

first pass of the data tape, average values for $|F_{\underset{\sim}{h}}|^2, \Sigma_j f_j^2$, and $\sin^2\theta/\lambda^2$ are calculated for each shell. The following quantities are then computed for each shell and printed out:

$$\ell n \frac{<|F_{\underset{\sim}{h}}|^2>_{\underset{\sim}{h}}}{<\Sigma_j f_j^2>_{\underset{\sim}{h}}} \qquad \text{and} \qquad <\sin^2\theta/\lambda^2> \quad .$$

The program also fits a straight line to these data points by the method of least squares, each point being given unit weight. The least squares values for k, the scaling factor for $F_{\underset{\sim}{h}}$, and for B, the over-all isotropic temperature factor, are printed out.

Care should be exercised when systematic extinctions are present, because those reflections which are not extinguished are expected to be stronger than normal by a factor which is equal to the multiplicity of the symmetry operation responsible for the extinctions. For example, a body-centered lattice causes half of the reflections to be extinguished and the other half to be twice as intense as normal. No problem results if the extinguished reflections are included on the data tape with $|F_{\underset{\sim}{h}}|$ identically zero.

However, these reflections are customarily not written on the data tape, and the following procedure is necessary. For centered space groups, the number of atoms in the unit cell multiplied by the multiplicity of the centering is entered on the NUMBERS OF ATOMS card (reference 1, chapter 5). For glide planes, the data are corrected by specifying the glide plane on a GLIDE PLANES card. For screw axes, the number of reflections which are affected is so small that no correction is made.

If the APPLY WILSON SCALING FACTOR card is recognized

by the program, a second pass of the data tape results. During this pass, the over-all isotropic temperature factor is written on the tape, each $|F_h|$ is multiplied by the least squares $k$, and each weight $(1/\sigma(I))^{\sim}$ is divided by $k^2$. The result is a data tape with the data on an approximately absolute scale.

## HOWELLS, PHILLIPS, AND ROGERS SUBROUTINE

### Introduction

The "Howells, Phillips, and Rogers Subroutine" is used (usually in conjunction with the "Wilson Statistics Subroutine") with the "Data Tape Preparation Program" (reference 1, chapter 5) in the prepare mode to decide, if possible from the distribution of the intensity data, if the structure possesses a center of symmetry. The method is based on the work of Wilson (11) and Howells, Phillips, and Rogers (3).

### Mechanics of the Calculation

If N(z) is the fraction of reflections whose intensities are less than a fraction, z , of the local average intensity, the following theoretical distributions are observed (3). For acentric crystals

$$N(z) = 1 - \exp(-z) , \tag{A7}$$

and for centric crystals

$$N(z) = \operatorname{erf}\left(\tfrac{1}{2}z\right)^{\frac{1}{2}} . \tag{A8}$$

The symbol "erf" represents the error function (5). Plots of these two functions are seen in figure 1, Part I, of this thesis. There is an appreciable difference inthe curves for the two theoretical cases, particularly for small values of z . These theoretical results are applicable only if other systematic variations in the distribution of the intensities,such as the attenuation which results from the fall in scattering factors and thermal vibration, are eliminated. Consequently, reciprocal space is divided into shells identical to those used in the "Wilson Statistics Subroutine." Local average intensities are com-

puted for each shell, and the N(z)'s are computed for selected values of z . The N(z)'s from the different shells are then averaged, and the average N(z) is plotted as a function of z .

This calculation requires local average intensities for each shell. If the "Wilson Statistics Subroutine" has been used, the local averages are in memory, but if not, this subroutine causes the local averages to be computed for ten shells of reciprocal space. (Once again, the innermost shell is disregarded.) The results, twenty values for N(z) for each z from 0 to 1.0 in increments of 0.05, are compared with the two theoretical distributions in the output.

It should be noted that if the "Wilson Statistics Subroutine" alone is used, only one pass of the data tape is necessary. However, either the APPLY WILSON SCALING FACTOR card or the DO HOWELLS, PHILLIPS, AND ROGERS CALC. card causes a second pass of the tape. Both operations (the scaling and the Howells, Phillips, and Rogers calculation) may be performed simultaneously during the second pass of the data.

# STATISTICAL PHASING PROGRAM

## Introduction

This program is useful as a starting point for most of the "direct methods" of X-ray crystallography. The unitary structure factor, $U_{\underset{\sim}{h}}$, normalized unitary structure factor, $E_{\underset{\sim}{h}}$, and the expectation value of $U^2$, $\epsilon_2$, are computed for each reflection during the first pass of the data tape. At the conclusion of the first pass of the tape, the distribution of the $E_{\underset{\sim}{h}}$'s is computed and compared with the theoretical two-tailed Gaussian. Other distribution criteria are also calculated. As an option, the normalized unitary structure factors, $E_{\underset{\sim}{h}}$'s, may be listed in the Sayer's relationships (8) which are essentially the same as the $\Sigma_2$ relationships of Hauptman and Karle (2).

In its present form, this program is applicable only to the centric space groups in the monoclinic and triclinic systems. If an acentric space group is detected, an error message will result. However, no serious error should occur if the centric space group which most closely approximates the desired acentric space group is used. If unitary structure factors are needed for a crystal not of the monoclinic or triclinic systems, the monoclinic or triclinic space group which is a subgroup of the desired space group should be used. However, the list of Sayer's relationships will be incomplete in this case.

## Mechanics of the Calculation

From the number of each kind of atom (from *the NUMBERS*

OF ATOMS card) and the scattering factors which are listed on the tape for each reflection, $\sum_j f_j$ , $\sum_j f_j^2$ , and $\sum_j f_j^3$ are computed, consideration being given to the attenuation which results from the overall isotropic temperature factor. Next, $\underset{\sim}{U_h}$ , $\epsilon_2$ , $\epsilon_3$ , and $\underset{\sim}{E_h}$ are computed according to the following equations.

$$\underset{\sim}{U_h} = \frac{\underset{\sim}{F_h}}{\sum_j f_j} \tag{A9}$$

$$\epsilon_2 = \frac{\sum_j f_j^2}{(\sum_j f_j)^2} \tag{A10}$$

$$\epsilon_3 = \frac{\sum_j f_j^3}{(\sum_j f_j)^3} \tag{A11}$$

$$\underset{\sim}{E_h} = \frac{\underset{\sim}{U_h}}{\epsilon^{\frac{1}{2}}} \tag{A12}$$

The $\underset{\sim}{E_h}$'s and $\underset{\sim}{U_h}$'s for certain classes of reflections must be divided by $\sqrt{2}$, $\sqrt{3}$, or 2 , depending on the symmetry elements which are present. This is done automatically for the centric monoclinic and triclinic space groups.

In addition to the distribution of the $\underset{\sim}{E_h}$'s , the expectation values for $|\underset{\sim}{E_h}|$ , $|\underset{\sim}{E_h^2}-1|$ , and $\underset{\sim}{E_h^2}-1$ are computed and compared with the theoretical values for both centric and acentric crystals (6).

The Sayer's, or $\Sigma_2$ , relationship is expressed in equation A13 and is a weighted sum of individual sign relationships of the type represented by equation A14.

$$s(\underset{\sim}{h}) \approx s \sum_{\underset{\sim}{h'}} (E_{\underset{\sim}{h'}} E_{\underset{\sim}{h}+\underset{\sim}{h'}}) \qquad \text{(A13)}$$

$$s(\underset{\sim}{h}) \approx s(\underset{\sim}{h'})\, s(\underset{\sim}{h}+\underset{\sim}{h'}) \qquad \text{(A14)}$$

The symbol s represents the sign (plus or minus) of the quantity which follows. For example, $s(\underset{\sim}{h'})$ means the sign of the structure factor for reflection $\underset{\sim}{h'}$. The "List Sayer's Relationships" option prints out the indices for reflection $\underset{\sim}{h}$, the $E_{\underset{\sim}{h}}$, and follows this with a list of all the pairs of reflections which fulfill the above relationships.

If the LIST SAYER'S RELATIONSHIPS card is recognized, a list is stored in memory of all the $E_{\underset{\sim}{h}}$'s which are greater than the E(MIN) (1.5 if no value is entered on the LIST SAYER'S RELATIONSHIPS card). The coefficient, $\epsilon_3/\epsilon_2^{3/2}$, for use in the probability relationship (equation A15) is stored along with the corresponding $E_{\underset{\sim}{h}}$'s. Next, a section of memory, "the sphere," is cleared for future storage of $E_{\underset{\sim}{h}}$'s as a function of $\underset{\sim}{h}$. The coefficient and the $E_{\underset{\sim}{h}}$ are combined into one 36-bit word for each reflection. The coefficient is put in bits s-17; the $E_{\underset{\sim}{h}}$, in bits 18-35. This compound word is stored as a function of $\underset{\sim}{h}$ in "the sphere" by the routine which is used for a similar purpose in the Fourier program (reference 1, chapter 7). The reflection $\underset{\sim}{h}$ (in equation A13) is taken from the list of $E_{\underset{\sim}{h}}$'s and is combined with every reflection in the list, $\underset{\sim}{h'}$, to form reflection $\underset{\sim}{h}+\underset{\sim}{h'}$. For each such reflection, $\underset{\sim}{h}+\underset{\sim}{h'}$, the appropriate word in "the sphere" is examined to see if the $E_{\underset{\sim}{h}+\underset{\sim}{h'}}$ is greater than E(MIN). Since "the sphere" had been cleared before the compound words were stored, the only non-zero words in "the sphere" are those for which

$E_{\underset{\sim}{h}+\underset{\sim}{h}'}$ is greater than E(MIN). When a sign relationship is found (i.e., when $E_{\underset{\sim}{h}+\underset{\sim}{h}'} > E(MIN)$), the indices of reflection $\underset{\sim}{h}'$ and $\underset{\sim}{h}+\underset{\sim}{h}'$ are printed within parentheses, separated by a /. This is followed by the signed product $E_{\underset{\sim}{h}'} \times E_{\underset{\sim}{h}+\underset{\sim}{h}'}$ and the probability (equation A15) that the particular sign relationship is true.

$$P_+(\underset{\sim}{h}, \underset{\sim}{h}') = \tfrac{1}{2} + \tfrac{1}{2} \tanh \{\epsilon_3/\epsilon_2^{3/2} |E_{\underset{\sim}{h}} E_{\underset{\sim}{h}'} E_{\underset{\sim}{h}+\underset{\sim}{h}'}|\} \qquad \text{(A15)}$$

The $\epsilon_3/\epsilon_2^{3/2}$ in equation A15 is the average value for the three reflections. (There usually is very little variation in the value of $\epsilon_3/\epsilon_2^{3/2}$, especially if the atoms are roughly equal in scattering power.)

When all of the possible relationships for a particular reflection are found, the maximum probability (i.e., the probability which would result if all the signs in the $\Sigma_2$ relationship are the same) is calculated according to equation A16.

$$P_+(\underset{\sim}{h}) = \tfrac{1}{2} + \tfrac{1}{2} \tanh \{\epsilon_3/\epsilon_2^{3/2} |E_{\underset{\sim}{h}}| \underset{\underset{\sim}{h}'}{\Sigma} E_{\underset{\sim}{h}'} E_{\underset{\sim}{h}+\underset{\sim}{h}'}\} \qquad \text{(A16)}$$

Next, the number of sign relationships in the $\Sigma_2$ relationship is printed out.

The reader is referred to page 13-3 of the "User's Guide to the CRYRM Crystallographic Computing System" (1) for an interpreted example of the output.

# HEXAGONAL LEAST SQUARES PROGRAM

## Introduction

The "Hexagonal Least Squares Program" is an integral part of the CRYRM library of least squares programs. All of these programs are called into memory by the LEAST SQUARES card or the STRUCTURE FACTOR CALCULATION card. The particular least squares program which is read into the computer is determined by the space group number. A space group number within the range 143-194 inclusive will call the "Hexagonal Least Squares Program" into memory.

This program, like all of the other CRYRM least squares programs, is based on the "Cubic Least Squares Program" which was written by N. C. Webb (reference 1, chapter 6). The basic matrix manipulation routines were taken directly from the cubic program. The cubic routines for the calculation of structure factors and derivatives have been replaced by routines specific for trigonal and hexagonal space groups. These trigonal and hexagonal routines are based upon the formulation of N. C. Webb (9).

## Mechanics of the Calculation

In the following discussion, all of the references to tables and page numbers refer to N. C. Webb's thesis (9). For each reflection, the structure factor and derivatives are calculated by summing over the atoms. All of the triple products in Table 1 on page 158 and Table 5 on page 173 are computed for each set of atomic coordinates. When the atom has anisotropic temperature factors, the twelve ex-

pressions in Table 6 on page 174 are also computed. From these quantities, the 18 expressions in Table 7, page 175, for trigonal space groups or the 24 expressions in Table 10, page 179, for hexagonal space groups, are computed. After all of these expressions have been calculated, the program goes to a routine which is specific for the particular space group and calculates the A's and B's and corresponding derivatives according to the expressions listed in Tables 8 and 9, pages 176 and 177, for trigonal space groups or in Tables 11 and 12, pages 180 and 181, for hexagonal space groups.

The matrix is assembled in the usual way, and the calculation continues by the least squares routines common to all the CRYRM least squares programs.

## REFERENCES FOR APPENDIX


1. D. J. Duchamp, "User's Guide to the CRYRM Crystallographic Computing System," Gates and Crellin Laboratories of Chemistry, California Institute of Technology, Pasadena, California (1964).

2. H. Hauptman and J. Karle, "Solution of the Phase Problem, I. The Centrosymmetric Crystal," A. C. A. Monograph No. 3, Edwards Brothers, Inc., Ann Arbor, Michigan (1953).

3. E. R. Howells, D. C. Phillips, and D. Rogers, Acta Cryst. 3, 210 (1950).

4. "I. B. M. 7090/7094 Programming System: Macro Assembly Program (MAP) Language," International Business Machines Corporation (1964).

5. E. Jahnke and F. Emde, Tables of Functions with Formulae and Curves, 4th Ed., Dover Publications, New York (1945).

6. I. L. Karle, K. Britts, and P. Gum, Acta Cryst. 17, 496 (1964).

7. "Reference Manual I. B. M. 7090 Data Processing System," International Business Machines Corporation (1962).

8. D. Sayer, Acta Cryst. 5, 60 (1952).

9. N. C. Webb, Ph. D. Thesis, California Institute of Technology (1963).

10. A. J. C. Wilson, Nature 150, 152 (1942).

11. A. J. C. Wilson, Acta Cryst. 2, 318 (1949).

# PROPOSITIONS

## PROPOSITION I

Thermochromism is the name given to any reversible dependence of color on temperature. This phenomenon is observed in many seemingly unrelated classes of compounds; however, the thermochromism of two types of molecules, the spiropyrans and the sterically hindered ethylenes, has seen extensive study (1, 4). Bianthrone I and dixanthylene II are the most striking examples of the latter class of compounds, and it is reasonable to assume that the mechanism for the color change is the same for both compounds in view of their similar structure. Briefly, the currently accepted theory involves a temperature dependent equilibrium between two molecular modifications; A, the pale yellow to colorless ground state, and B, the blue thermochromic modification. Solutions of bianthrone reversibly form a similar blue color at liquid nitrogen temperature when irradiated by ultraviolet light, and recent evidence indicates the existence of a third molecular modification in addition to form B which is present in these solutions (5). Photochromism is the name given to this latter phenomenon. In the crystal structure of type A bianthrone, the molecule exists in a folded conformation, rings A and B above the plane of the paper and rings C and D below the plane of the paper (2). Chemical evidence (8, 9) indicates the ability of the two molecular halves to pass one another in the transition to the thermochromic state. Speculation, therefore, holds the thermochromic form B to be a conformation in which both molecular halves are planar and twisted about the central double bond, i.e., rings A and D are above the plane of the paper and rings B and C are below. This theory apparently was

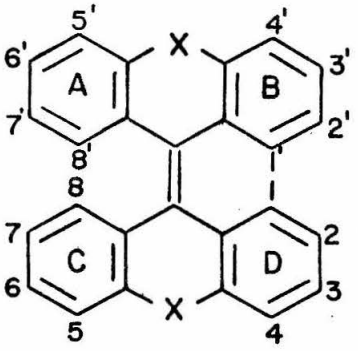


I X = C=O

II X = O

disproved by Mills and Nyburg (6) who reported the folded molecular conformation for both the ground state and the thermochromic state of dixanthylene on the basis of an X-ray crystal structure analysis.

It is proposed that the two structures reported by Mills and Nyburg are really two different crystalline forms of the ground state of dixanthylene. They claim to have produced crystals of the thermochromic form of dixanthylene by subliming the colorless type A crystals at 250°C and $10^{-3}$ mm. Hg. The crystals produced by this procedure exhibit the thermochromic color, but a rough calculation from the spectroscopic data (7) indicates the concentration of the thermochromic form at 250°C to be 0.81 per cent. This is sufficient to impart the blue color, but could hardly be considered sufficient to be observed by X-ray diffraction. These authors have examined their data for lattice disorder and found none; however, this is not surprising,as disordered carbon atoms present in this concentration correspond to the scattering power of 0.05 electrons. Hence, it is doubtful that the thermochromic form can be thermally produced in sufficient concentration for X-ray studies.

There are, however, other methods of producing the colored modification B. Low temperature irradiation has already been mentioned, but because of the complex nature of the colored modification (5), and because this is purely a liquid phase phenomenon, it is not suited for production of crystals of the colored modification B. Kortüm, et al. (3, 10) have observed the precipitation of an intensely green-colored, solid material when red sulfuric acid solutions of various derivatives of bianthrone are added to ice water. Generally, the green solid produced in this way reverts to the colorless state when exposed to light; however, the green modification of 1, 3, 6', 8'-tetramethylbianthrone (which is not attainable thermally) was reported to be stable to light (3). Kortüm and Bayer (5) have subsequently produced solutions of this green modification by adding a sulfuric acid solution of the 1, 3, 6', 8'-tetramethyl derivative to a 10 per cent water, 90 per cent alcohol solution at 183°K. By spectroscopic measurements, they distinguished this colored modification from the photochromic state (5). This particular derivative does not exhibit the temperature-dependent change of color, presumably because of the increased activation energy and enthalpy of transition associated with the increased steric hindrance at the 1, 8'-positions; however, the similarity of the ultraviolet and visible spectrum with that of the thermochromic B modification of I led to the identification of this green modification as a thermochromic B state (5). Moreover, the intensity of the thermochromic band in the visible spectrum of this derivative indicated a concentration of the B modification twenty-five times as great as the B form of I at 455°K (5). Since the concentra-

tion of the colored modification of I is 4. 5 per cent at 455°K (7), this low temperature solution of the colored 1, 3, 6', 8'-tetramethyl derivative is presumably pure form B. By inference, the solid material which was precipitated from the ice water (vide ultra) is also pure form B.

Because of the stability of the B form of 1, 3, 6', 8'-tetramethylbianthrone, it is suggested that attempts be made to obtain large single crystals of this substance suitable for X-ray studies. Either slow addition of the sulfuric acid solutions to the ice water or some method of growing crystals from the water - alcohol solution should be tried. A three-dimensional X-ray crystal structure analysis of such crystals is proposed. The results of such a study would be of considerable interest in explaining the mechanism of thermochromism in compounds of this type.

References for Proposition I

1. J. H. Day, Chem. Rev. 63, 65 (1963).

2. E. Harnik and G. M. J. Schmidt, J. Chem. Soc., 1954, 3295.

3. G. Kortüm, W. Theilacker, H. Elliehausen, and H. Zeininger, Chem. Ber. 86, 294 (1953).

4. G. Kortüm, Angew. Chem. 70, 14 (1958).

5. G. Kortüm and G. Bayer, Ber. Bunsen Ges. Physik Chem. 67, 24 (1963); Angew. Chem. 75, 96 (1963).

6. J. F. D. Mills and S. C. Nyburg, J. Chem. Soc. 1963, 308 927.

7. W. Theilacker, G. Kortüm, and G. Friedheim, Chem. Ber. 83, 508 (1950).

8. W. Theilacker, Angew. Chem. 65, 216 (1953).

9. W. Theilacker, G. Kortüm, and H. Elliehausen, Z. Naturforsch. 9b, 167 (1954).

10. W. Theilacker, G. Kortüm, H. Elliehausen, and H. Wilski, Chem. Ber. 89, 1578 (1956).

## PROPOSITION II

The thermochromic properties of rubrene (5, 6, 11, 12-tetraphenylnapthacene) I, first reported by Schönberg, Mustafa, and Asker (7), have recently been investigated by Kim, Smith, Beineke, and Day (5). The observed thermochromism in rubrene is thought to be due to a thermal quenching of the yellow fluorescence along with measurable changes in the absorption spectrum. It was found that the absorption intensity is approximately doubled at each absorption maximum as the temperature is lowered from room temperature to -195°C; however, the explanation given by Kim, et al. is unsatisfactory. The fact that no new peaks appear in the spectrum and no old peaks disappear was interpreted as evidence against thermal generation of any new molecular species (5). However, integration of the area under the absorption curves in the region of the $^1$La peak at both room temperature and -195°C yields a value for the ratio of the area at -195°C to the area at room temperature of 1.44, whereas the ratio expected from the known contraction of the solvent (22.5 per cent at -195°C) is 1.29. Hence, it is seen that the oscillator strength of the transition responsible for this band changes as the temperature is decreased to -195°C. Such a change in oscillator strength is impossible when only one molecular species is present.

It is proposed that the temperature dependence of the absorption spectrum of rubrene can be explained in terms of a temperature dependent equilibrium between two molecular conformations of rubrene. The absorption spectra of both molecular conformations

are almost identical, differing only in intensity*. Inasmuch as rubrene represents a highly strained structure, such an equilibrium between two conformations separated by a sizable barrier is reasonable, and as will be shown, there is a fair amount of evidence in support of this mechanism.

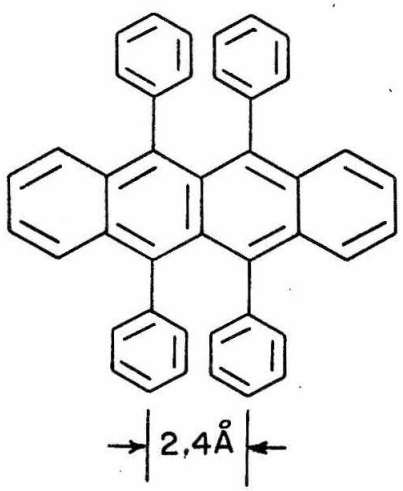


I

Figure 1.

The ultraviolet and visible spectrum of rubrene is essentially that of the napthacene nucleus shifted to longer wavelengths by the phenyl groups (4). The strongest peak is the $^1B_b$ band at 303 mμ. (log ε = 5.07). The $^1L_b$ peak is masked by the stronger $^1L_a$ peak which has considerable vibrational structure with three maxima occurring at 465 mμ. (log ε = 3.79), 495 mμ. (log ε = 4.07), and

* Such a temperature dependent equilibrium between two molecular species, along with the appearance of no new peaks and the disappearance of no old peaks, is only possible if one of the species has no absorption in the region measured or has an absorption very similar to that of the other species. An aromatic molecule with no absorption in the region measured is very unlikely.

530 mμ. (log ε = 4.08) (2, 3). Thus, it is reasonable that if the different conformations involve differences in the positions of the overcrowded phenyl groups alone, very little effect would be noticed in the spectrum.

Figure 1 indicates a distance between adjacent phenyl groups of 2.4 Å, whereas the equilibrium distance between two parallel phenyl groups is 3.4 Å (6). Hence, even with the phenyl groups perpendicular to the plane of the naphthacene nucleus, considerable strain is apparent in the structure. Some relief of this strain is realized if the phenyl groups slide past one another, i.e., up and down with respect to the plane of the naphthacene nucleus, as shown in Figure 2. Two conformations result if the strain is relieved in

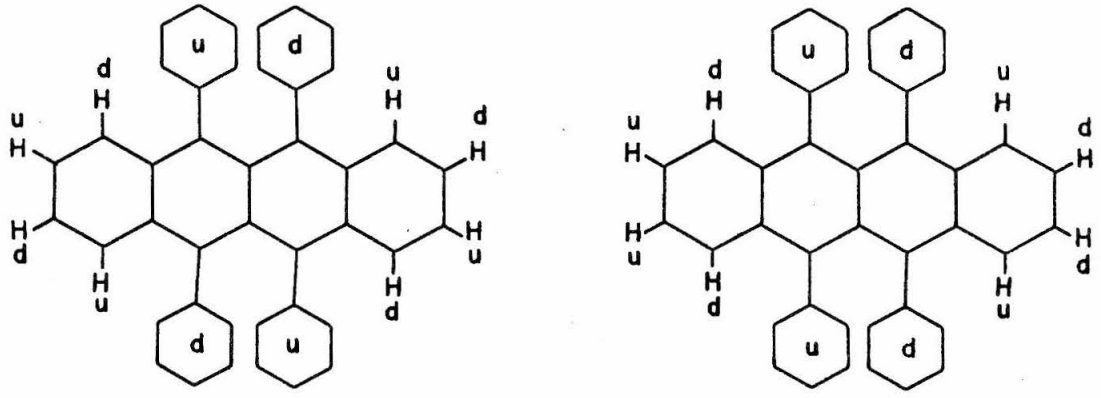


Acentric rubrene structure  Centric rubrene structure

Figure 2. Proposed structures for rubrene. u means above the plane of the paper, and d means below the plane of the paper.

this way, one centrosymmetric and one acentric. Presumably these structures would be approximately equal in energy, but the eclipsed hydrogens of the centrosymmetric structure could require a slightly higher energy content.

Evidence for the existence of two molecular conformations is obtained from crystallographic investigations. Taylor (8) reported two kinds of rubrene crystals, which he called rubrene A and rubrene B. Rubrene A could be distinguished from rubrene B only by X-rays because no well developed faces were present. Crystals of rubrene A belong to the triclinic system and are so badly twinned that Taylor was unable to measure the b-axis. He reported the following cell parameters for rubrene A:

$$\underset{\sim}{a} = 14.3\ \text{Å} \qquad \underset{\sim}{c} = 7.0\ \text{Å} \qquad d_{010} = n \times 7.3\ \text{Å}$$

$$\beta = 107^{\circ}$$

Assuming $n = 1$, the volume of the unit cell calculates to 698 $\text{Å}^3$.

Rubrene B is monoclinic, $P2_1/n$ with two molecules per unit cell and with the following cell parameters:

$$\underset{\sim}{a} = 17.9\ \text{Å} \qquad \underset{\sim}{b} = 10.1\ \text{Å} \qquad \underset{\sim}{c} = 8.8\ \text{Å}$$

$$\beta = 120^{\circ}$$

The structural investigation was not pursued beyond this point; however, the space group and number of molecules per unit cell yield valuable information about the molecular symmetry. Space group $P2_1/n$ with two molecules per unit cell requires a centrosymmetric molecule. Hence a centrosymmetric rubrene molecule is known to exist.

The only other crystallographic investigation of rubrene was

made by Akopyan, Avoyan, and Struchkov (1). These authors mention only one kind of rubrene crystal, with the following unit cell parameters:

$\underset{\sim}{a} = 7.16 \pm 0.02$ Å  $\underset{\sim}{b} = 9.15 \pm 0.05$ Å  $\underset{\sim}{c} = 14.65 \pm 0.04$ Å

$\alpha = 52^{\circ}20' \pm 15'$  $\beta = 115^{\circ}24' \pm 15'$  $\gamma = 112^{\circ}58' \pm 15'$

$V = 675$ Å$^3$

The unit cell volume agrees fairly well with that for Taylor's rubrene A, and they are presumed to be the same. The space group is P1 with one molecule per unit cell. Again, the structural investigation was halted at this stage; however, the molecular symmetry is determined by the space group and the number of molecules per unit cell. Space group P1 with one molecule per unit cell requires an acentric molecule. Rubrene A is, therefore, acentric, while rubrene B is centrosymmetric. The existence of both conformations in the same system may be inferred from the mixture of crystals obtained by Taylor, presumably at room temperature.

If it is assumed that rubrene B is slightly above rubrene A in energy content, it must also be assumed that the oscillator strength for the $^1L_a$ and $^1B_b$ transitions in rubrene B is slightly less than the corresponding oscillator strengths in rubrene A. The spectral behavior can then be explained in terms of the following equilibrium:

$$\delta \text{ energy} + \text{rubrene A} \rightleftharpoons \text{rubrene B} \ .$$

## References for Proposition II


1. Z. A. Akopyan, R. L. Avoyan, and Yu. T. Struchkov, Journal of Structural Chemistry 3, 576 (1962) (English translation).

2. G. M. Badger, R. S. Pearce, H. J. Rodda, and I. S. Walker, J. Chem. Soc., 1954, 3151.

3. H. H. Jaffe and M. Orchin, Theory and Application of Ultraviolet Spectroscopy, John Wiley and Sons, New York (1962), p. 321.

4. H. H. Jaffe and O. Chalvet, J. Am. Chem. Soc. 85, 1561 (1963).

5. K. H. Kim, L. Smith, T. Beineke, and J. H. Day, J. Org. Chem. 28, 1890 (1963).

6. L. Pauling, The Nature of the Chemical Bond, Cornell University Press, Ithaca, New York (1960), p. 260.

7. A. Schönberg, A. Mustafa, and W. Asker, J. Am. Chem. Soc. 76, 4134 (1954).

8. W. H. Taylor, Z. Krist. A93, 151 (1936).

## PROPOSITION III

During the past two years, considerable activity has been seen in the chemistry of polyhedral carboranes. These compounds are of theoretical interest because of their isoelectronic relationship to the polyhedral $B_nH_n^{-2}$ series of ions which, with the exception of tetrahedral $B_4H_4^{-2}$, should exist as stable ions with closed electronic shells (9). Of the series $B_nH_n^{-2}$, only $B_6H_6^{-2}$ (3), $B_{10}H_{10}^{-2}$ (7, 12), and $B_{12}H_{12}^{-2}$ (16) are known. The structure of $B_6H_6^{-2}$ is a regular octahedron (18); $B_{10}H_{10}^{-2}$, a bicapped square antiprism (10); and $B_{12}H_{12}^{-2}$, a regular icosahedron (26). Other interesting structures have been observed in the carborane series, $B_nC_2H_{n+2}$. The following carboranes are known: $B_3C_2H_5$ (trigonal bipyramid) (21, 25); $B_4C_2H_6$ (two isomers, sym- and antisym-octahedra) (21, 22); $B_5C_2H_7$ (pentagonal bipyramid) (1, 21); $B_9C_2H_{11}$ (structure unknown) (2, 23); and $B_{10}C_2H_{12}$ (three isomers, o-, m-, and p- icosahedra) (4, 5, 8, 15, 17, 19, 20, 24, 27). The $B_3C_2H_5$ and $B_5C_2H_7$ carboranes are isoelectronic respectively with the unknown $B_5H_5^{-2}$ and $B_7H_7^{-2}$ anions. The two $B_4C_2H_6$ carboranes are isoelectronic with the recently discovered $B_6H_6^{-2}$ anion, and the three $B_{10}C_2H_{12}$ carboranes, of course, are isoelectronic with the well known $B_{12}H_{12}^{-2}$ anion. However, no carborane analog of the $B_{10}H_{10}^{-2}$ anion has been reported. Because of the great theoretical and practical interest in $B_{10}H_{10}^{-2}$, it is proposed that the synthesis of $B_8C_2H_{10}$ II be attempted.

Carboranes have been prepared by three different synthetic routes: 1) for the carboranes containing 3 to 5 borons, the reaction of acetylene with diborane or pentaborane-9 in a silent discharge tube

has been successful (21, 22, 25); 2) carboranes, $B_4C_2H_6$, $B_5C_2H_7$, and $B_9C_2H_{11}$ have been prepared through the pyrolysis of the appropriate dihydrocarborane (14, 23); 3) decaborane reacts with acetylene in the presence of a Lewis base to form o-$B_{10}C_2H_{12}$ (4, 8, 27) from which the m- and p-isomers are obtained by thermal isomerization (5, 15). This latter reaction has also been successful if the Lewis base substituted decaborane is used as starting material (8). This is the synthetic route which is chosen for the synthesis of $B_8C_2H_{10}$ II. The starting material is the Lewis base substituted $B_8$ icosahedral fragment, $C_2H_5NH_2B_8H_{11}NHC_2H_5$ I (6, 13), which has the following structure (11).

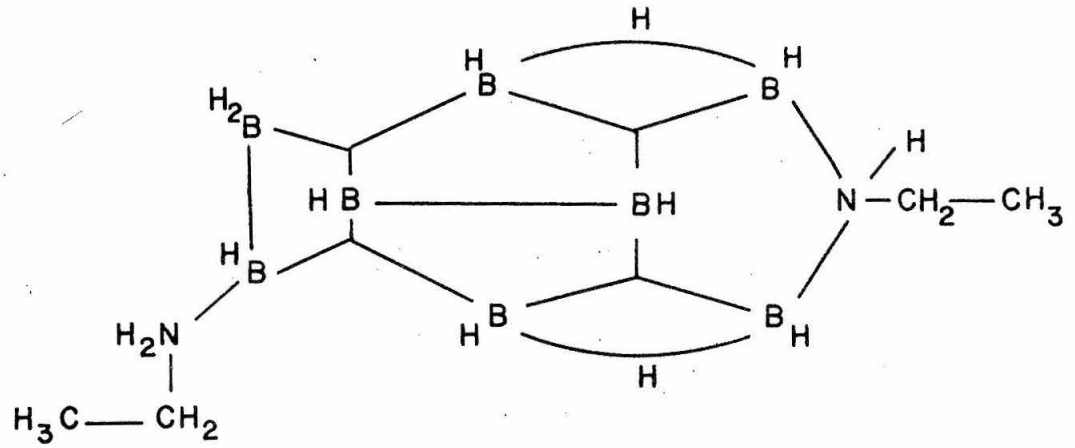

I

The reaction of I with acetylene is reasonable in that amines were listed among the Lewis bases which were successfully used in the corresponding reaction with decaborane (8). The rearrangement of the $B_8$ icosahedral fragment to the bicapped square antiprism geometry is expected because of the enhanced stability of the latter structure

and the parallel rearrangement of the decaborane icosahedral fragment to $B_{10}H_{10}^{-2}$ when treated with $(C_2H_5)_3N$ (7, 12).

The synthesis of II could probably be accomplished by dissolving I in a suitable solvent (di-n-propyl ether was used for the synthesis of $B_{10}C_2H_{12}$) and bubbling purified acetylene through the solution at about 90°C under a reflux condenser. Because of the

$$C_2H_5NH_2B_8H_{11}NHC_2H_5 + HC \equiv CH \rightarrow H_2\uparrow + B_8C_2H_{10} + 2NH_2C_2H_5$$

lower symmetry of the bicapped square antiprism relative to the icosahedron, seven isomers (the 2, 7(8)- and 2, 6(9)- enantiomorphic pairs being counted each as one isomer instead of two) are possible

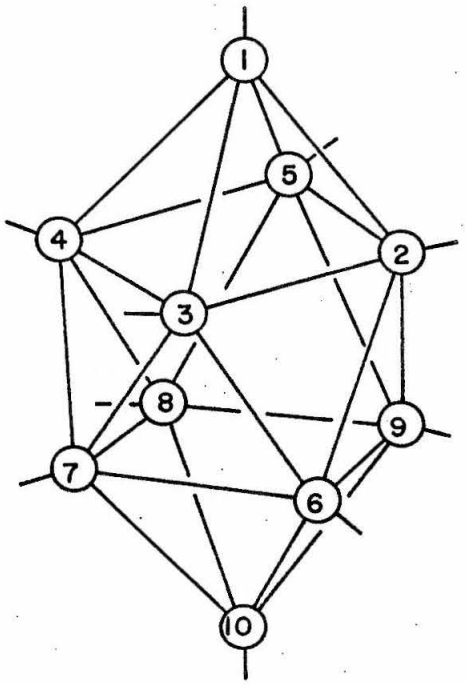


Numbering of the Atoms in the $B_8C_2H_{10}$ Structure.

for $B_8C_2H_{10}$, whereas only three isomers are possible for $B_{10}C_2H_{12}$. Of the seven isomers, the structure for II will probably be one of the

three structures in which the carbons are adjacent, i.e., the 1, 2-, the 2, 6- , or the 2, 3- isomer, although the latter is unlikely from geometric considerations.

## References for Proposition III


1. R. A. Beaudet and R. L. Poynter, J. Am. Chem. Soc. 86, 1258 (1964).

2. T. E. Berry, F. N. Tebbe, and M. F. Hawthorne, Tetrahedron Letters 1965, 715.

3. J. Boone, J. Am. Chem. Soc. 86, 5036 (1964).

4. M. M. Fein, J. Bobinski, N. Mayes, N. Schwartz, and M. S. Cohen, Inorg. Chem. 2, 1111 (1963).

5. D. Grafstein and J. Dvorak, Inorg. Chem. 2, 1128 (1963).

6. B. M. Graybill, A. R. Pitochelli, and M. F. Hawthorne, Inorg. Chem. 1, 626 (1962).

7. M. F. Hawthorne and A. R. Pitochelli, J. Am. Chem. Soc. 81, 5519 (1959).

8. T. L. Heying, J. W. Ager, S. L. Clark, D. J. Mangold, H. L. Goldstein, M. Hillman, R. J. Polak, and J. W. Szymanski, Inorg. Chem. 2, 1089 (1963).

9. R. Hoffmann and W. N. Lipscomb, J. Chem. Phys. 36, 2179 (1962).

10. A. Kaczmarczyk, R. Dobrott, and W. N. Lipscomb, Proc. Natl. Acad. Sci. U. S. 48, 729 (1962).

11. R. Lewin, P. Simpson, and W. N. Lipscomb, J. Am. Chem. Soc. 85, 478 (1963).

12. W. N. Lipscomb, A. R. Pitochelli, and M. F. Hawthorne, J. Am. Chem. Soc. 81, 5833 (1959).

13. W. N. Lipscomb, Boron Hydrides, W. A. Benjamin, Inc., New York (1963), p. 15.

14. T. P. Onak, F. J. Gerhart, and R. E. Williams, J. Am. Chem. Soc. 85, 3378 (1963).

15. S. Papetti and T. L. Heying, J. Am. Chem. Soc. 86, 2295 (1964).

16. A. R. Pitochelli and M. F. Hawthorne, J. Am. Chem. Soc. 82, 3228 (1960).

17. A. Potenza and W. N. Lipscomb, J. Am. Chem. Soc. 86, 1874 (1964); Inorg. Chem. 3, 1673 (1964).

18. R. Schaeffer, Q. Johnson, and G. S. Smith, Inorg. Chem. 4, 917 (1965).

19. H. Schroeder, T. L. Heying, and R. Reiner, Inorg. Chem. 2, 1092 (1963).

20. H. Schroeder and G. D. Vickers, Inorg. Chem. 2, 1317 (1963).

21. I. Shapiro, C. D. Good, and R. E. Williams, J. Am. Chem. Soc. 84, 3837 (1962).

22. I. Shapiro, B. Keilin, R. E. Williams, and C. D. Good, J. Am. Chem. Soc. 85, 3167 (1963).

23. F. Tebbe, P. M. Garrett, and M. F. Hawthorne, J. Am. Chem. Soc. 86, 4222 (1964).

24. D. Voet and W. N. Lipscomb, Inorg. Chem. 3, 1679 (1964).

25. R. E. Williams, C. D. Good, I. Shapiro, and B. Keilin, Abstracts, 140th National Meeting of the American Chemical Society, Chicago, Illinois, Sept. 1961, p. 14N.

26. J. Wunderlich and W. N. Lipscomb, J. Am. Chem. Soc. 82, 4427 (1960).

27. L. I. Zakharin, V. I. Stanko, V. A. Brattsev, Yu. A. Chapovskii, and Yu. Okhlobystin, Izv. Akad. Nauk SSSR, Otd. Khim. Nauk, 2238 (1963).

## PROPOSITION IV

Oxidation of the polyhedral $B_{10}H_{10}^{-2}$ ion by either aqueous $FeCl_3$ or $Ce(HSO_4)_4$ has been reported to produce the $B_{20}H_{18}^{-2}$ ion (1, 2, 3, 4, 8, 9). X-ray (1, 4) and $^{11}B$ n. m. r. (1-4, 8, 9) measurements have shown that the $B_{20}H_{18}^{-2}$ ion is a centrosymmetric combination of two $B_{10}H_9^-$ polyhedra; however, the exact nature of the bond between the two polyhedra is not clear.

Of the many $^{11}B$ n. m. r. spectra which have been reported for this ion, the 60 Mc./sec. spectrum of Pilling, et. al. (8), because of its higher resolution, contains the most useful structural information. Relative to $BF_3 \cdot O(C_2H_5)_2$ there is a low field doublet of area 2 at -29.9 p.p.m., a low field singlet of area 2 at -15.3 p.p.m., and five high field doublets of areas 2:4:4:4:2 at 7.6, 13.4, 16.7, 20.1, and 26.1 p.p.m., respectively (see figure 2, reference 8). The division of the spectrum into a low field part and a high field part with the ratio of areas 4:16 is characteristic of the $B_{10}$ polyhedra for which the low field part corresponds to the apical borons (5). The appearance of boron resonances as doublets results from splitting by the terminal hydrogens which are bonded to most of the borons. Hydrogens which are involved in three-center B-H-B bridge bonds generally do not cause a splitting in the resonance of either boron involved in the bridge.

In the earlier $^{11}B$ n. m. r. spectra (4), the high field resonance was not well resolved, and the appearance of the low field singlet was attributed to B-H-B bridge bonds involving apical borons. (The pres-

ence of another singlet,presumably in the unresolved high field resonance, was assumed.) Consequently, the original interpretation of the $^{11}B$ n. m. r. data (4) lent support to the proposed structure (6) involving two B-H-B bridges linking an apical boron atom in one $B_{10}$ unit to an equitorial boron of the other $B_{10}$ unit (see figure 1, reference 8). The presence of only one singlet in the 60 Mc./sec. spectrum, however, precluded the bridged structure (8). Two other structures, I and II, which involve B-B-B three-center bonds were then considered. (In Figure 1, the shaded areas represent three-center bonds. The numbered circles are boron atoms, and terminal hydrogens are represented by the short lines pointing outward from the polyhedra.) Pilling, et. al. (8) expressed a preference for structure I over structure II on the basis of more favorable bond angles and thereby ignored the fact that the low field singlet indicates the presence of apical borons to which are bonded no terminal hydrogens. It is, therefore, proposed that structure II is the correct structure for $B_{20}H_{18}^{-2}$.

It can be argued that the involvement of an equatorial boron in a three-center bond may cause a shift to lower magnetic field, and that the low field singlet observed in the 60 Mc./sec. spectrum of $B_{20}H_{18}^{-2}$ results from the equatorial borons 6 and 6' to which no terminal hydrogens are bonded (in structure I), but such an argument demands an equal shift to higher magnetic field in the resonance of the apical borons 10 and 10', so that the resulting doublet falls in the high field part of the spectrum. In order to effectively answer

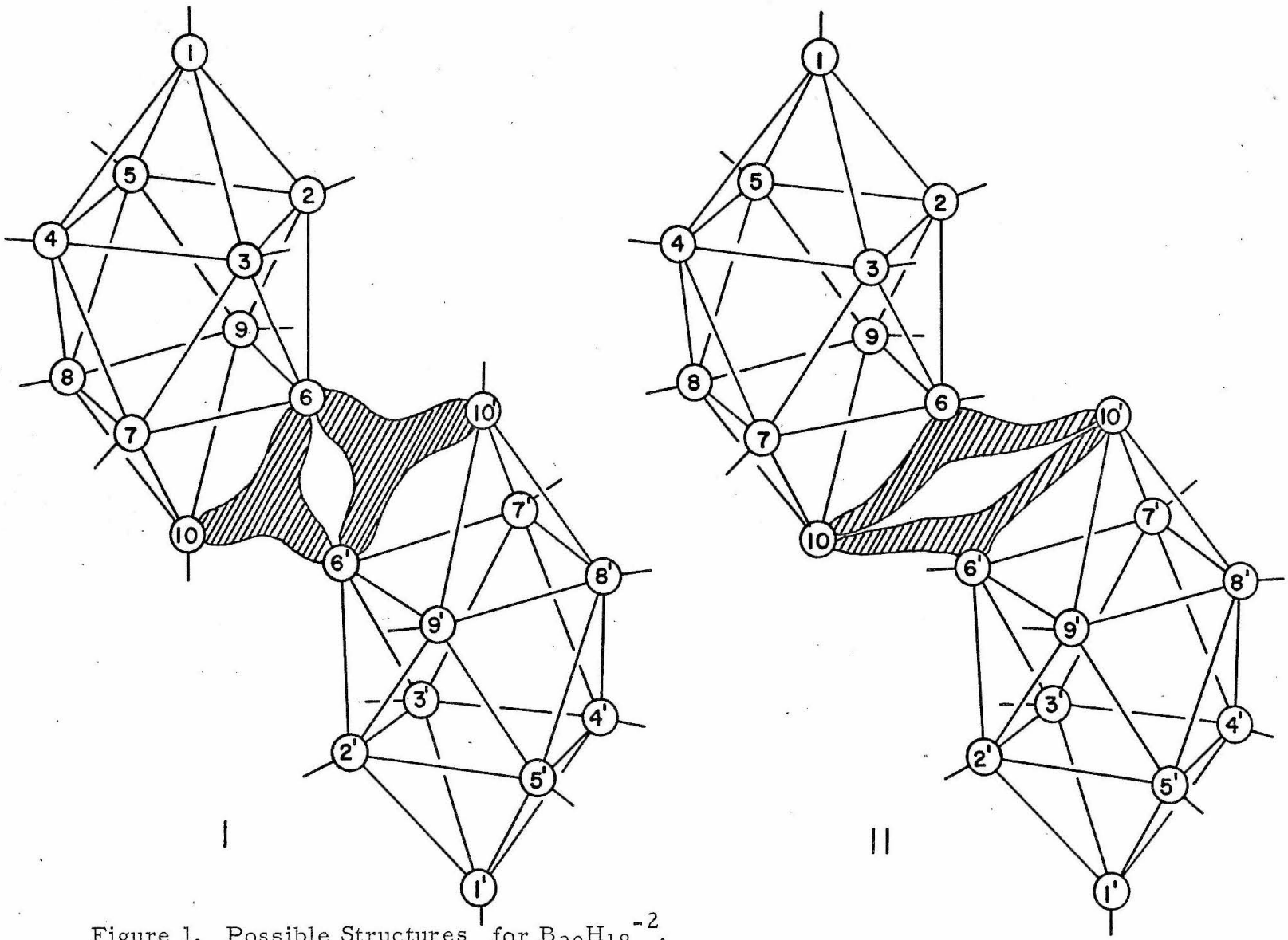


Figure 1. Possible Structures for $B_{20}H_{18}^{-2}$.

this argument, it is suggested that the very similar $B_{24}H_{22}^{-2}$ ion be synthesized and studied by n. m. r. techniques. The $B_{24}H_{22}^{-2}$ ion, which has not yet been reported, should be easily attainable by oxidation of the well known $B_{12}H_{12}^{-2}$ ion (7). In the $B_{12}$ icosahedron, there is only one kind of boron, and the n. m. r. spectrum of the $B_{24}H_{22}^{-2}$ ion should consist of a poorly resolved multiplet on the high field side of $BF_3 \cdot O(C_2H_5)_2$. However, if the interpretation of Pilling, et al. (8) is correct, a singlet of area 2 resulting from the very similar icosahedral borons in $B_{24}H_{22}^{-2}$, which correspond to borons 6 and 6' in $B_{20}H_{18}^{-2}$, should be observed on the low field side of the multiplet in the spectrum of $B_{24}H_{22}^{-2}$.

## References for Proposition IV


1. B. L. Chamberland and E. L. Muetterties, Inorg. Chem. 3, 1450 (1964).

2. M. F. Hawthorne, R. L. Pilling, P. F. Stokely, and P. M. Garrett, J. Am. Chem. Soc. 85, 3704 (1963).

3. M. F. Hawthorne, R. L. Pilling, and P. F. Stokely, J. Am. Chem. Soc. 87, 1893 (1965).

4. A. Kaczmarczyk, R. Dobrott, and W. N. Lipscomb, Proc. Natl. Acad. Sci. U. S. 48, 729 (1962).

5. W. N. Lipscomb, A. R. Pitochelli, and M. F. Hawthorne, J. Am. Chem. Soc. 81, 5833 (1959).

6. W. N. Lipscomb, Proc. Natl. Acad. Sci. U. S. 47, 1791 (1961).

7. W. N. Lipscomb, Boron Hydrides, W. A. Benjamin, Inc., New York (1963), p. 188.

8. R. L. Pilling, M. F. Hawthorne, and E. A. Pier, J. Am. Chem. Soc. 86, 3568 (1964).

9. A. R. Pitochelli, W. N. Lipscomb, and M. F. Hawthorne, J. Am. Chem. Soc. 84, 3026 (1962).

## PROPOSITION V

Evidence for restricted rotation of a methyl group has recently been observed in the e. p. r. spectrum of α-methylanthrasemiquinones (3). However, no such effect has ever been observed by nuclear magnetic resonance spectroscopy, presumably because of the longer time constants involved in the latter method. It is proposed that systems of the type described below will inhibit the rotation of methyl groups to the extent that the different methyl hydrogens should exhibit different proton chemical shifts in the n. m. r. spectra.

10-methyldibenzo [c, g] phenanthrene I is probably the simplest of these overcrowded molecules; however, in view of the unsuccessful synthetic attempt of Bell and Waring (1), it is doubtful that it can be prepared. A similar overcrowded compound, 1, 3, 6', 8'-tetramethylbianthrone IIa , has been known for several years (7), but no n. m. r. spectrum has been reported. An X-ray structural investiga-

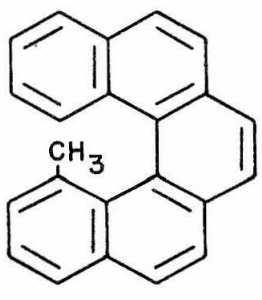


I

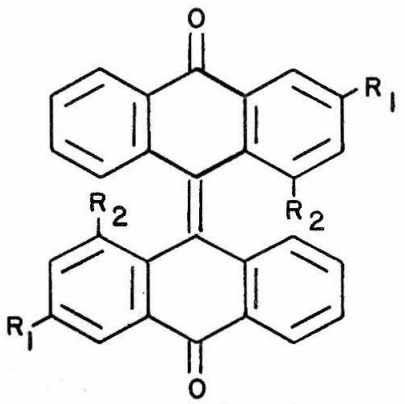


IIa : $R_1 = R_2 = CH_3$

IIb : $R_1 = COOH$ ; $R_2 = H$

IIc : $R_1 = COOH$ ; $R_2 = CH_3$

tion of the unsubstituted bianthrone (5) has shown that because of the steric strain at the 1, 8, 1', and 8' positions, the molecule exists in the folded conformation shown in Figure 1. Ultraviolet and visible spectral studies (7, 8) indicate a similar conformation for the 1, 3, 6', 8-tetramethyl derivative. Molecular scale models (see figures 6 and 7, reference 7) show that one of the hydrogens on both the 1- and the

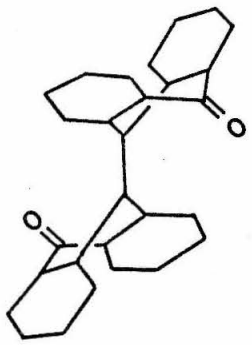

Figure 1. Folded Conformation for Bianthrone (5).

8'-methyl groups can be directed toward the center of the opposite six-membered ring. This is very similar to the "nesting" phenomenon described by Fritchie (4) for large molecules which contain phenyl groups. Such a nesting arrangement is evidently energetically favorable. This, together with the tremendous overcrowding at the methyl positions, should substantially increase the barrier to rotation and permit the observation of different methyl proton chemical shifts in the n. m. r. spectrum.

The "nested" protons at the centers of six-membered rings in

IIa should experience the shielding effect of induced ring currents. The ring current shielding of protons within the cavity of π-electron systems has been observed previously in 14- and 18-carbon ring systems (2, 6, 10), but the shielding of the "nested" protons in IIa should be greater because of the more intense ring current in benzenoid systems. The resonance of the "nested" protons is, therefore, expected to occur on the high field side of the resonance (14.03τ) of the previously observed shielded protons (2). The other two methyl hydrogens will experience the same shielding, but to a far lesser extent. There is no way of predicting whether the other two hydrogens will have the same or different chemical shifts, but there is little doubt that they will couple with the "nested" proton to split its resonance into either a triplet or a double doublet.

The solubilities of the unsubstituted bianthrone and 1, 3, 6', 8'-tetramethylbianthrone IIa are rather low in most solvents, but bianthrone-3, 6'-dicarboxylic acid IIb and its esters (11) are very soluble in a number of solvents. For this reason, it is suggested that 1, 8'-dimethylbianthrone-3, 6'-dicarboxylic acid IIc be prepared and used for an n. m. r. investigation of "nesting." IIc should be easily obtainable by the usual synthetic route (7, 11) from 4-methylanthrone-2-carboxylic acid III which probably could be prepared from IV by the method of Limpricht (9).

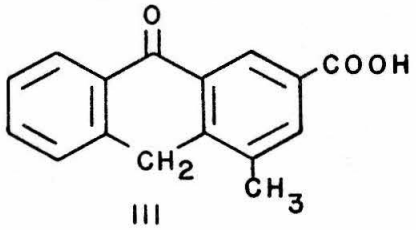


III

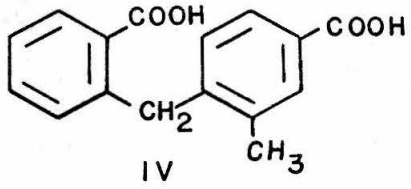


IV

References for Proposition V

1. F. Bell and D. H. Waring, J. Chem. Soc. 1949, 2689.

2. V. Boekelheide and J. B. Phillips, J. Am. Chem. Soc. 85, 1545 (1963).

3. R. M. Elofson, K. F. Schulz, B. E. Galbraith, and R. Newton, Can. J. Chem. 43, 1553 (1965).

4. C. J. Fritchie, Ph. D. Thesis, California Institute of Technology, Pasadena, California (1963).

5. E. Harnik and G. M. J. Schmidt, J. Chem. Soc. 1954, 3295.

6. L. M. Jackman, F. Sondheimer, Y. Amiel, D. A. Ben-Efraim, Y. Gaoni, R. Wolovsky, and A. A. Bothner-By, J. Am. Chem. Soc. 84, 4307 (1962).

7. G. Kortüm, W. Theilacker, H. Elliehausen, and H. Zeininger, Chem. Ber. 86, 294 (1953).

8. G. Kortüm and G. Bayer, Ber. Bunsen Ges. Physik. Chem. 67, 24 (1963); Angew. Chem. 75, 96 (1963).

9. H. Limpricht, Ann. 309, 121 (1899).

10. F. Sondheimer, Y. Gaoni, L. M. Jackman, N. A. Bailey, and R. Mason, J. Am. Chem. Soc. 84, 4595 (1962).

11. W. Theilacker, G. Kortüm, H. Elliehausen, and H. Wilski, Chem. Ber. 89, 1578 (1956).

Beineke, T. A
1966

PLEASE NOTE:

Tables pages are not original copy. Some have extremely small print. Figure pages tend to "curl". Filmed in best possible way.

University Microfilms, Inc.